Bikash Chaudhary

ASSESSMENT ON PLASTIC DEFORMATION AT THE POWERHOUSE CAVERN AND TAILRACE TUNNEL OF ANDHIKHOLA HYDROELECTRIC PROJECT

Master's thesis in Hydropower Development
Supervisor: Krishna Kanta Panthi

June 2020

Master's thesis

NTNU
Norwegian University of Science and Technology
Faculty of Engineering
Department of Geoscience and Petroleum

NTNU
Norwegian University of
Science and Technology

NTNU
Norwegian University of
Science and Technology

NTNU
Norwegian University of
Science and Technology

Department of Geoscience and Petroleum

Your ref.: MS/I18T54/IGP/BCKP

Date: 06.01.2020

TGB4910 Rock Engineering - MSc thesis
for
Bikash Chaudhary

ASSESSMENT ON PLASTIC DEFORMATION AT THE POWERHOUSE CAVERN AND TAILRACE TUNNEL OF ANDHIKHOLA HYDROELECTRIC PROJECT

Background

Plastic deformation (tunnel squeezing) is a phenomenon which is frequently confronted while tunnelling through Himalayan rock mass. Schistose rocks like shale, slate, phyllite, schist, highly schistose and sheared rocks and the rock mass of the tectonic fault zones are incapable of sustaining medium to high stresses. While carrying upgrading work at Andhikhola Hydroelectric project it was observed that substantial plastic deformation (tunnel squeezing) was noticed along the tailrace tunnel and in the underground powerhouse cavern. The deformation data collected during upgrading work are important to understand the deformation phenomenon.

In this respect, documentation and analysis of plastic deformation phenomenon at this tunnel project would be an important issue for the engineers, project developers and as a whole to the scientific community involved in rock and tunnel engineering.

MSc thesis task

Hence, this MSc thesis is to focus on the documentation and evaluation of plastic deformation at the underground powerhouse cavern and tailrace tunnel of the Andikhola Hydroelectric Project, with a main focus on the following issues:

- Review existing theory on the stability issues in underground excavation with focus on plastic deformation.
- Briefly describe about Andhikhola Hydroelectric Project covering history of project development, recent upgrading work and engineering geological conditions at the project site.

- Document the extent of plastic deformation observed during upgrading work and rock support principle used while upgrading.
- Back-analyse the plastic deformation using empirical and analytical approaches including production of support characteristics curve based on applied support, measured final deformation and reviewed theory.
- Analyse plastic deformation using numerical modelling for both underground powerhouse cavern and selected tailrace segments.
- Compare and discuss the analysis results from empirical, analytical and numerical approaches.

Relevant computer software packages

Candidate shall use *rocscience package* and other relevant computer software for the master study.

Background information for the study

- Relevant information about the project such as reports, maps, information and data collected by the candidate.
- Scientific papers, reports and books related to the Himalayan geology and tunnelling.
- Scientific papers and books related to international tunnelling cases.
- Literatures in rock engineering, rock support principles, rock mechanics and tunnelling.

Mr. Bibek Neupane will be the co-supervisor of this MSc thesis.

The thesis work is to start on January 15, 2020 and to be completed by June 10, 2020.

The Norwegian University of Science and Technology (NTNU)
Department of Geoscience and Petroleum (IGP)

January 06, 2020

Dr. Krishna Kanta Panthi
Professor of rock and tunnel engineering, main supervisor

FOREWORD

This master thesis titled "**ASSESSMENT ON PLASTIC DEFORMATION AT THE POWERHOUSE CAVERN AND TAILRACE TUNNEL OF ANDHIKHOLA HYDROELECTRIC PROJECT"** is submitted to the Department of Geoscience and Petroleum as the final requirement for fulfillment of Master of Science in Hydropower Development Program (2018-2020).

The thesis mainly focuses on the documentation and evaluation of plastic deformation analysis of tailrace tunnel and powerhouse cavern of Andhikhola Hydropower Project (AKHP), Nepal. The applied methods for plastic deformation analysis involve empirical, semi-empirical, analytical, and numerical methods. The results obtained from these methods were compared and discussed with the measured deformation from the site during upgrading work of the AKHP.

_ _ _ _ _ _ _ _ _ _ _

Bikash Chaudhary

NTNU, Norway

June 2020

ACKNOWLEDGEMENT

ABSTRACT

There are several risks and challenges associated with underground excavation especially in case of weak and schistose rock mass. One of the major instability issues is the high induced stress around the excavation boundary. Once the magnitude of these induced stresses exceeds the rock mass strength, the yielding of rock mass occurs resulting in displacement around the excavation contour. Tunnels and caverns excavated in weak and deformable rock mass under high rock cover are more likely to experience instability in the form of deformation. In many cases, those deformation is of significant magnitude and is irreversible, which is often called as plastic deformation also known as tunnel squeezing in case of weak rock. Squeezing phenomena in underground excavation are very common in weak rocks such as shale, slate, phyllite and schist of the lesser Himalayan and Siwaliks zones, and in weakness/fault zones (Panthi, 2006).

In this thesis, Andhikhola Hydropower Project (AKHP), located in lesser Himalayan of Nepal has been taken as case study. This hydropower project experienced substantial plastic deformation (squeezing phenomena) in some stretches of tailrace tunnel and minor squeezing in powerhouse cavern which were initially in complete stable condition for last 3 decades. The squeezing phenomena was noticed only after upgrading the project to higher capacity which demanded the existing tailrace tunnel and cavern to be enlarged in cross section. The major squeezing occurred in tailrace tunnel in which the most critical section was from chainage 0+390 to 0+410. The convergence measurement of those squeezed tailrace sections was carried out which showed maximum plastic deformation of 14.5cm. Powerhouse cavern experienced 50-100mm of plastic deformation on walls just after the longitudinal extension. The rock types along the powerhouse cavern and tailrace tunnel are fresh to moderately weathered slate intercalated with phyllite.

The main focus of this thesis is the documentation and assessment of plastic deformation of the powerhouse cavern and tailrace tunnel of AKHP. The objective involves an evaluation of available methods for prediction and assessment of squeezing of underground excavation. For this study, the methods that have been used to analyze the plastic deformation are: empirical methods such as Singh et al. (1992) and Q-system (Grimstad and Barton, 1993), semi-analytical method Hoek and Marinos (2000), and numerical modeling in RS2 and RS3. Calibration of the major input parameters like stress conditions and rock mass deformability has been carried out using the numerical analysis. As per the squeezing prediction criteria such as Singh et al. (1992), Q-system and Hoek and Marinos (2000) , there is severe squeezing

problem in the selected tailrace sections and minor squeezing in the powerhouse cavern. Hoek and Marinos (2000) show there is substantial amount of plastic deformation in tailrace tunnel. The numerical analysis was carried out for the tailrace tunnel section (chainage 0+400) which experienced the maximum deformation whereas for powerhouse cavern, the existing powerhouse cavern was modeled both in 2D and 3D so investigate the effect of extension.

The accuracy of the plastic deformation analysis largely depends on the correct estimation of input parameters mainly: induced rock stress and rock mass deformability parameters. The induced stress over the excavation opening are the resultant of stress due to gravity and tectonic stresses. Since there were not any rock stress measurement carried out at the site, the RS2 program has been used to calibrate these values using the measured deformation. However, stress measurement will be necessary to verify this value. Also, the Uniaxial unconfined strength of intact rock of the tunnel sections has been back calculated from measured deformations using RS2 program and found to be in the range of 10 Mpa for tailrace sections and 30Mpa for powerhouse cavern. The analysis from all the above-mentioned methods indicates that that there is significant plastic deformation in the selected sections of tailrace tunnel and minor deformation in cavern.

TABLE OF CONTENTS

List of Abbreviation

AKHP	Andhikhola Hydropower Project
CCM	Convergence confinement method
GRC	Ground Reaction Curve
GSI	Geological Strength Index
ISRM	International Society for Rock Mechanics
LDP	Load displacement curve
MBT	Main Boundary Thrust
MCT	Main Central Thrust
Mpa	Mega Pascal
MW	Mega Watt
RMR	Rock Mass Rating
RQD	Rock Quality Designation
SCC	Support Characteristic Curve
SFR	Shotcrete Fiber Reinforced
SRF	Strength Reduction Factor
UCS	Uniaxial Compressive Strength
σ_0	Far-field stress

1 Introduction

1.1 Background

Nepal is a land-bound country gifted with massive geographical diversity and water resources. Most of the major rivers in Nepal have steep gradient, emerging from snowmelt and glaciers of the Himalayas thus creating considerable potential for hydropower generation. Because of the huge scale of its potential for energy production, the hydropower sector in Nepal can be a major ladder to economic prosperity. Tunnels and underground caverns are inevitable in most of the hydropower projects of Nepal since they are located in topographically steep areas with risk of landslide and high tectonic activity. However, the complex geological setup of Himalayan region and the ongoing tectonic activities have increased geological uncertainties and caused considerable stability problems for tunnels and underground caverns (Panthi, 2006).

Due to persistent compressive tectonic stress, the rock mass of Himalaya has been subjected to intense deformation causing faulting, shearing, folding and jointing. Therefore, rock mass in this region, mainly sedimentary and metamorphic rocks are highly anisotropic, sheared and schistose (Panthi, 2006). Along with that, steep topography and high mountains have further increased the gravity induced stresses. These all factors have caused various stability problems for tunnels and caverns. Out of which, plastic deformation or squeezing in case of weak and deformable rock mass has been a major challenge in Himalayan rock masses. Weak rocks such as Phyllite, schist, schistose gneiss, shale, slate of lesser Himalayan and Siwaliks zones and rock mass in weakness and fault zones have experienced severe tunnel squeezing (Panthi, 2006).

Experiences from several hydropower projects in the Himalayan region have shown that the tectonized and young formations typically show plastic behavior, even for small overburdens (Panthi, 2006). Severe tunnel squeezing cases has been encountered in many hydropower tunnels in Nepal like Kaligandaki HP, Khimti HP, Modi HP (Panthi, 2006), Chameliya HEP (Basnet et al., 2013) and many more. Andhikhola hydropower project (AKHP) is also one among them which faced similar problem. Located in Syangja district, Gandaki province of Nepal, AKHP had been upgraded from 5.1 MW to 9.4 MW which demanded the enlargement of the existing powerhouse cavern and the tailrace tunnel. During the construction, there was substantial plastic deformation in tailrace tunnel and minor squeezing in powerhouse cavern.

The focus of the thesis is therefore the documentation and analysis of plastic deformation at the tailrace tunnel and powerhouse cavern of AKHP.

1.2 Objective and Scope of the Study

MSc thesis is to focus on the documentation and evaluation of plastic deformation at the underground powerhouse cavern and tailrace tunnel of the Andikhola Hydropower Project, with a main focus on the following issues:

- Review existing theory on the stability issues in underground excavation with focus on plastic deformation.
- Briefly describe about Andhikhola Hydropower Project covering history of project development, recent upgrading work and engineering geological conditions at the project site.
- Document the extent of plastic deformation observed during upgrading work and rock support principle used while upgrading.
- Back-analyze the plastic deformation using empirical and analytical approaches including production of support characteristics curve based on applied support, measured final deformation, and reviewed theory
- Analyze plastic deformation using numerical modelling for both underground powerhouse cavern and selected tailrace segments.
- Compare and discuss the analysis results from empirical, analytical, and numerical approaches.

1.3 Methodology of the study

The following methodology has been applied during the study:

1.3.1 Literature review:

- Background theories on rock mass properties and stress induced instability with major focus on plastic deformation.
- Background theories on stability analysis and deformation calculation

1.3.2 Study of Andhikhola Hydropower Project

- Study of AKHP development history, overview of project layout with more focus on powerhouse cavern and tailrace tunnel
- Data collection of deformation measurements, feasibility and project completion report, photographs, lab test results, hydropower projects from same geological area

- Study of engineering geological conditions and rock mass properties of tailrace and powerhouse cavern

1.3.3 Plastic deformation analysis

Based on the data collected, the plastic deformation analysis has been carried out using following approaches:

Empirical methods: Singh et al. (1992) and Q-system

Semi-Analytical method: Hoek and Marinos (2000)

Numerical method: Numerical modeling using RS2 and RS3 (Rocscience Software)

1.3.4 Comparison and evaluation of results

The results from the analysis has been compared to the measured deformations from the tailrace tunnel and powerhouse cavern. The applicability of these methods on deformation analysis in non-circular tunnel and cavern has been assessed based on limitations and assumptions for each method.

1.4 Limitations of the Study

The major challenge in this study has been to establish reliable input parameters for the analysis. Since this project was constructed 30 years ago, very few geological information was available for the study of existing stability state of powerhouse cavern and tailrace tunnel. The main source of input data has been the Feasibility study report 2005, AKHP Project completion report 2015, project photographs and project drawings which lacked field testing data on rock mass parameters. Therefore, many literatures such as journals, books, thesis reports and discussions with supervisor have been used to estimate the rock mass parameters. Also, the project in the same geological area has been used as reference. The parameters estimated from these references may not represent the reality of the case study project. The deformation measurement of tailrace tunnel lacks the data monitoring of almost 3 weeks after the excavation date. Furthermore, the maximum number of convergence monitoring data available for the squeezed stretches of the tailrace tunnel is only for 19 days. Although the powerhouse cavern experienced minor squeezing, no exact convergence monitoring has been done at the site. However, the outward shifting of rail-track of EOT crane by 50-100mm has been noticed during inspection of post construction which has been assumed as final deformation value for analysis of the powerhouse cavern.

2   Rock and Rock mass properties

2.1   Introduction

A rock is a heterogeneous material smaller and larger blocks/pieces composed of naturally occurring solid aggregates of one or more minerals. These minerals differ significantly in physical properties with one another. Hence the physical properties of the rock will considerably depend on the type and amount of the minerals it contains. Moreover, size, shape, orientation of the minerals and also the mineral binding forces significantly influence the physical and mechanical properties of rocks (Nilsen and Thidemann, 1993). While investigating the mechanical and physical properties, usually two terms are considered i.e. intact rock and rock mass. It is because, only intact rock properties are not sufficient to understand the behavior of actual ground. In fact, the actual ground behavior is more relatable to the term rock mass which is the total in-situ material containing intact rock, all joints and other discontinuities and structural features which makes its properties quite different from that of intact rock and has more concern in practical life (Nilsen and Thidemann, 1993).

The rock mass is a heterogeneous medium which is mostly exemplified by two main features: rock mass quality and the mechanical processes acting on the rock mass (Panthi, 2006). These two features are highly dependent on each other and are very important function to the stability of underground excavation as shown in Figure 2-1.
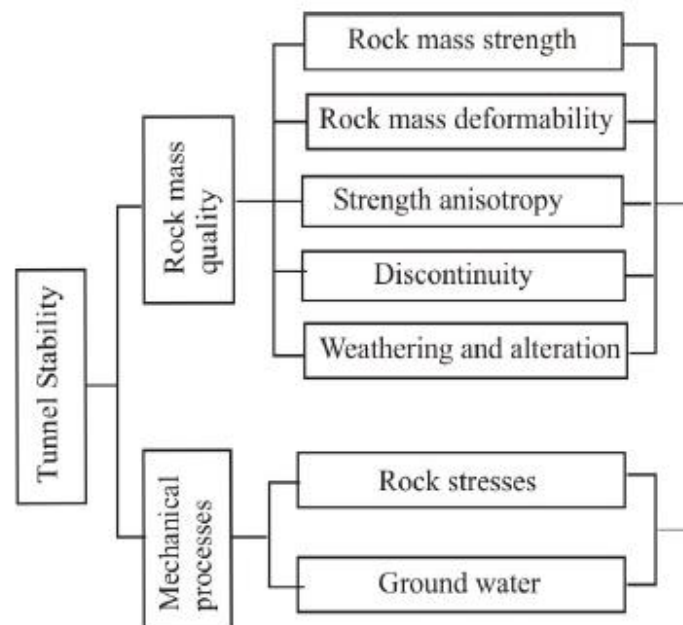
Figure 2-1: Factors influencing on tunnel stability (Panthi, 2006)

In this chapter, a brief introduction of some of the factors influencing rock mass quality are presented and more emphasis is given on rock mass in the Himalaya due to the location of the

study. These factors are very important during the evaluation of the stability of underground excavation.

2.2 Rock mass structures

Rock mass structure is basically the nature and distribution of structural features within the rock mass. The major structural features of the rock mass are bedding plane, joints, folds, faults, shear zones and dykes (Brady and Brown, 2007). The occurrence of these structural features largely influences the properties of rock mass which are described below:

2.2.1 Bedding plane

Bedding planes divide the rock into bed or strata basically in sedimentary rocks and are highly persistent features. It may contain parting material of different grain size from sediment forming the rock mass or may have been partly healed by low-order metamorphism. Arising from the depositional process, there may be a preferred orientation of particles in the rock, giving rise to planes of weakness parallel to bedding (Brady and Brown, 2007).

2.2.2 Jointing of rock mass

Joints are the most common structural features present in the rock mass. A group of parallel joints is called a joint set and joint sets intersect to form a joint system. Joints may be open, filled or healed. They frequently form parallel to bedding planes, foliations or cleavage, where they may be termed bedding joints, foliation joints or cleavage joints (Brady and Brown, 2007)
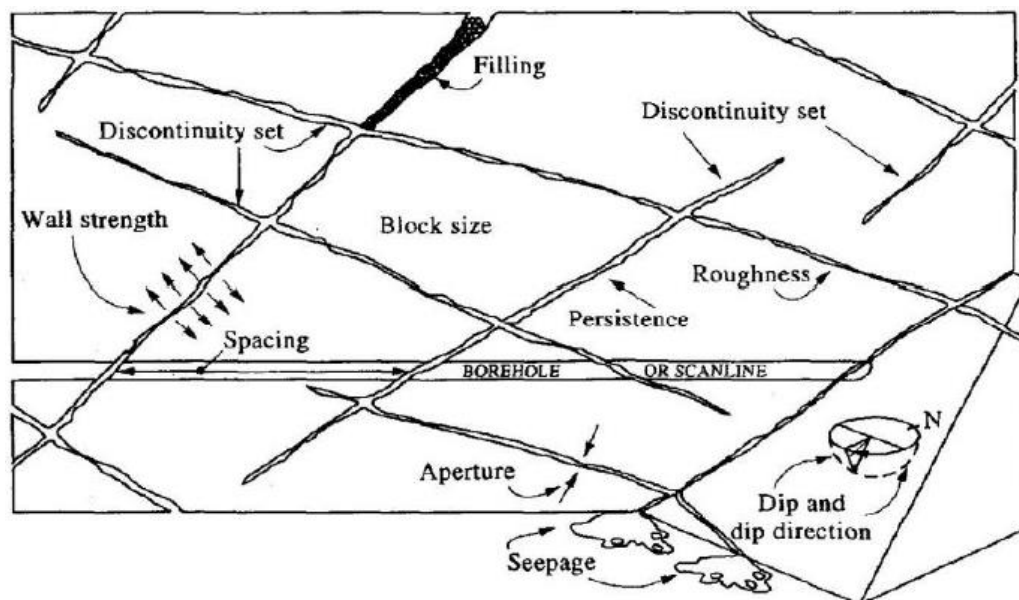
Figure 2-2: Schematic of the primary geometrical properties of discontinuities in rocks (Hudson and Harrison, 2000)

2.2.3 Weakness zones and faults

There are two major groups of weakness zones; those formed by tectonic activity, or those formed by other processes ((Nilsen and Palmström, 2000). Faults are tectonically formed minor to major structures in the rock mass and are identified by the occurrence of shear displacement as shown in Figure 2-3. Minor faults normally range in thickness from a decimeter to a meter whereas, the major faults range from several meters to hundred meters.

A weakness zone may be beds or layers of particularly weak rock in a series of sedimentary or metamorphic rocks (Nilsen and Thidemann, 1993). Weakness zones and faults form patterns in the surface, or lineaments, and may be identified by inspection of aerial photos or maps, or during field mapping.

The filling materials within weakness zones are called gouge materials. The main gouge materials are often coarse rock fragments. But some minerals may be altered or changed into new minerals and form clay minerals. Some clay minerals, e.g. smectites, have a swelling capacity when exposed to water. This could cause severe instability problem during pre-excavation and post excavation.
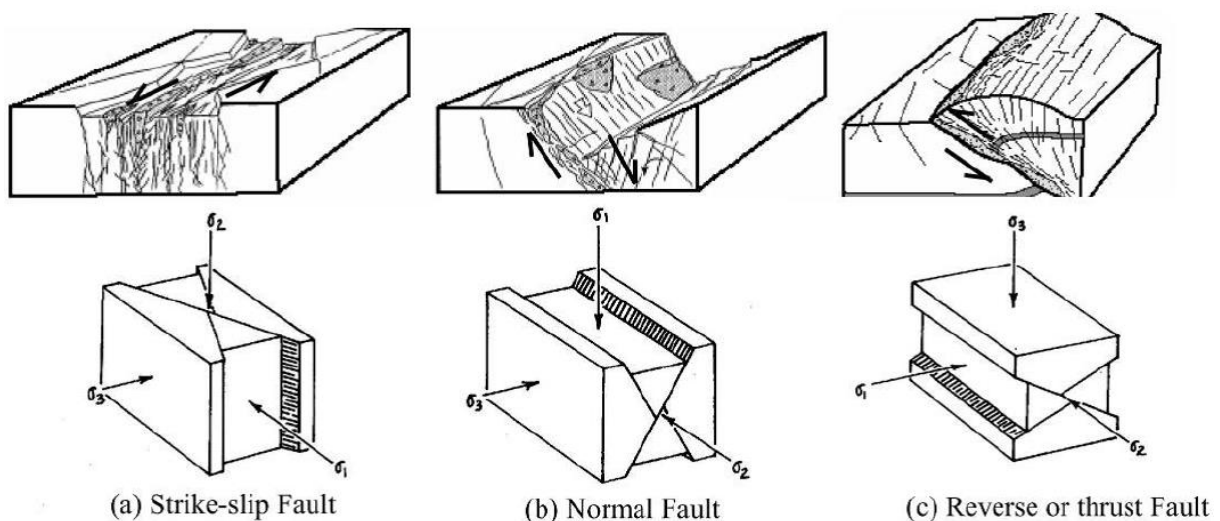
Figure 2-3: Types of faults and weakness zones (Panthi, 2006)

2.3 Rock mass strength and deformability

Rock strength and elastic properties play a major role in all aspects of rock engineering. Determination of the strength for the intact rock (σ_{ci}) is done by laboratory testing or field tests. The rock mass strength (σ_{rm}) is typically estimated by empirical relationships. Common intact rock strength tests include uniaxial compressive test, triaxial strength test and the point load test. Methods for field estimation have also been developed but are only good as a firsthand estimate. No tests were performed especially for this study, although results from previous tests

have been used. The reader will in either case be referred to other sources for theory on rock strength testing.

2.3.1 Factors influencing rock mass strength

Most methods for estimating rock mass strength depends on the uniaxial compressive strength of the intact rock. The factors influencing the strength of intact rock are therefore just as important for the discussion of factors for rock mass strength. Some of the many factors will be discussed below:

2.3.1.1 The scale effect

An intact rock test specimen is usually strong and close to homogeneous with few discontinuities. The specimen does not represent the strength and deformability of the rock mass; there is a considerable scale effect. The more discontinuous features in the rock mass, the more size dependence should be expected. Crystalline unweathered rocks have small size effect. Highly schistose, foliated and deformed rocks of sedimentary and metamorphic origin like shale, slate, phyllite and schist have considerable size and directional effect on their strength (Panthi, 2006). As shown in Figure 2-4, it can be noticed that increasing the specimen diameter from 50mm to 200mm reduces the intact rock strength by almost 25 percent.
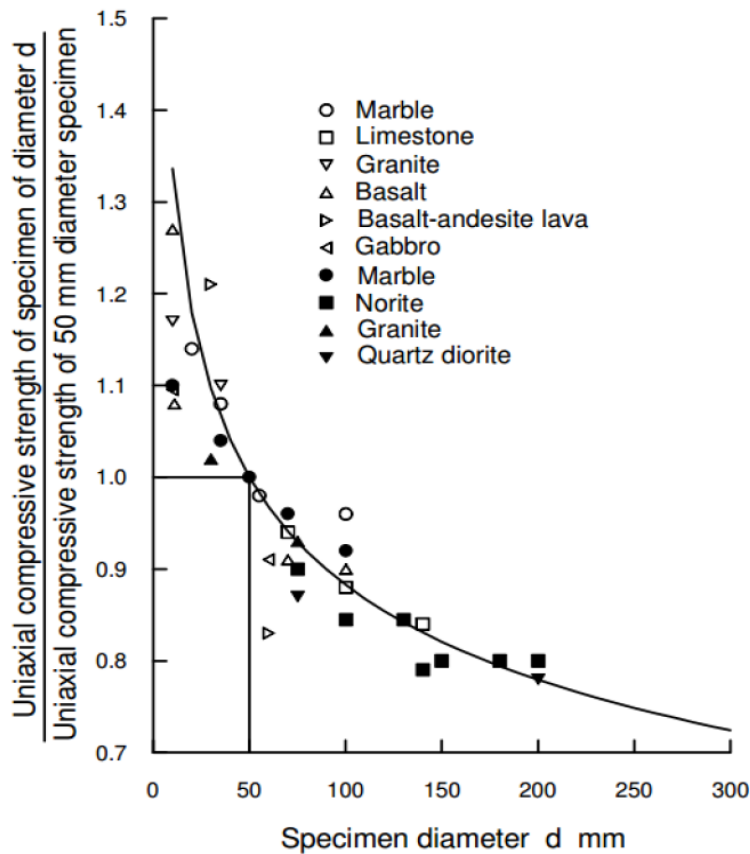
Figure 2-4: Influence of specimen size on the strength of intact rock (Hoek, 2007c)

2.3.1.2   The effect of anisotropy

Anisotropy in rocks is mainly caused by a preferred orientation of mineral grains and directional stress history. This is especially common in sedimentary and metamorphic rocks as a result of bedding, foliation and schistocity (Goodman, 1989). According to Panthi (2006), the Himalayan rocks often consist of thin bands of very weak and highly sheared rocks such as slate, phyllite and schists interlayered within the bands of relatively strong and brittle rocks such as gneisses, quartzite and dolomite. The layers of weak and schistose rocks lack sufficient bonding/friction and have reduced self-supporting capacity and may result in severe stability problems while tunneling.
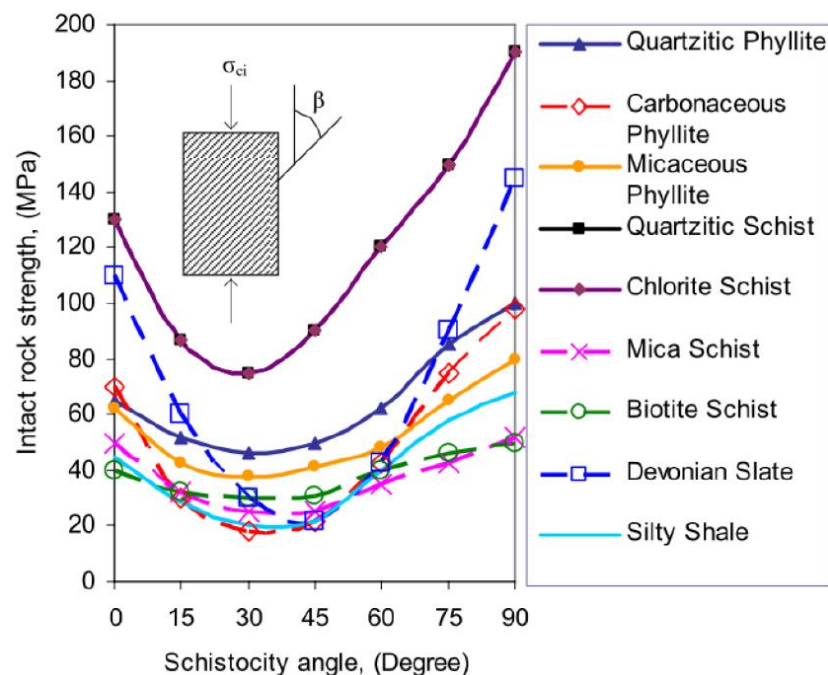
Figure 2-5: Uniaxial compressive strength of intact rock at different angle of schistocity plane (Panthi, 2006)

As illustrated in Figure 2-5, strength of intact rock is lowest when the schistosity plane angle is inclined at around 30 degrees and highest when the plane is perpendicular to the direction of loading. The test results may therefore give the false impression of strength characteristics (Panthi, 2006).

2.3.1.3   The effect of water

The occurrence of water has a considerable effect on rock mass strength, especially for highly schistose or porous rocks like sandstone and shale. Laboratory tests of moist sand-stone and shale have shown a reduction in strength of 40% and 60% respectively, compared to dry

strength (Nilsen and Palmström, 2000). The reduction in strength is due to the effect of pore and fissure water pressure and can be reduced by drying the samples before testing.

2.3.1.4 The effect of weathering and alteration

Rock weathering is the process of disintegration and decomposition of the rock material. The rock loses its coherence by mechanical disintegration or breakdown of the material. This causes opening or new formation of joints, opening of grain boundaries and fracturing of individual mineral grains (Nilsen and Palmström, 2000). Chemical decomposition involves rock decay accompanied by changes in chemical and mineralogical composition. This leads to discolorations, decomposition and alteration of silicate minerals to clay minerals and leaching or solution of calcite, anhydrite and salt minerals (Nilsen and Palmström, 2000). Generally, the weathering starts in the walls of the discontinuities and migrates to the rock material (Panthi, 2006). Weathering reduces the mechanical properties of the rock mass, such as strength, deformability, slaking durability, and frictional resistance. In ISRM, 1978 , weathering classification has been done and rock mass have been graded from I to IV based on weathering condition.
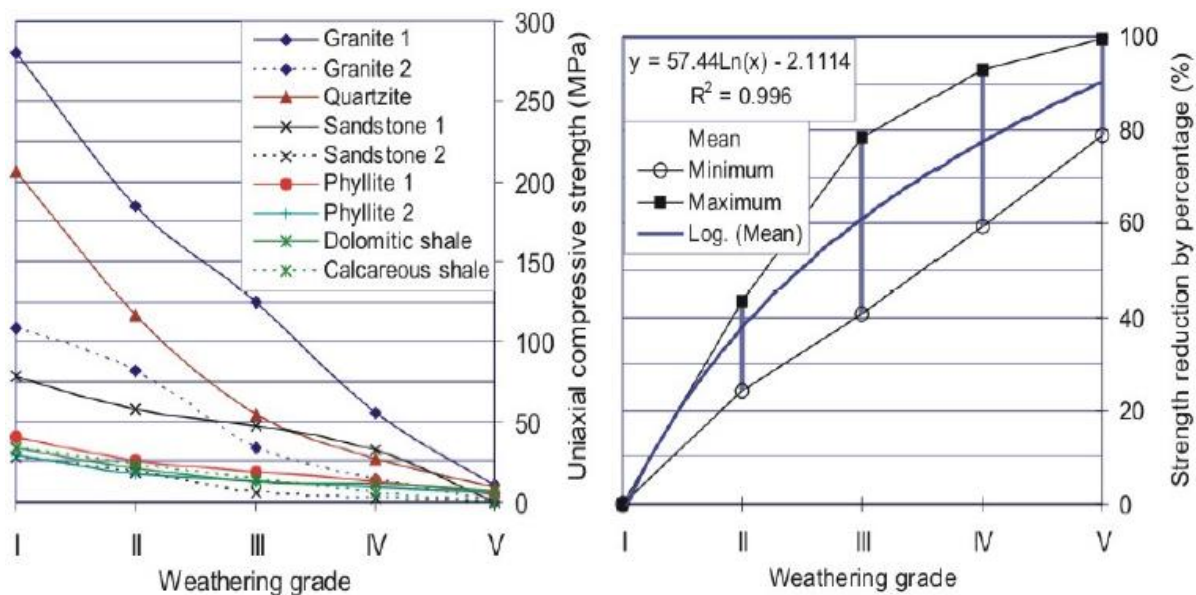
Figure 2-6: Compressive strength of rock (left) and strength reduction in percentage (right) as function of weathering grade (Panthi, 2006)

2.3.2 Failure Criteria

The term failure can be regarded as the "loss of integrity" of the material, which in engineering is interpreted as the loss of the materials load carrying capacity. There are several theories or criteria for the attempt to explain and predict when and where failure will occur in the rock mass. This has been done by assuming that the failure will occur due to a specific mechanism,

when a specific mechanical property is exceeded (Myrvang, 2001). Further it is evaluated which principal stress condition will lead to such a failure. Among the classical theoretical failure criteria are the Tresca criterion (max. shear stress), Mohr-Coulomb (max effective shear stress), Drucker Prager criterion and Griffith's criterion (Myrvang, 2001). The theoretical criteria rarely reflect the true nature of the failure mechanism. Out of many empirical relationships, the Mohr-Coulomb criterion and Hoek-Brown criterion are widely applied in rock engineering. In this thesis, only Hoek and Brown criteria has been described further since this criterion has been used in the deformation analysis.

The Hoek-Brown Criterion

Hoek and Brown introduced their failure criterion as an attempt to provide input data for the analysis required for the design of underground excavations in hard rock (Hoek et al., 2002). The criterion is an empirical relation derived from a best fit of strength data plotted in a principal stress space ($\sigma1$-$\sigma3$) (Hudson and Harrison, 2000). Further adjustment of the criterion was done based on tangents of the principal stress plot (Mohr-envelope). From various practical situations, they found that the Mohr-envelope could be adjusted with a variable constant a instead of the square root term (Hoek, 1990). The generalized Hoek-Brown criterion was introduced:

$$\sigma'_1 = \sigma'_3 + \sigma_{ci}\left(m_b\frac{\sigma'_3}{\sigma_{ci}} + s\right)^a \qquad \text{2-1}$$

Where the material constant mb, s and a are defined as:

σ'_1 and σ'_3 are the major and minor effective principal stresses at failure, σ'_{ci} is the uniaxial compressive strength of intact rock material which is discussed in section 2.3.

$$m_b = m_i \exp\left(\frac{GSI - 100}{28 - 14D}\right) \qquad \text{2-2}$$

$$s = \exp\left(\frac{GSI - 100}{9 - 3D}\right) \qquad \text{2-3}$$

$$a = \frac{1}{2} + \frac{1}{6}\left(e^{-GSI/15} - e^{-20/3}\right) \qquad \text{2-4}$$

In the 2-2, m_i is a material constant for intact rock and GSI is the Geological Strength Index. D is the disturbance factor, and depend upon the degree of disturbance of the rock mass by blasting and stress relaxation (0 for undisturbed masses). The determination of these are given in Appendix A.

Relationship between Hoek-Brown and Mohr-Coulomb Failure Criteria

Selection of failure criterion should be done based on the type of rock mass being investigated. Mohr-Coulomb is best fitted for situations with rock mass consisting of one or two joint sets; or when one of the discontinuity sets is significantly weaker than the others. Hoek-Brown is best suited for intact rock, or for rock masses with a sufficient number of closely spaced discontinuities with similar characteristics. Then isotropic behavior involving failure on discontinuities can be assumed(Hoek, 2007c) as shown in Figure 2-7.
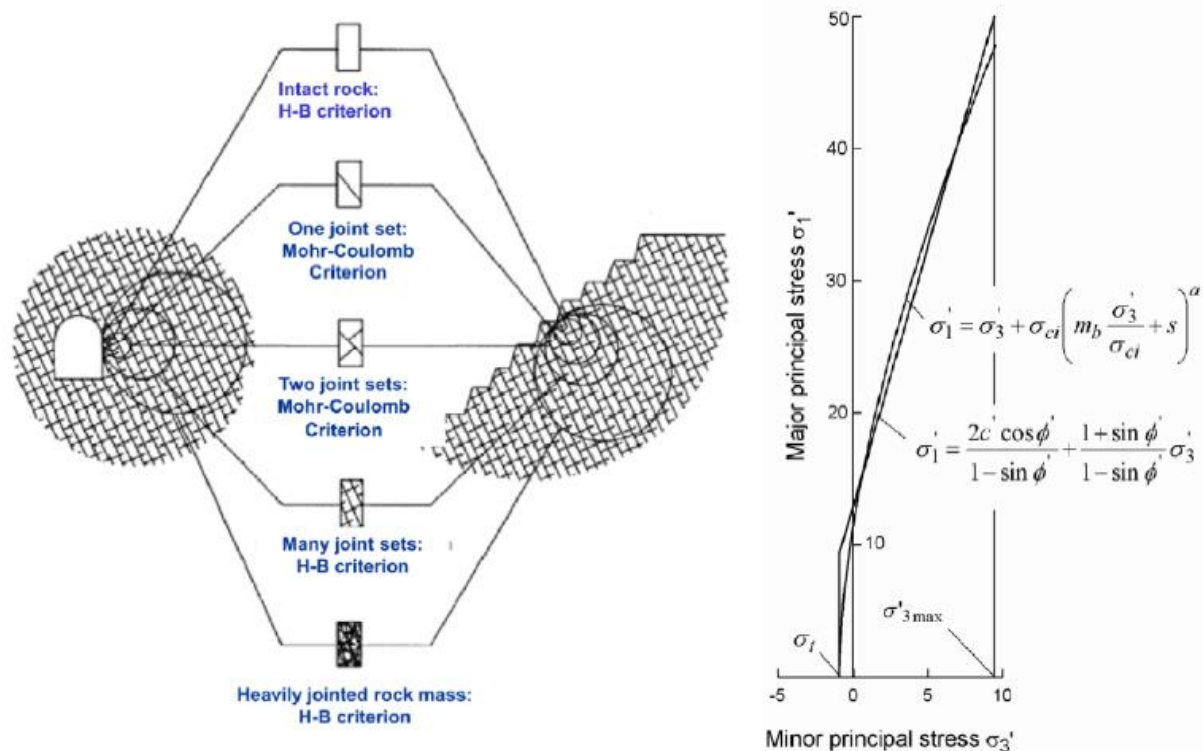
Figure 2-7: Selection of failure criteria according to rock mass condition (left) and Relationship between major and minor principal stresses for Hoek-Brown and equivalent Mohr-Coulomb criteria. (Hoek et al., 2002)

2.3.3 Estimation of rock mass strength

Rock mass strength and deformation is different from that of an intact rock specimen. An intact rock specimen is usually strong and homogeneous with few discontinuities and can therefore not represent the strength and deformability of the total rock mass. As discussed above, there are several factors influencing the strength of intact rock, and by this the strength of the rock mass. Evaluation of strength of the rock mass will additionally include the influence of discontinuities, foliation or schistocity planes, and the orientation of these relative to the direction in which the strength is assessed (Panthi, 2006). Rock mass strength is difficult to estimate in the field, or by laboratory testing, and many authors have therefore suggested

11

empirical relationships for estimation of rock mass strength (σ_{cm}) as presented in Table 2-1. Typically, the methods include intact rock strength (σ_{ci})) and a form of rock mass characterization parameter like Q-value or Rock Mass Rating (RMR).

Table 2-1: Empirical formulas for estimation of rock mass strength

Proposed by	Empirical relationship
Bieniawaski (1993)	$$\sigma_{cm} = \sigma_{ci} \times exp\left(\frac{RMR - 100}{18.75}\right)$$
Hoek et al. (2002)	$$\sigma_{cm=}\sigma_{ci}\left(\frac{(m_b + 4s - a(m_b - 8s))((m_b/4 + s)^{a-1}}{2(1 + a)(2 + a)}\right)$$
Barton (2002)	$$\sigma_{cm} = 5_\gamma\left(\frac{\sigma_{ci}}{100} \times 10^{\frac{RMR-50}{15}}\right)^{1/3}$$
Panthi (2006)	$$\sigma_{cm} = \frac{\sigma_{ci}^{1.5}}{60}$$

In the above equations, σ_{cm} is the unconfined compressive strength of rock mass in MPa, σ_{ci} is the uniaxial compressive strength of intact rock in MPa, RMR is the Wieniawski's rock mass rating and the detail is given in Appendix A, s and a are the material constant related to Hoek-Brown failure criteria (calculated using equations 2-3 and 2-4 respectively), GSI is the geological strength index, γ is the rock density in t/m^3.

In case of availability of Q-value; RMR and GSI value can be calculated using the equations 2-5 and 2-6 and proposed by Barton (1995) and Hoek and Diederichs (2006) as follows:

$$RMR = 15 \times logQ + 50 \tag{2-5}$$

$$GSI = RMR - 5 \tag{2-6}$$

The methods relating both rock mass rating and intact rock strength have been found to have a weakness when evaluating weak, fractured and schistose rocks. There is reduction in strength of discontinuous rock twice; once in the laboratory while determining σ_{ci} and again while determining the rock mass rating (RMR, Q or GSI) (Hoek and Marinos, 2000). However, the relation by Panthi (2006) depends on only σ_{ci}. According to Panthi (2006) the relation may be used for highly schistose, foliated, thinly bedded and anisotropic rocks of metamorphic and sedimentary origin with low compression strength.

2.3.4 Estimation of rock mass deformability

Deformability of the intact rock is referred to as the Young's modulus or modulus of elasticity (E_{ci}) and is the ratio between applied stress and corresponding strain within the elasticity limit. Rock mass deformability or modulus of deformation (E_m) is defined as the ratio of stress to corresponding strain during loading of the rock mass, and includes both elastic and inelastic behavior (Panthi, 2006). A jointed rock mass does not behave elastically, and it is therefore necessary with the term modulus of deformation rather than modulus of elasticity (Bieniawski, 1989). As for rock mass strength, the deformability of the rock mass is lower than for the intact rock, and may be reduced down to 10% of the intact deformability (Panthi, 2006)

The modulus of deformation may be measured directly in the field (e.g. plate bearing, dilatometer test, flat-jack test, hydraulic chamber etc.), but often provide values that differ considerably (Nilsen and Palmström, 2000). The tests are also considered time consuming and costly. Many authors have therefore proposed empirical equations for estimating the modulus of deformation, some of the selected are presented in Table 2-2.

Table 2-2: Empirical formulas for estimation of rock mass deformation modulus

Proposed by	Empirical relationship
Bieniawski (1989)	$E_m = 2\text{RMR-100}$
Hoek et al. (2002)	$E_m = \left(1 - \dfrac{D}{2}\right)\sqrt{\dfrac{\sigma_{ci}}{100}}\,10^{\left(\frac{GSI-10}{40}\right)}$
Barton (2002)	$E_m = 10 \times \left(\dfrac{Q \times \sigma_{ci}}{100}\right)^{1/3}$
Hoek and Diederichs (2006)	$E_m = E_{ci} \times \left(0.02 + \dfrac{1 - \dfrac{D}{2}}{1 + e^{\left(\frac{60+15D-GSI}{11}\right)}}\right)$
Panthi (2006)	$E_m = \dfrac{1}{60} \times E_{ci} \times \sigma_{ci}^{0.5}$

3   Stress induced instabilities in tunneling

Rock stresses is the intensity of internal forces (force per unit area) induced in a rock mass under the influence of set of applied forces. Even in undisturbed rock mass contains nonzero stress condition due to the weight of overlying material, confinement, and pass stress history. Creating an underground excavation changes the stress conditions in the rock mass surrounding the opening. The final stress state will be a result of the initial stress conditions and the stresses induced by the excavation. The stability of an underground excavation will depend on the rocks ability to sustain failure induced by the stresses around the opening. Since the final stress condition is dependent on the initial stresses, specification and determination of the pre-excavation stress state is a key component of any stability and design analysis (Brady and Brown, 2007)

3.1   In situ rock stress

The stress condition existent in the rock mass prior to excavation is in-situ stresses. This stresses are formed as a result of following components (Nilsen and Palmström, 2000):

> ➢ Gravitation stresses: stress formed due to gravity alone.
> ➢ Tectonic stresses: stress caused by plate tectonics.
> ➢ Topographic stresses: mainly occurs when the surface is not horizontal, and the topography will have a considerable influence on rock stress situation.
> ➢ Residual stresses: when stresses locked into the rock mass from earlier stages of its geologic history.

There are several theory and information about the origin, influence, and determination of each of these stresses. However, in rock engineering, the most important stress for the stability analysis of underground opening is the magnitude and direction of major and minor principal stresses (Panthi, 2006). The gravitational and tectonic components of the in-situ stresses are generally regarded as the two most influencing stress components.

Gravitational stresses

This stress is the result of gravity alone and divided into vertical and horizontal component. In case of horizontal surface, the vertical gravitational stress at a depth H (in meters) is given by:

$$\sigma_v = \sigma_z = \gamma H \qquad\qquad\qquad 3\text{-}1$$

Where, γ is specific gravity of rock in MN/m^3

The total horizontal stress is the sum of gravitational stress component and a tectonic stress (Panthi, 2006) and is calculated as:

$$\sigma_h = \frac{\nu}{1-\nu} \times \sigma_v + \sigma_{tec} \qquad\qquad 3\text{-}2$$

Where, σ_h and σ_v are the horizontal and vertical stresses in MPa, σ_{tec} is the tectonic stresses in Mpa and ν is the Poisson's ratio of the rock mass
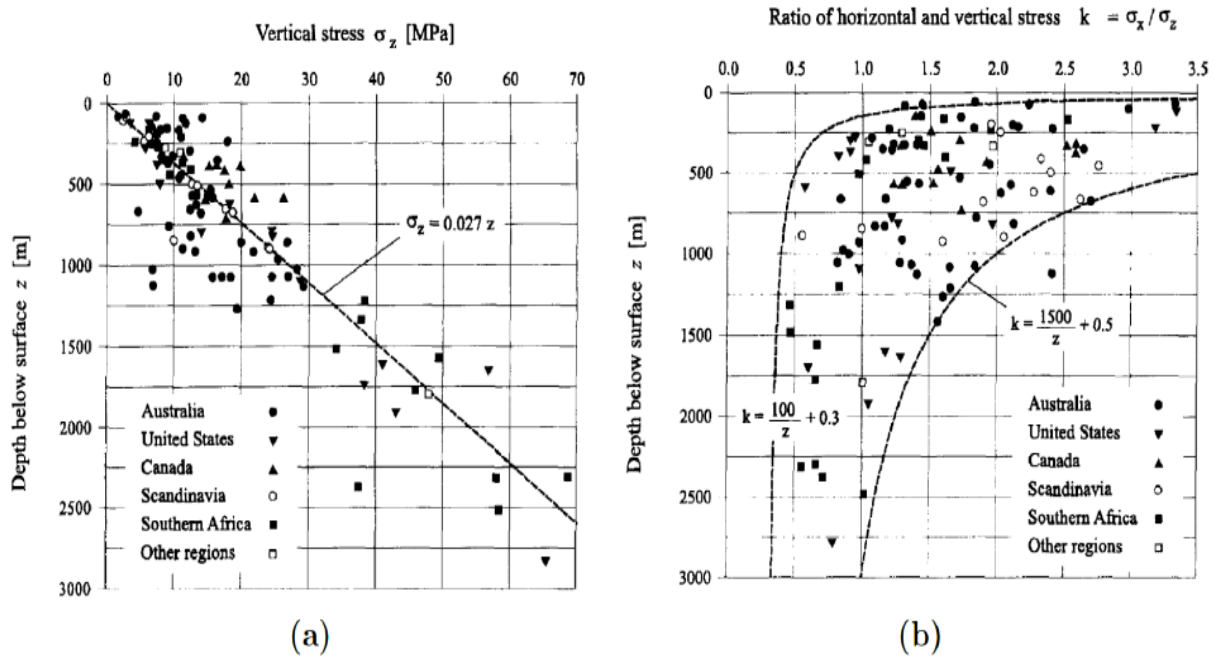
Figure 3-1: Plot of a) vertical stress against depth below surface, and b) variation in ratio of average horizontal stress to vertical stress with depth below surface (Hoek and Brown, 1980)

Figure 3-1(a) shows that the measured vertical stresses are in fair agreement with the simple prediction given by calculating the vertical stress due to the overlying weight of rock at a particular depth from the equation 3-1. At shallow depths, there is a considerable amount of scatter which may be associated with the fact that these stress values are often close to the limit of the measuring accuracy of most stress measuring tools. On the other hand, the possibility that high vertical stresses may exist cannot be discounted, particularly where some unusual geological or topographic feature may have influenced the entire stress field (Hoek and Brown, 1980)

Figure 3-1(b) provides the value of "k" which is the ratio of average horizontal to vertical stress against depth below surface. It can be seen that for most of the values plotted, k lies within the limits defined by following equation:

$$\frac{100}{z} + 0.3 < k < \frac{1500}{z} + 1.5 \qquad \text{3-3}$$

It is seen that at depths of less than 500 meters, horizontal stresses are significantly greater than vertical stresses. For depths in excess of 1 kilometer (3280 feet), the average horizontal stress and the vertical stress tend to equalize (Hoek and Brown, 1980). If very high horizontal stresses existed at depths in excess of 1 kilometer, these would have induced fracturing, plastic flow and time-dependent deformation in the rock, and all of these processes would tend to reduce the difference between horizontal and vertical stresses (Hoek and Brown, 1980).

Tectonic stress

The convergence of Indian and Asian tectonic plates has subjected the Himalayn region to undergoing persistent compression for more than million years. The compressional tectonic deformation and active reverse faulting mechanism have considerable influence on the magnitude of major tectonic principal stress in the Himalaya (Panthi, 2006). As shown in Figure 3-2, (world stress map,2016) tectonic principal stress in the Himalaya is oriented horizontally with Northeast-Southwest trend.

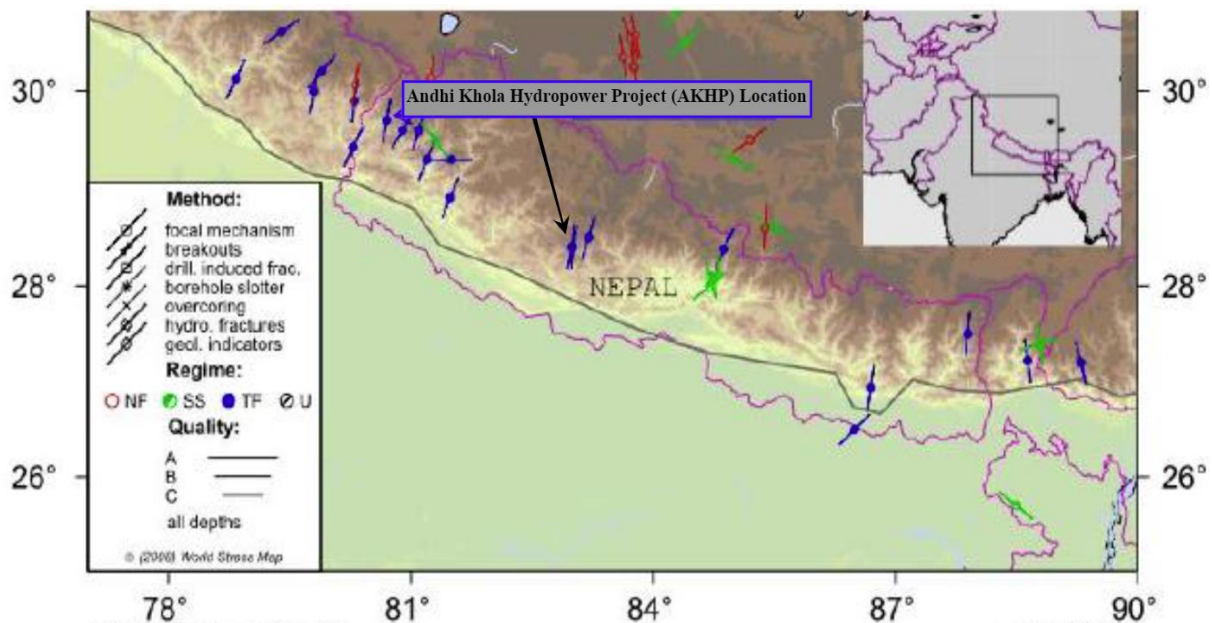Figure 3-2: Stress map of the Nepal with project location (World Stress Map,2016)

3.2 Stress distribution around excavation

During and after excavation of an underground opening, the stresses in the rock mass will be redistributed around the periphery of the excavation. The load carried by the mass removed must be transferred to the remaining mass. The stresses induced by the excavation will depend

on the magnitude and direction of the principal stresses and the geometry of the opening (Nilsen and Palmström, 2000).
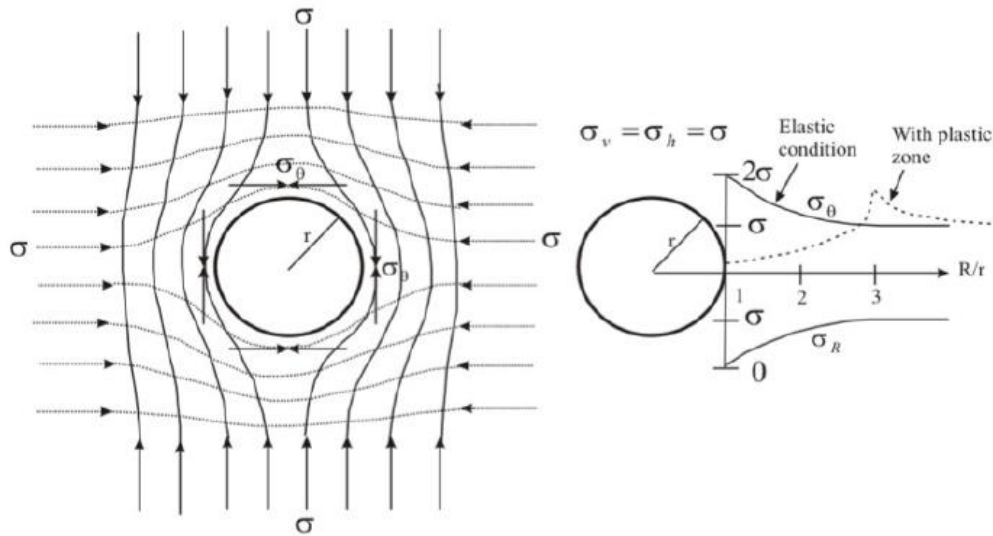
Figure 3-3: Stress trajectories around an circular opening (left), Tangential and radial stress distribution in elastic and non-elastic conditions (Panthi, 2006)

In Figure 3-3, the mechanism of stress redistribution around the opening of circular tunnel under isostatic stress condition is displayed. In elastic material the tangential stress (σ_θ) will be twice the principal stress (σ) at the wall of the opening, and the radial stress (σ_R) equal to zero. Moving away from the opening, the stresses will normalize as the ratio between radial distance (R) and opening radius (r) increases (Figure 3-3 right). This theory is known as the Kirsch solution:

$$\sigma_\theta = \sigma\left(1 + \frac{r^2}{R^2}\right)$$
3-4

$$\sigma_R = \sigma\left(1 - \frac{r^2}{R^2}\right)$$
3-5

In case of non-isostatic stress conditions, the Kirsch solution states that the maximum tangential stress ($\sigma_{\theta max}$) will occur in the direction where the major principal stress (σ_1) is tangent to the contour and the minimal tangential stress ($\sigma_{\theta min}$) occur where minor principal stress (σ_3) is tangent to contour . According to the Kirsch solution, the magnitude of the tangential stresses is defined as:

$$\sigma_{\theta max} = 3\sigma_1 - \sigma_3$$
3-6

$$\sigma_{\theta min} = 3\sigma_3 - \sigma_1$$
3-7

The Kirsch solution is valid for a homogeneous, isotropic, and elastic rock mass with widely spaced and tight joints (Panthi, 2006). For weak and anisotropic rocks, the tangential stresses

17

will cause destruction and cracking of the material, resulting in a gradual reduction of the strength. A zone of broken rock will form around the opening, so called plastic zone, where the material loses its load carrying ability. In such rock masses, the maximum tangential stresses are moved further from the periphery of the opening, until the elastic zone is reached (Panthi, 2006)

A non-circular opening will change the locational and magnitude of the tangential stresses. Sharp corners in particular, may strongly influence the magnitude; the sharper the corner, the higher the stress concentration in that corner will be (Nilsen and Palmström, 2000). The magnitude of the maximum tangential stress depends in theory on the shape of the excavation, and not its size. However, the zone of influence increases when the size increases. Consequently, the more masses are removed, the more stress is redistributed to the remaining masses (Myrvang, 2001)

3.3 Stress induced instabilities

When the tangential stress around the excavation exceeds the strength of the rock, the material will fail and cause instabilities in the underground opening. The problems are normally connected to the maximum tangential stress, causing compressive failure of the rock. However, if the minimum tangential stress is very low, this may cause tangential failure in the rock mass.

3.3.1 Problem due to tensile stress

Due to its discontinuous character, the rock mass has a low tolerance for tensile stress. Even a small tensile stress may cause radial failure. Tensile failure will occur if the minimal tangential stress (Eq.3-7) exceeds the tangential strength of the rock mass. In most cases, tensile fracturing will not have much influence on rock stability in a tunnel. However, for high-pressure hydropower tunnels the presence of open fractures may increase the possibility of water leakage, causing a decrease in water-pressure (Nilsen and Palmström, 2000).

3.3.2 Problem induced by high compressive stress

Compressive failure of the rock mass will occur if the compressive tangential stress (Eq. 3-6) exceeds the compressive strength of the rock. Depending on the character of the rock, the failure usually takes the form of either: i) rock/burst spalling, or ii) squeezing or plastic deformation.

Rock burst/Rock spalling

Rock spalling is fracturing parallel to the tunnel contour induced by high compressive stresses, and typically occurs for strong brittle rocks. The fracturing process is often accompanied by loud noises and vibrations and is then referred to as heavy spalling or rock burst. Rock burst or

heavy spalling typically only occur for very high rock stresses and are therefore most relevant for deep excavations. For moderate stress levels, the fracturing will result in loosening of thin rock slabs, referred to as rock slabbing or spalling (Nilsen and Palmström, 2000). Rock bursting may at times be quite violent and dramatic. In extreme cases the process can have the character of popping of large rock slabs with considerable force and speed. The activity is often most intensive in the vicinity of the face (10-20m behind face) and may therefore be a major threat to the safety of the workers if the appropriate support is not installed (Nilsen and Thidemann, 1993). The analysis and risk assessment of rock burst/spalling is not an objective of this study and will not be discussed further.

Squeezing or plastic deformation

Weak and soft rocks will due to its plastic nature behave very differently when subjected to tangential stress. In such rocks, the potential problems will be squeezing deformation. In extreme cases reduction of the original tunnel diameter of several tens of centimeters due to squeezing may occur (Nilsen and Palmström, 2000). As this is the major cause of stability problems at the tailrace tunnel of AKHP, the review on the plastic deformation has been discussed in detail in Chapter 6.

4 Andhikhola Hydropower Project

4.1 Project Development History

The Andhikhola Hydropower Project (AKHP) was commissioned in 1991 with an installed capacity of 5.1 MW. It is owned and operated by Butwal Power Company Ltd (BPC). The project was built under the aegis of UMN with old used equipment from Norway.

The Andhikhola Hydropower Project (5.1 MW) was designed for firm power supply i.e. with 93 percentage exceedance level. Since, old electro-mechanical equipment was installed in the powerhouse, the physical lifetime of the equipment was already over and therefore it was necessary to change the electro-mechanical equipment of the powerhouse as soon as possible. Furthermore, availability of more water for power generation, BPC decided to upgrade the project to a higher capacity (9.4 MW) and give the name of the project as Andhikhola Hydropower Project (Upgrading). The detail design and construction of the upgrading work started in 2012 and was completed and commercially operated in 2015.

To accommodate higher capacity electromechanical units, the powerhouse cavern had been extended longitudinally. Similarly, additional excavation in the existing tailrace tunnel was done to increase its discharge carrying capacity. During the upgrading work, substantial plastic deformation (squeezing) was noticed in some stretches of the tailrace tunnel and minor squeezing was observed in the powerhouse cavern.

4.2 Project Description

Andhikhola Hydropower project is in Syangja district, Gandaki Province of Nepal. The project area is about 80 km south-west from Pokhara on the Siddhartha highway near Galyang Bazar. The location map of the project is shown in Figure 4-1. AKHP is a run-of-river project with the rated turbine discharge is 4.9 m^3/s and the gross head of the project is 246m. The design discharge for the intake is 6.2m^3/s considering additional 1.3m^3/s discharge for irrigation purpose.

The 1284m long headrace tunnel conveys the discharge to the start of the penstock pipe. Two penstock pipes (one new and one old) of variable diameter then takes the rated design discharge to three turbine units in the powerhouse cavern. The powerhouse cavern is extended length wise to accommodate new higher capacity electro-mechanical units having 45m length, 6.6m wide and 11m height. Three units of horizontal axis Pelton turbine are installed with synchronous generators to generate the installed capacity of 9.4 MW. The discharge from the turbine is released in Kaligandaki River via 1084m long tailrace tunnel.
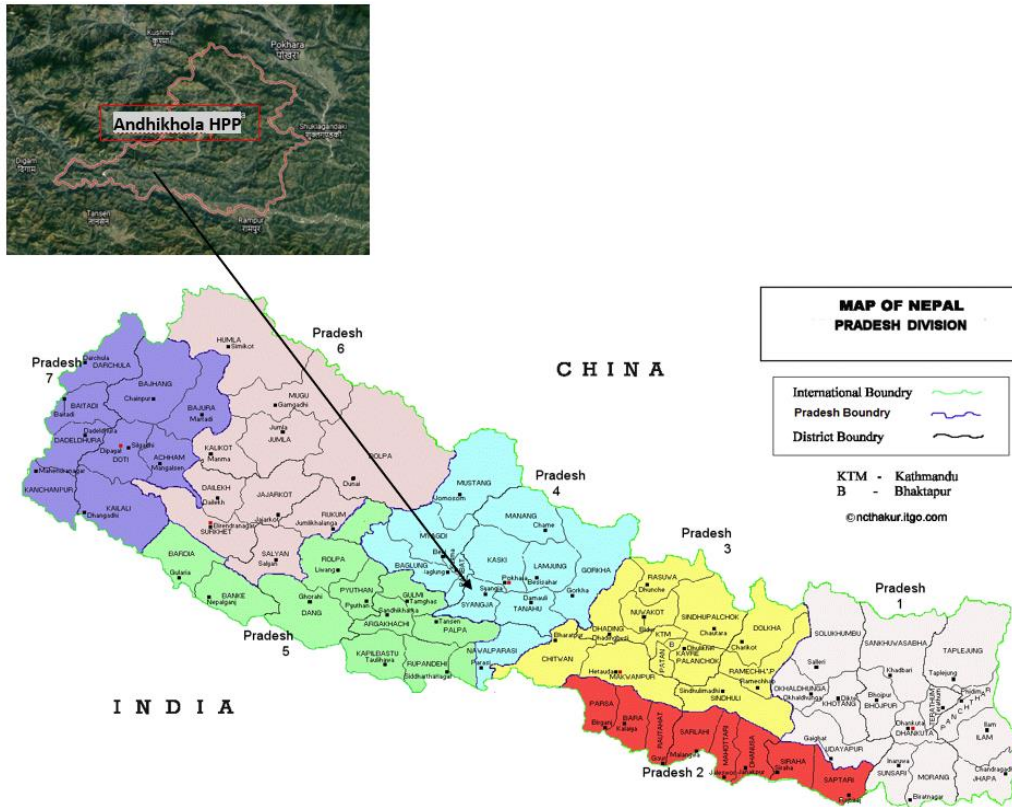
Figure 4-1: AKHP location map
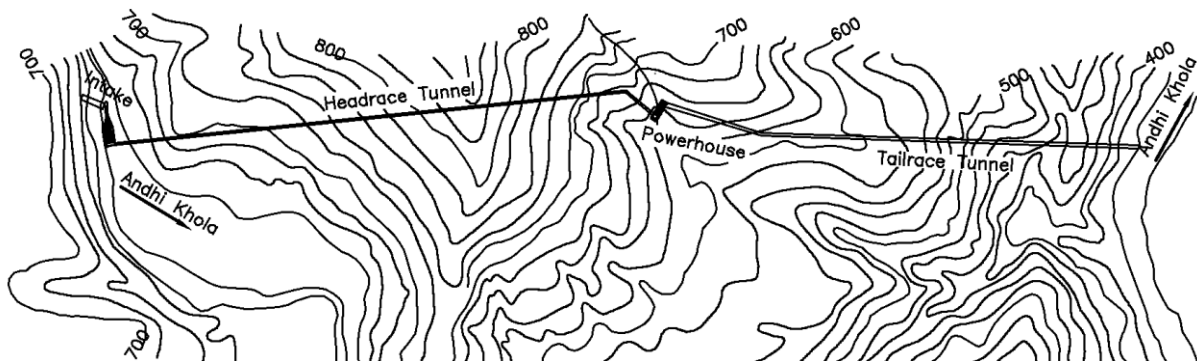
Figure 4-2: General layout of the AKHP
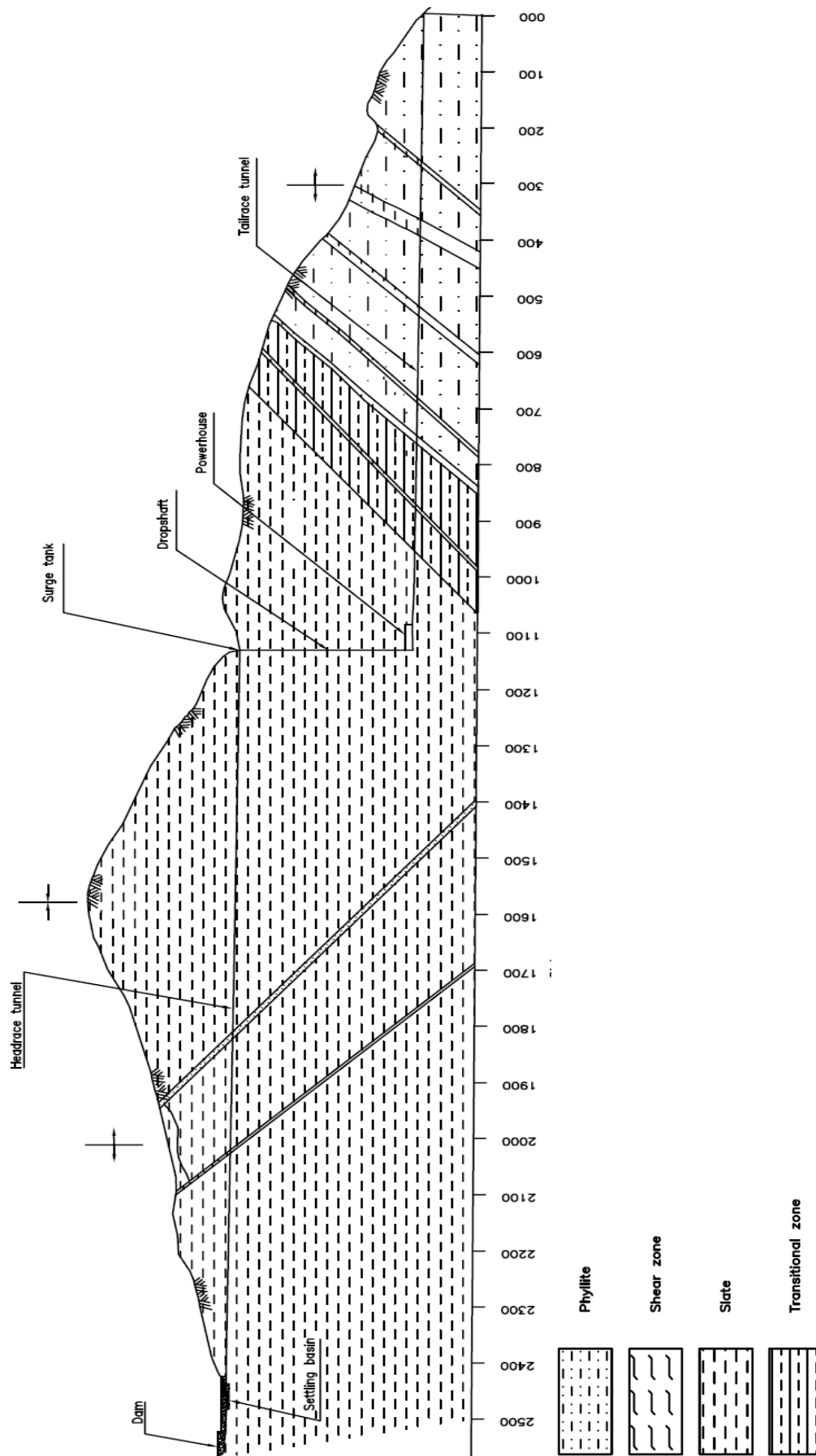
Figure 4-3: Geological longitudinal profile of the AKHP project

4.3   Regional Geology

4.3.1   Engineering Geology of the project area

The project area lies in Kali Gandaki Supergroup, Lower Kali Gandaki Group of the Lesser Himalaya. The rocks of the project area belong to Andhi formation, which is predominantly argillaceous formation, which is distributed along the Kali Gandaki and Andhikhola. The Formation is monotonous and consists of thick sequences of phyllitic slates with occasional interbeds of thin, calcareous siltstone. The Slate is dark bluish grey to black and yellow when weathered. Frequent inter layering of black laminae is the notable features of the formation. The foliation structure in the area having a steep south dipping nature. No major faults were observed within the project area.

4.3.2   Engineering Geological Condition at Project Site

Black laminated slate and phyllites are the pre-dominant rock type in the project area. The slate is often intercalated with phyllite and together form unstable substrates. In the project area, intense fracturing and jointing is common making the rocks to be very friable and easily weathered. No major faults were observed within the project area during the field investigation.
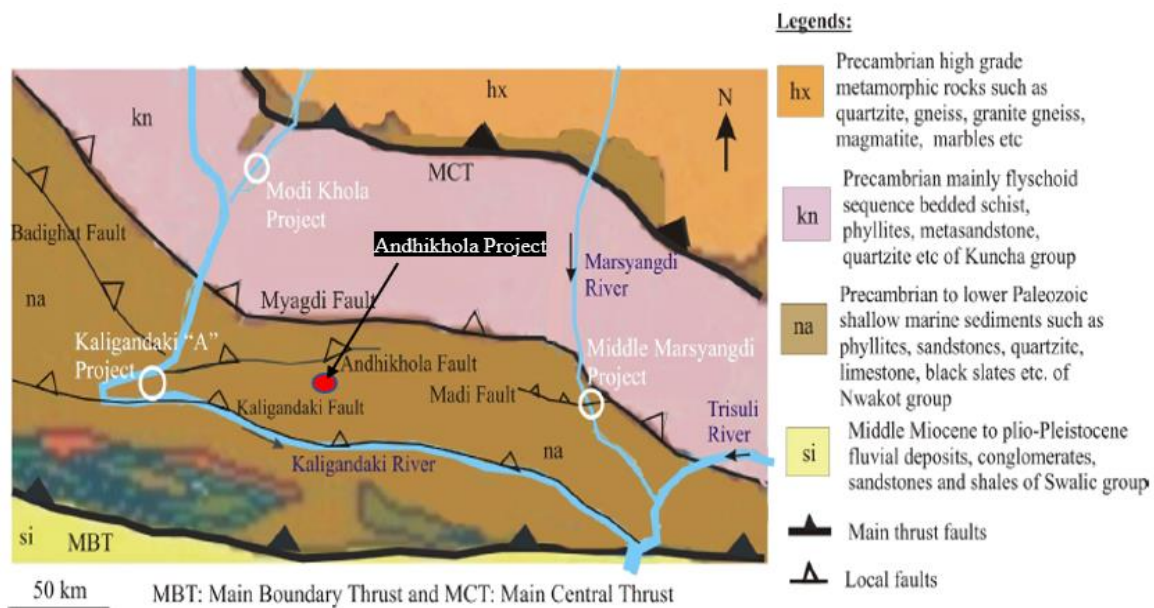
Figure 4-4: Regional Geology of the project area (Modified after Panthi (2006))

Headrace tunnel and shaft

The rock mass in the headrace tunnel and shaft area are slightly to moderately weathered, closely foliated, jointed (three prominent joint sets), fractured, laminated black slates. The joints are generally open. There had been no any modification or construction work along HRT during the upgrading of the project.

Powerhouse cavern

Fresh to moderately weathered, weak, closely spaced slate with quartz vein in upper part. Some shear zones are found in the bottom of right wall. Ground water condition is dry.

Figure 4-5: Powerhouse cavern after first step of excavation

The rock mass quality assessment of the powerhouse cavern rock mass as per the AKHP Upgrading, Project completion report is presented below in Table 4-1.

Table 4-1: Rock mass quality assessment of powerhouse cavern using RMR system

Parameter	Ranges of Value	Remarks
Uniaxial Compressive Strength (UCS)	2	Low range (5-25 Mpa)
RQD	3	< 25%, Poor
Spacing of discontinuities	5	< 60mm
Condition of discontinuities	20	Slightly rough surfaces, Separation < 1mm, Highly weathered walls
Ground water condition (dry)	15	Completely dry
Orientation of discontinuities	-5	Fair
RMR = 40		

Tailrace tunnel

Black slates, phyllitic slate and occasionally intercalation of thin quartzite is typical lithology of the tailrace tunnel area. Rock mass present are highly fractured, moderate to highly weathered and highly crushed at several tunnel sections. The Figure 4-6 shows the geological longitudinal profile of the tailrace tunnel. The rock mass classification of the squeezed section of the tailrace section using Q system is presented in Table 4-2.
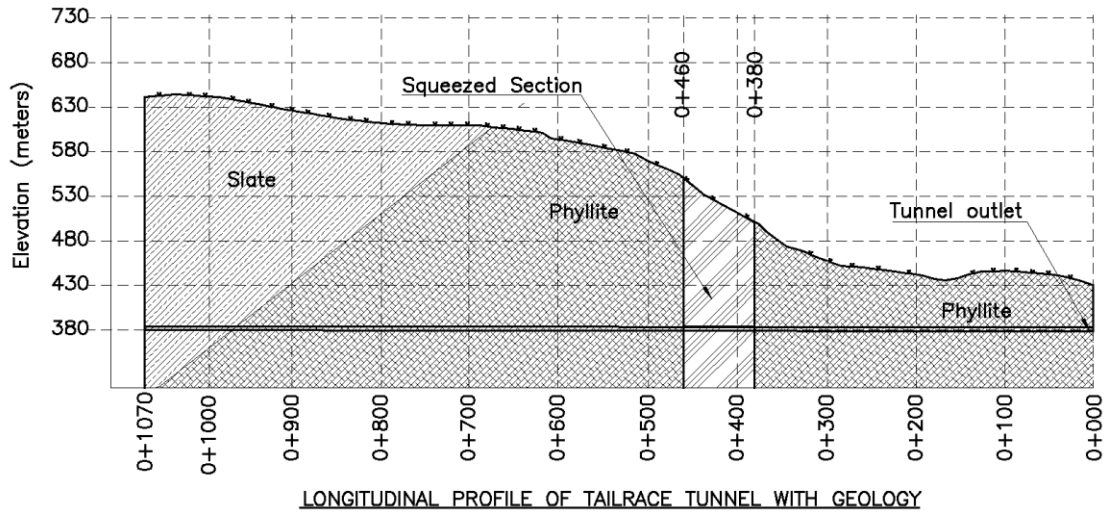
Figure 4-6: Longitudinal profile of tailrace tunnel of Andhikhola Hydropower Project

Table 4-2: Rock mass classification of squeezed section using Q system (AKHP Project completion report,2015)

Parameters	Ranges of Value
Rock Quality Designation (RQD)	10
Joint Set Number (Jn)	15
Joint Roughness Number (Jr)	1.5
Joint Alteration Number (Ja)	4
Joint Water Condition (Jw)	1
Stress Reduction Factor (SRF)	10
Rock mass quality = Q =	0.04

5 Inspection and Data Synthetization

5.1 Inspection Overview

The upgrading of Andhikhola Hydropower Project (AKHP) demanded the longitudinal enlargement of powerhouse cavern and cross-sectional enlargement of tailrace tunnel. In case of powerhouse cavern, minor squeezing phenomena was noticed on the side wall. However, during the excavation of existing tailrace tunnel base, the support provided initially was not sufficient which caused squeezing in various section of the tunnel. The most critical section was from chainage 0+390 to 0+410. Later the support condition was revised, new support design was updated for the squeezed section of tailrace tunnel. The deformed tailrace tunnel was re-excavated to its required size using temporary supports.

5.1.1 Overall condition

5.1.1.1 Powerhouse Cavern

Dimension of existing powerhouse cavern of AKHP was 37m long, 6.6m wide and 11m high semicircular. During the upgrading, the existing powerhouse cavern was extended about 8m in length with same width and height to accommodate the new electromechanical components. The powerhouse cavern is located approximately 240m vertically down from the surface and is accessible through a 4m diameter drop shaft accommodated with a crane. During inspection, the stability condition of powerhouse cavern before extension or upgrading work are presented below:

- Existing power cavern was found stable and not any remarkable instability features were observed. However, big cavities exist at the crown near drop shaft indicates the huge over break which was probably formed during excavation.
- Towards the downstream end, drainage system was found to handle the seepage water. It indicates that there would be ground water ingression problem at this stretch.
- Schmidt Hammer Rebound test carried on shotcrete face on cavern walls shows the equivalent compressive strength varying in between 12.25 Mpa to 33.35 Mpa.

Figure 5-1: AKHP Powerhouse cavern before upgrading

Existing rock support and in situ geology in the powerhouse cavern

- Rock bolts installed are of 20 mm dia. with base plate (15 cm *15 cm) and nut bolts (40 mm). Spacing of those bolts is varying in different part of the cavern from 0.7 to 1.5 m. whereas the length of bolt is unknown.

- Sprayed shotcrete on walls are plain as well as steel fiber reinforced.

- At both walls of cavern, thickness of shotcrete measured in test holes show the installation of two layers of liners.
    - Inner liners: 7-10cm thick plain shotcrete with combination of wire mesh.
    - Outer liner: 2-5cm thick of steel fiber shotcrete.

- Rock exposed in test holes 1 and 3 resembles fragile and poor quality. In situ rocks are laminated, weathered black to grey slate. Some bands of slate contain quartz veins and schist.

5.1.1.2 Tailrace Tunnel

The typical dimensioning of the tailrace tunnel before the upgrading was inverted D, modified horseshoe shaped with 2.5m finished height and 1.8m wide. Upgrading of AKHP demanded

lowering the invert of existing tailrace tunnel to pass the increased design discharge. This was done by keeping the existing rock support intact at the place and excavating the floor. The excavation depth for the first 400m from the powerhouse is 1.8m and 2.2m for the remaining length. The tailrace tunnel was in stable condition since almost 30 years before the upgrading construction.

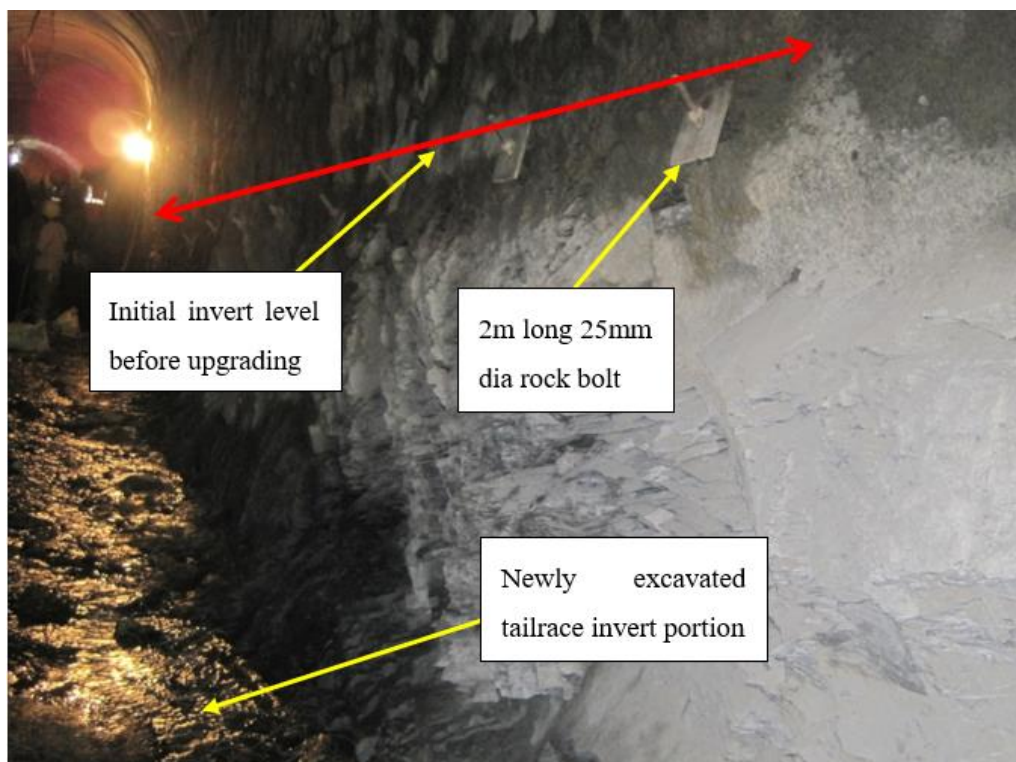Figure 5-2: Existing tailrace tunnel before the enlargement

Figure 5-3: Tailrace tunnel during upgrading work

The dimension of new tailrace tunnel after excavation is 4.2m height and 2.1m width. As per Q-system, for Span or Height to ESR ratio of 2.6 and Q value of 0.04 , the rock support required is Rock bolt at 1.2m spacing and Shotcrete of 12cm thickness. The rock support provided in the newly excavated portion was 15cm thick steel fibre shotcrete along with rock bolts installed at 1m spacing which was in line as required by Q-system. However, the installed rock support was found to be inadequate and squeezing occurred.

5.1.2 Rock support registration

5.1.2.1 Rock support registration of Powerhouse cavern

As per the as built drawing, the proposed rock support in the excavated powerhouse cavern is presented in the Table 5-1.

Table 5-1: Rock support in the existing powerhouse cavern before upgrading

Area	Rock Bolt (20 mm dia.)	Shotcrete
Crown	4 m long @ c/c 1 m alternately	2 layers of 75 mm thick of steel fiber reinforced (sfr)
Wall	3m long @ c/c 1.5 m alternately	1 layer of 75 mm thick sfr
Floor	2 m long dowel @ c/c 2 m alternately	
End wall	3 m long @ c/c 1.5 m alternately 3m long @ c/c 1 m around tailrace opening	1 layer of 75 mm sfr

5.1.2.2 Rock support registration of Tailrace Tunnel

As per the AKHP project completion report, the support in the existing tailrace tunnel before cross section enlargement before the upgrading is presented in Table 5-2.

Table 5-2: Rock support proposed in the construction drawing of the existing tailrace tunnel before upgrading

Area	Rock Support type
Crown	- Precast concrete arch 75mm thick and stone masonry - Dry stone packing (in overbreak sections) 20mm diameter, 1.5m long rock bolt (varies along the tailrace tunnel)
Wall	0.35 m thick stone masonry (varies along the tailrace tunnel section)
Floor	10 cm thick structural concrete lining

Rock support design during tailrace tunnel enlargement:

Before carrying out the tunnel enlargement, the existing tunnel wall was supported by providing 2m long, 25mm diameter rock bolts inclined at two corners of existing invert as shown in Figure 5-4. Then enlargement of the tunnel cross-section was done by excavating the bottom slab and benching up to 2 m below the existing tunnel invert level. In the new excavated enlarged portion of tailrace tunnel, 15cm thick steel fiber shotcrete was applied on the wall and 0.2m thick concrete lining at invert was provided as permanent rock support.
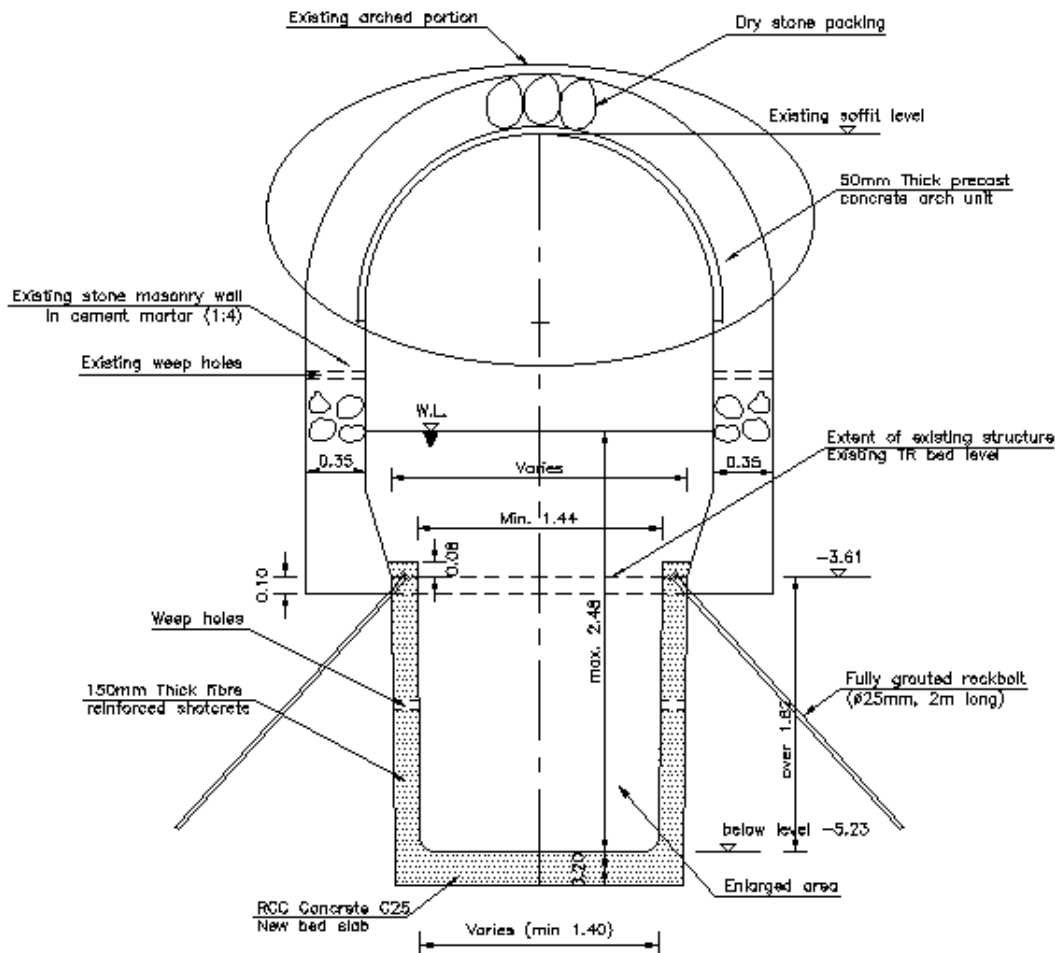
Figure 5-4: Typical tailrace tunnel support provision during tunnel enlargement

5.1.3   Deformation condition

Powerhouse cavern

Due to the extension of powerhouse cavern and blasting activity during the excavation, there was minor squeezing of 0.75% to 1.4% on the wall of the existing powerhouse cavern. This was identified when the EOT crane could not be moved on old rail-track. The rail-track was shifted outwards by 50-100mm. There was not any accurate measurement of powerhouse deformation.

Tailrace Tunnel

Squeezing was observed in tailrace tunnel from chainage 0+380 m to 0+460 m from the outlet portal as shown in Figure 5-5. However, the most critical squeezed sections were from chainage 0+390 to 0+410.

Figure 5-5: Squeezed tailrace tunnel section along chainage 390-410m dated 22nd July 2013
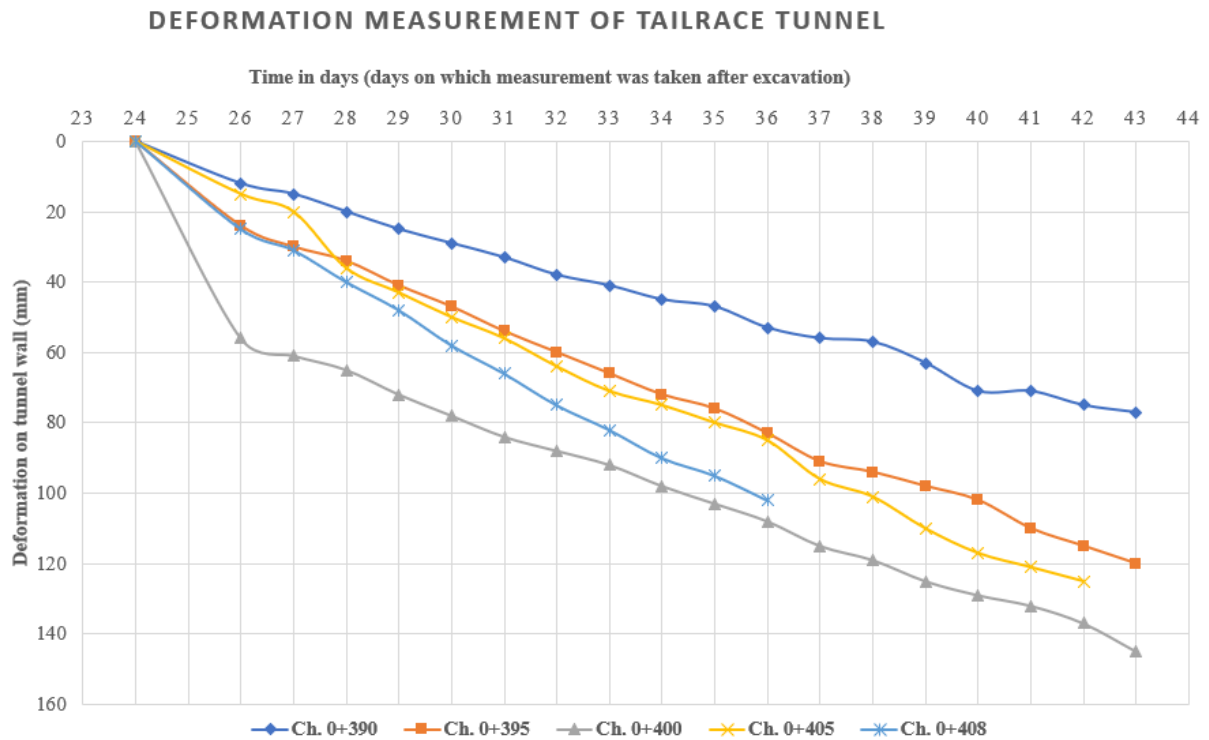
Figure 5-6: Time Vs Deformation measurement of the squeezed section for various chainage

5.2 Support in the squeezed section of Tailrace tunnel

The initial provided rock support in the enlarged section of the tailrace tunnel were found to be inadequate and caused squeezing. Later, support was revised and new support system in two stages were provided which are discussed below.

5.2.1 Temporary Support

The squeezed tunnel section was in use for mucking and other construction activities. Because of the risk of collapse, the permanent support was to be applied by excavating a short section and concreting it immediately. Since it would take longer time to install, it was agreed to use a temporary steel support option which will take a short time to install and would not disturb the construction work for a long time. Thus initially, temporary support was applied that consists Reinforced Shotcrete Rib (RSR) which is to be a part of permanent support in future. The RSR has been applied throughout the tunnel perimeter including invert as shown in Figure 5-8. It consists of 4 number of 16 mm diameter rebars. The RSRs are held together by using steel channel (ISMC 75*150) at 1m above the invert levels.

5.2.2 Permanent support

Before application of the final rock support, the critical squeezed section from Chainage 0+390 m to 0+410 m were re-excavated as per the hydraulic requirement for the upgraded discharge section shown in Figure 5-7. Finally, the structural concrete lining of C25 grade with 250mm thickness and the reinforcement of Fe500 with 16mm diameter bar at 150mm center to center spacing has been provided in the invert. At the existing crown for the chainage 0+390m to 0+400m, the shotcrete rib of 200mm thickness and 250mm width with four numbers of 16mm diameter bars has been provided at every 2m along the longitudinal direction. Also, the rock bolts of 25mm diameter and 2m in length were also provided which are two in number for each wall.
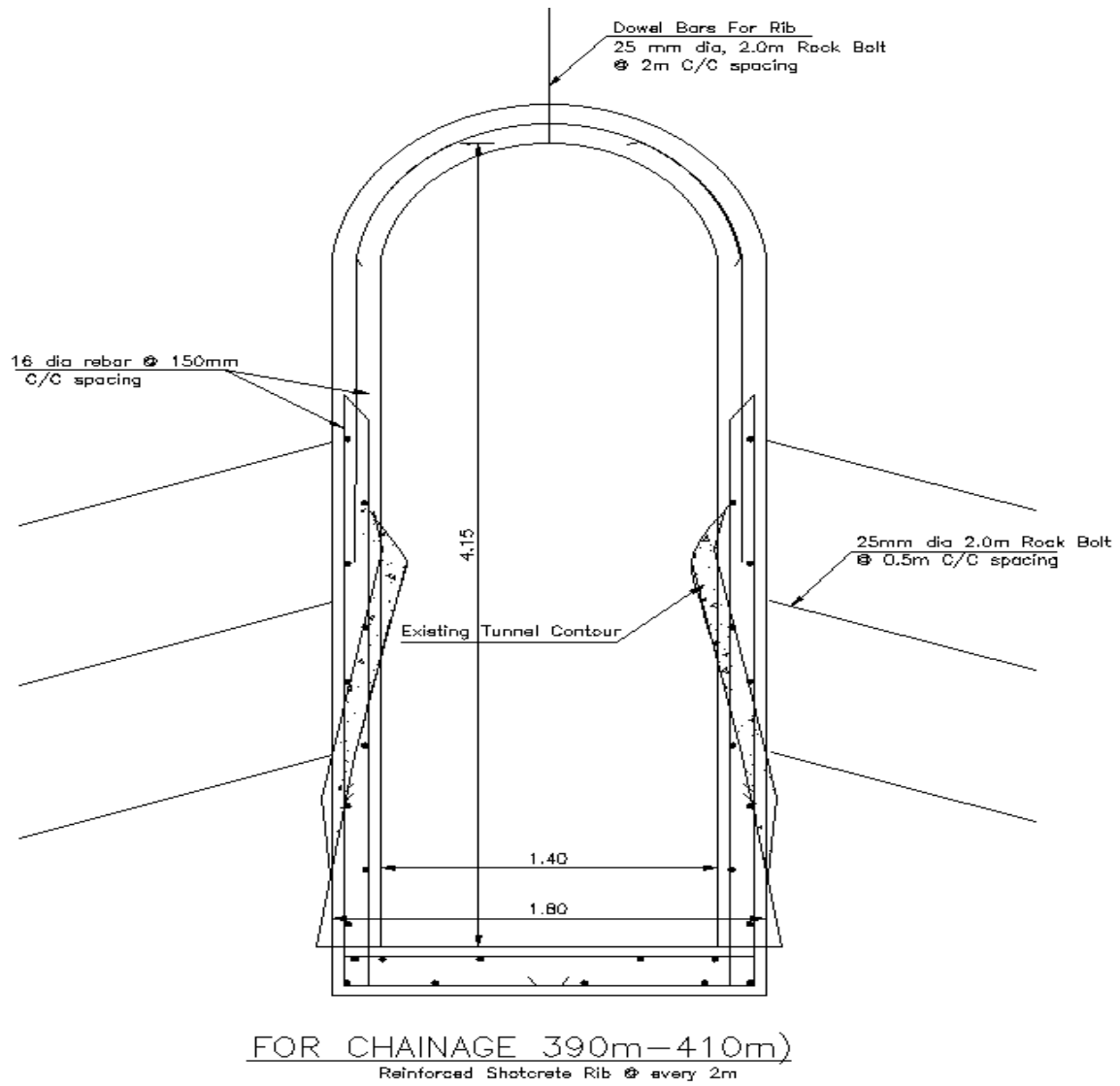
Figure 5-7: Final rock support at the squeezed section
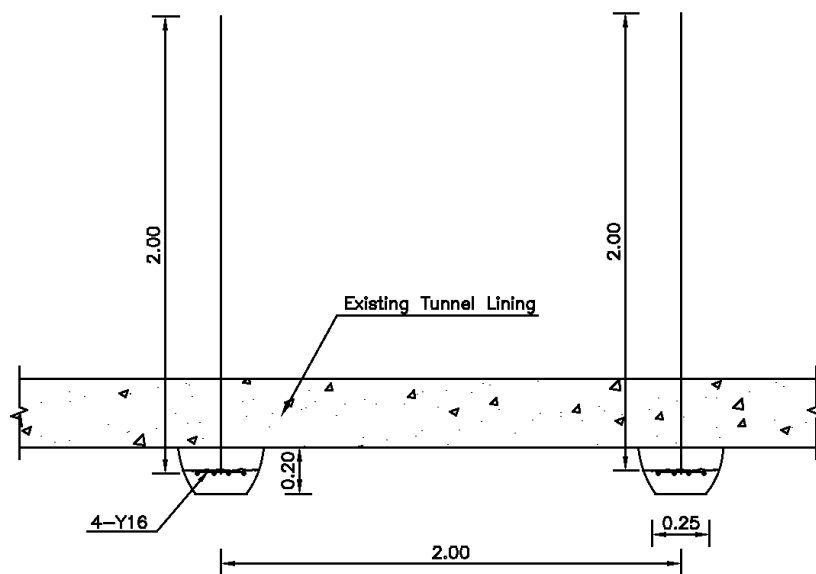
Figure 5-8: Typical Detail of Shotcrete Rib at the crown

5.3   Support in deformed powerhouse cavern

The deformation noticed on the walls of powerhouse cavern after the 8 m longitudinal extension was 5 to 10 cm which is about 0.75% to 1.4% strain. Thus, it falls under minor squeezing problem (Hoek and Marinos, 2000) and are generally dealt with by rock bolts and shotcrete; sometimes with light steel sets or lattice girders for additional factor of safety.

The support in the newly excavated powerhouse cavern as per as built drawing are:

Temporary support:

Perimeter grouting was carried out as per real ground mass condition during excavation. 4 m long spiling bolt at spacing of 25 cm to 30 cm above the existing crane beam level with minimum overlapping of 1.5m. 5 cm thick fiber reinforced shotcrete with pattern rock bolting at 1.5 m spacing alternatively.

Permanent Support

Steel Ribs of ISMB 150 are placed at interval of 1.5m c/c along the cavern axis and 15 cm thick fiber reinforced shotcrete.

6 Review on Plastic deformation

6.1 General

Plastic deformation, also known as squeezing in case of weak rocks, is the response of rock mass to the induced stresses. It is comprised of instantaneous deformation and time dependent deformation (Barla et al., 2010). Plastic deformation in the tunnel periphery starts before and immediately after the excavation and continues even after the rock support has been applied. The 'rock support interaction analysis' (Carranza-Torres and Fairhurst, 2000) assumes that the time-independent maximum deformation takes place when the tunnel face effect has ceased. However, time-dependent deformation will continue for long time even after the excavation elapses. Total plastic deformation in underground excavations, passing through weak and schistose rock mass exhibit both time-independent (instantaneous) and time-dependent deformations(Shrestha and Panthi, 2014a). For a long-term stability of the tunnel, support design should be made by considering both time independent and time dependent deformation. Panthi (2006) exemplified the phenomenon of plastic deformation process, as when the induced tangential stresses exceeds the strength of weak and deformable rocks, micro-cracks are gradually formed along the foliation plane or schistosity which results in the development of visco-plastic zone along the periphery of tunnel opening as shown in Figure 6-1. This plastic zone finally results in convergence of rock material towards the center of the tunnel opening.
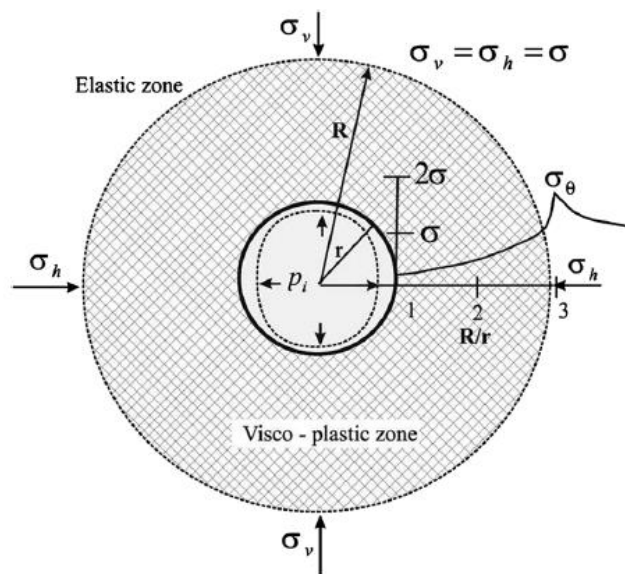
Figure 6-1: Illustration of plastic deformation in tunnel (Panthi, 2006)

The illustration of longitudinal deformation profile of tunnel at various stages is shown in Figure 6-2. As a tunnel is excavated, it will have displacement of value Ue at the tunnel face. By the time applied rock support comes in effect, an additional displacement Us will occur.

Under such conditions, tunnels will exhibit a deformation profile like curve ABC. If the tunnel is unsupported, it will have a displacement of Uf represented by curve ABD. Weak and deformable rock mass under stress also exhibits time-dependent behavior of deformation. Deformation of tunnel contour without support will have a profile like the curve ABE. But when the tunnel is supported, the time dependent behavior will be additional displacement U't represented by curve ABE'.
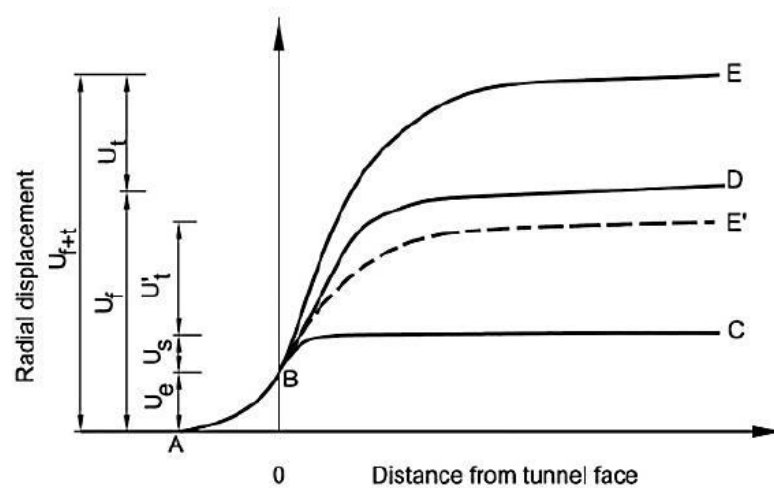
Figure 6-2: Idealized tunnel longitudinal deformation profiles (Shrestha, 2014)

Underground opening is mainly an interaction of rock mass properties, induced stresses and stiffness of the applied support. (Hoek and Brown, 1980). Underground excavation disturbs the in-situ stresses and equilibrium conditions prevailing in the rock mass before excavation. This stress changes require displacements to occur and the excavated ground tries to converge toward the opening. Such phenomena is mainly noticed in rock mass of weak and schistose character, highly deformable with low strength (Panthi, 2006).

6.1.1 Instantaneous deformation

In a rock mass when excavation is made, the existing nature of in-situ stress is disturbed and re-distributed around the opening periphery. Depending upon the magnitude and direction of principal stresses and geometry of the opening, the new induced stresses are set up around opening periphery in the form of tangential and radial stresses. Once the magnitude of these induced stresses exceeds the rock mass strength, the yielding of rock mass occurs resulting in displacement around the excavation contour. This is called as Instantaneous deformation. Thus, it is a kind of stress failure condition caused by overstressing.

6.1.2 Time dependent deformation

Time-dependent deformation (squeezing) as defined by ISRM is related to creep caused by exceeding a limiting shear stress (Shrestha, 2006). Materials that may not show much deformation right after the excavation could during constant stress over a long-time experience increasing strain (deformation) which ultimately can lead to failure. This is called creep and may continue for a long time before the material completely fails. Creep is important at low pressures only in a few rock types: shale, soft chalks and evaporite rocks (e.g. rock salts, gypsum and anhydrites) (Shrestha, 2006).

Creep in rock mass can be categorized into three stages: primary creep, secondary creep and tertiary creep (Goodman, 1989). First the material immediately responds to the applied load by initiation of crack propagation, causing elastic strain (early primary stage). As the rock "adjusts" to the stress, the crack propagation slows down, and the strain rate decelerates. Entering the secondary stage, the crack propagation reaches a stable almost constant rate during which the material slowly continues deforming. Tertiary stage initiates when the strain rate starts accelerating, and uncontrolled crack propagation continues until failure. Tertiary stage may be avoided with adequate support.
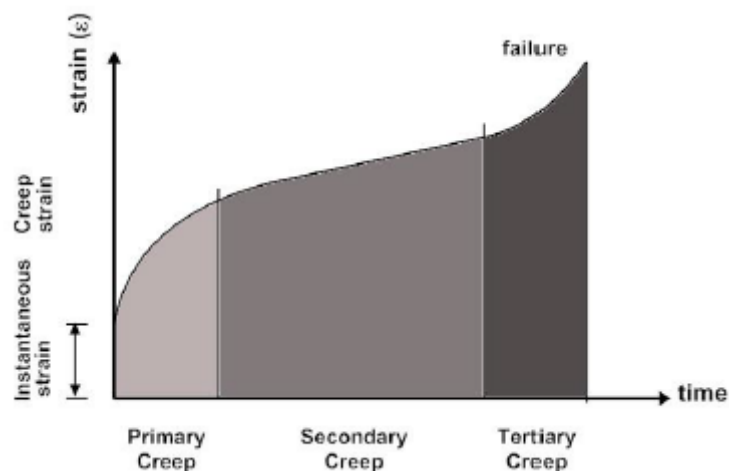
Figure 6-3: Idealized creep curve (Goodman, 1989)

Panthi and Shrestha (2018) have assessed the long-term plastic deformation records of three hydropower tunnel projects from Nepal Himalaya and found the relation between the time independent and time dependent deformation using convergence law proposed by (Sulem et al., 1987).The long-term plastic deformation records of 24 tunnel sections representing four different rock types of three different headrace tunnel cases from Nepal Himalaya are used for the analysis. Panthi and Shrestha (2018) have established a link between tunnel strain (for both instantaneous and total tunnel strain), vertical gravitational stress (σv), horizontal to vertical stress ratio (k),

support pressure (pi) and rock mass deformability properties expressed by shear modulus (G). The instantaneous closure and final closure values are indirectly proportional to the rock mass shear modulus and support pressure values and directly proportional to the in-situ stress conditions.
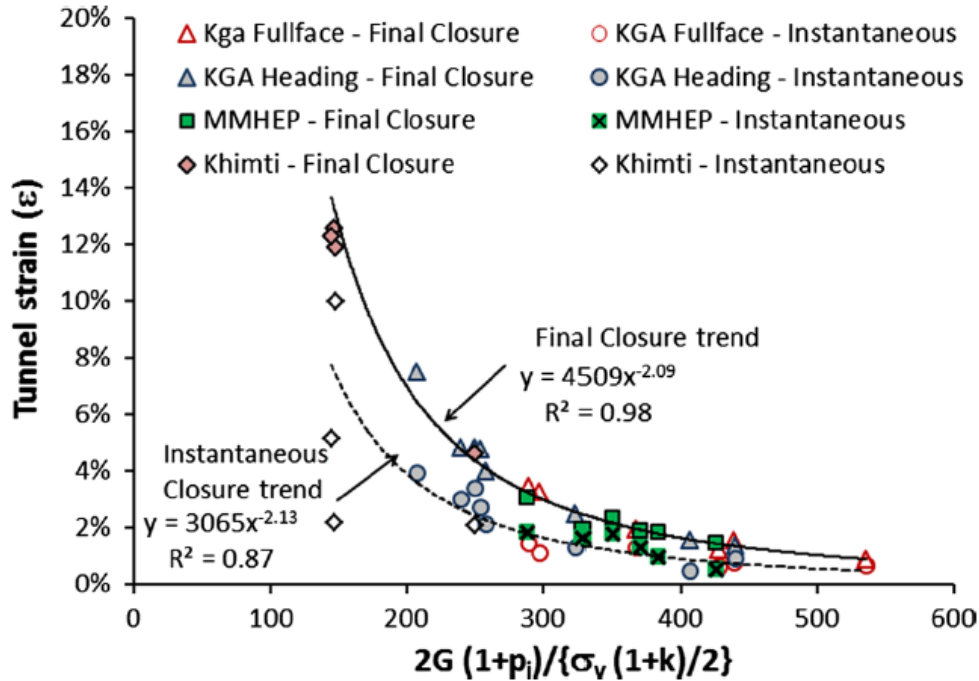
Figure 6-4: Correlation of instantaneous and final closure with rock mass property, support pressure and in situ stress (Shrestha, 2014)

Using the trendline as presented in Figure 6-4, the relationships for instantaneous and final strain are presented as equation 6-1and 6-2.

$$\varepsilon_{IC} = 3065 \left(\frac{\sigma v * (1 + k)/2}{2G(1 + pi)} \right)^{2.13} \qquad \text{6-1}$$

$$\varepsilon_{FC} = 4509 \left(\frac{\sigma v * (1 + k)/2}{2G(1 + pi)} \right)^{2.09} \qquad \text{6-2}$$

Where, ε_{IC} = instantaneous strain, ε_{FC} = final deformation, G= Shear modulus, pi=support pressure, k = stress ratio

6.2 Factors influencing squeezing phenomena

Squeezing condition in rock mass conditions are influenced by several factors to different degrees. Many authors have analyzed case studies to identify the influencing factors, and have each presented their results differently (Panthi (2006) ; Shrestha and Panthi (2014b); Kovári and Staus (1996); Aydan et al. (1996, 1993)). Shrestha (2006) gave the following summary of the factors influencing the occurrence and degree of squeezing:

- Stress conditions

- Strength and deformability of the rock mass

- Rock type

- Orientation of the geological structures

- Water pressure and porosity of the rock mass

- Construction procedures and support systems

The occurrence and degree of squeezing highly depend on the ratio between rock mass strength and in-situ stress. This means that for weak or strongly foliated (crushed) rocks, squeezing may occur even at low overburdens (low in-situ stress). At which ratio squeezing will occur is not defined, but a study on squeezing in tunnels in Japan showed that a ratio less than 2 resulted in squeezing (Aydan et al., 1996). According to Chapman et al. (2010)severe squeezing may occur when the uniaxial compressive strength (intact rock strength) of the rock is less than 30% of the in-situ stress. The degree of squeezing depends on the rocks ability to deform; high deformability causes large deformation. Large long-term deformations or large long-term rock pressures is only possible in weak and deformable rocks (Shrestha, 2006).

Squeezing is typically seen in weak rocks like phyllite, shale, schist, claystone, mudstone, serpentine, flysh and weathered clayey and micaceous metamorphic rocks (Shrestha, 2006).. According to Panthi (2013)the high degree of schistosity (extent of thin foliation) in a rock is the dominating characteristic that leads to the formation of the visco-plastic zone around the opening. Accordingly, highly sheared material and fault gauge is especially prone to squeezing. Highly tectonized rocks lack sufficient bonding or confinement which results in a considerably reduced self-supporting capacity (Panthi, 2006).

The orientation of the rock foliation relative to the structure is critical for the degree of squeezing. As for all instability issues in tunneling, rock structures (e.g. foliation, fracture sets, fault zone) parallel to the tunnel alignment is the least preferable. According to Steiner (2000) substantially higher convergences, up to one order of magnitude greater, is observed where the foliation strikes parallel rather than perpendicular to the tunnel. For parallel structures also the dip relative to the opening is important. Overbreak due to buckling of schistose layers mainly occurs where the schistocity is parallel to the tunnel perimeter (Shrestha, 2006).

6.3 Methods in accessing plastic deformation

Many researchers have developed various methods that can be used in prediction and assessment of tunnel deformation under stress conditions in underground openings. The available methods include:

Empirical methods (Singh et al., 1992), Q-system (Grimstad and Barton, 1993), (Goel et al., 1995), semi-analytical methods such as (Hoek and Marinos, 2000) and analytical methods such as convergence confinement methods (Carranza-Torres and Fairhurst, 2000), probabilistic approach of uncertainty analysis (Panthi, 2006, Panthi and Nilsen, 2007) and numerical methods such as 2-Dimensional elasto-plastic finite element program, RS2 are used for the squeezing analysis. However, a common limitation in empirical, semi-analytical and analytical solution is that stress anisotropy in non-cylindrical tunnel has not been incorporated in the analysis. The selected methods are presented further in this chapter.

6.3.1 Empirical Method

Based on experience and comparison of cases of numerous underground structures, the authors have developed several empirical relationships for predicting plastic deformation. These methods are generally based on experience and comparison of various cases. Depending on the indicators used, the approaches can be grouped in the following three categories:

➢ Strength-stress ratio approach
➢ Strain estimation approach
➢ Rock mass classification approach

Strength-stress ratio approach:

As per (Wood, 1972) , when Competence Factor 'Fc' is less than 2, the ground will be over-stressed immediately and can result into potential squeezing problem. The Fc is ratio of unconfined compressive strength of rock mass (σ_{cm}) to overburden stress.

$$\text{For squeezing condition, } \boldsymbol{F_c} = \frac{\sigma_{cm}}{\gamma H} < \boldsymbol{2} \qquad \text{6-3}$$

Where γ is unit weight of rock mass and H is depth of overburden.

Strain estimation approach:

Tangential strain can be used as parameter to access the degree of squeezing of rock (Saari, 1982). For tunnels constructed in Taiwan, (Chern et al., 1998) showed that problems with tunnel stability occurred when the 'strain' exceeds about 1%. The data plotted is the basis for his conclusion (Figure 6-5).
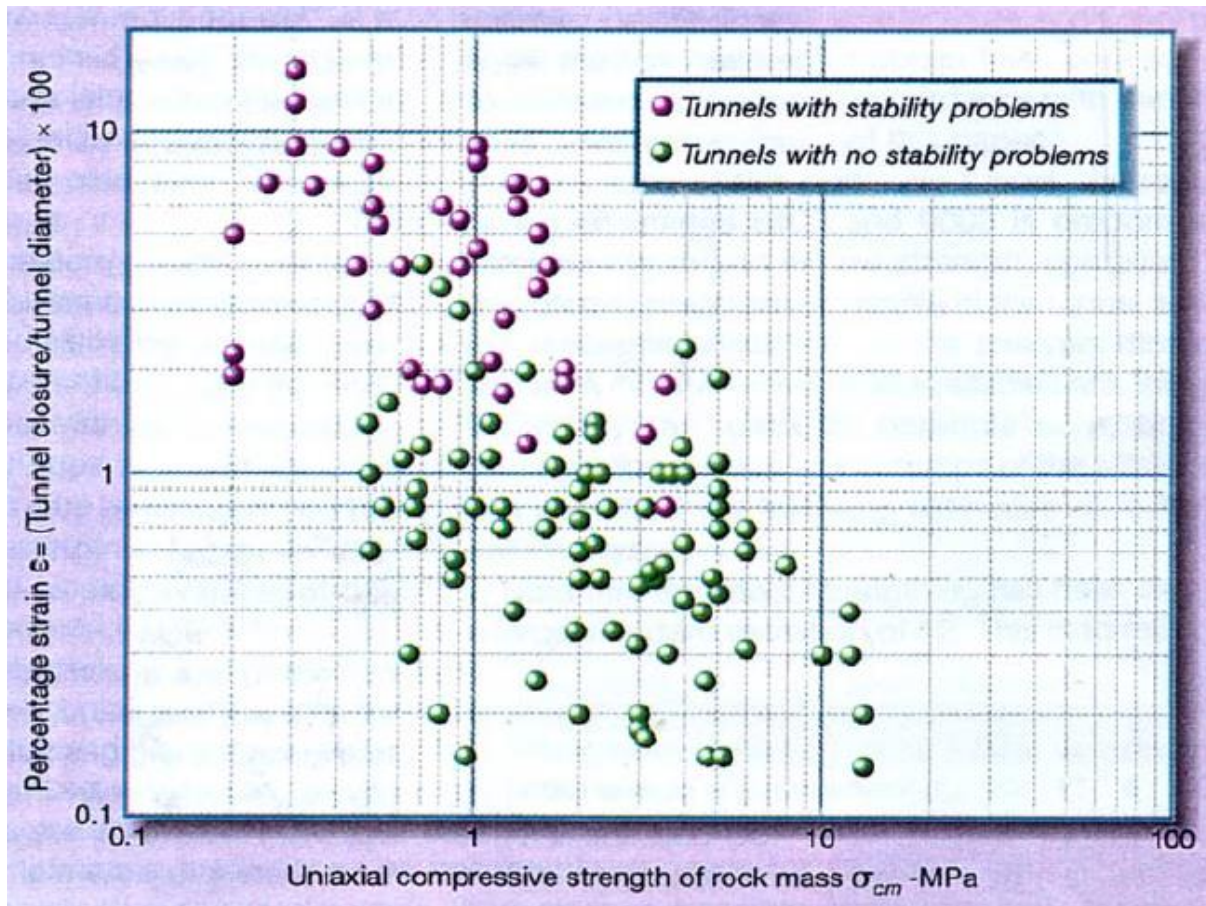
Figure 6-5: Percentage strain for different rock mass strengths. (Chern et al., 1998)

Rock mass classification approach

6.3.1.1   Singh et al approach

Singh et al. (1992) has developed an empirical relationship between overburden depth (H) and logarithm mean of rock mass quality Q, based on plot generated using 41 tunnel section data. Out of 41 data, 17 tunnel sections data were taken from case histories in (Barton et al., 1974) and 24 tunnel sections data from Himalayan region. A demarcation line has been given to differentiate between non-squeezing and squeezing condition is shown in Figure 6-6. The equation of the line is given as:

$$H = 350Q^{1/3}$$
<div align="right">6-4</div>

As presented in Figure 6-6 , the squeezing phenomena may occur in the rock mass when overburden depth of tunnel exceeds $350Q^{1/3}$. This criterion being simple and easy to use, the difficulty lies in selection of SRF value which is very sensitive for correct estimation of Q-value.

Figure 6-6: Singh et al. (1992) approach to predict squeezing condition

6.3.1.2 Q-system

The Q-system for rock mass classification was developed at Norwegian Geotechnical Institute (NGI) by (Barton et al., 1974). Later , Grimstad and Barton (1993) updated it by including more than 1000 cases. This system is based on numerical assessment of rock mass quality and estimates the required tunnel support using the following six parameters:

➢ Rock quality designation (RQD)

➢ Number of joint sets (Jn)

➢ Roughness of the most unfavorable joint or discontinuity (Jr)

➢ Degree of alteration or filling along the weakest joint (Ja)

➢ Water inflow (Jw)

➢ Stress condition given as the stress reduction factor (SRF)

Based on the six parameters, the overall rock mass quality(Q-value) is calculated as follows:

$$Q = \frac{RQD}{Jn} \times \frac{Jr}{Ja} \times \frac{Jw}{SRF} \qquad \text{6-5}$$

Detail description of estimation of these six parameters are shown in Appendix A.

The last term in Eq 6-5 i.e Jw/SRF named as "Active stress" incorporates the effect of water, faulting, strength /stress ratio, squeezing or swelling (Barton, 2002). The Q-system has briefly addressed squeezing condition based on the values of $\sigma_{\theta max}/\sigma_{cm}$ ratio and assigning the value of SRF as presented in Table 6-1 ($\sigma_{\theta max}$ and σ_{cm} are maximum tangential stress and rock mass strength respectively):

Table 6-1: Squeezing condition according to Q-system (Barton, 2002).

Squeezing rock: plastic flow of incompetent rock under the influence of high rock pressure	$\sigma_{\theta max}/\sigma_{cm}$	SRF
Mild squeezing rock pressure	1-5	5-10
Heavy squeezing rock pressure	>5	10-20

The tangential stress can be estimated using Krich Equation and whereas the rock mass strength is difficult to quantify. As per NGI (1997) " Squeezing of rock mass occur if overburden depth H> 350 $Q^{1/3}$ (Singh et al., 1992), where rock mass strength (σ_{cm}) $= 0.7 \, \gamma \, Q^{1/3}$ (Mpa) where γ is rock density in kN/m^3. However according to (Shrestha, 2006) these method lead to the loop dependency among the parameters. Since to calculate σ_{cm} , Q value has be known which depends on SRF and to estimate SRF, it should be known whether there is the case of squeezing or not. Thus, to overcome this loop dependency, other various empirical methods can be used as section 6.3.2.

6.3.2   Semi-Analytical Method

Some of the semi-analytical methods have been proposed for estimation of the deformation caused by squeezing and also the support requirement during squeezing of tunnel. Some of these methods are (Kovári, 1998), (Aydan et al., 1993), (Hoek and Marinos, 2000), etc. In the chapter, the (Hoek and Marinos, 2000) approach is described and used for analysis in the thesis.

6.3.2.1   Hoek and Marinos Approach

According to Hoek and Marinos (2000), the ratio of uniaxial compressive strength of rock mass (σ_{cm}) and in-situ stress (p_o) can be used to predict potential squeezing problem in a circular tunnel. The authors followed (Sakurai, 1984) approach to find the relationship between σ_{cm}/ p_o and the percentage strain (ε) of the tunnel. The result of this study is based on closed form analytical solutions of a circular tunnel in a hydrostatic stress field, published by (FAMA, 1993), (Carranza-Torres and Fairhurst, 1999). Hoek and Marinos (2000) used Monte Carlo simulation to determine strain in the tunnels for a wide range of tunnel conditions and found a

clearly defined pattern of tunnel convergence which could be predicted by equation shown in Figure 6-7 .
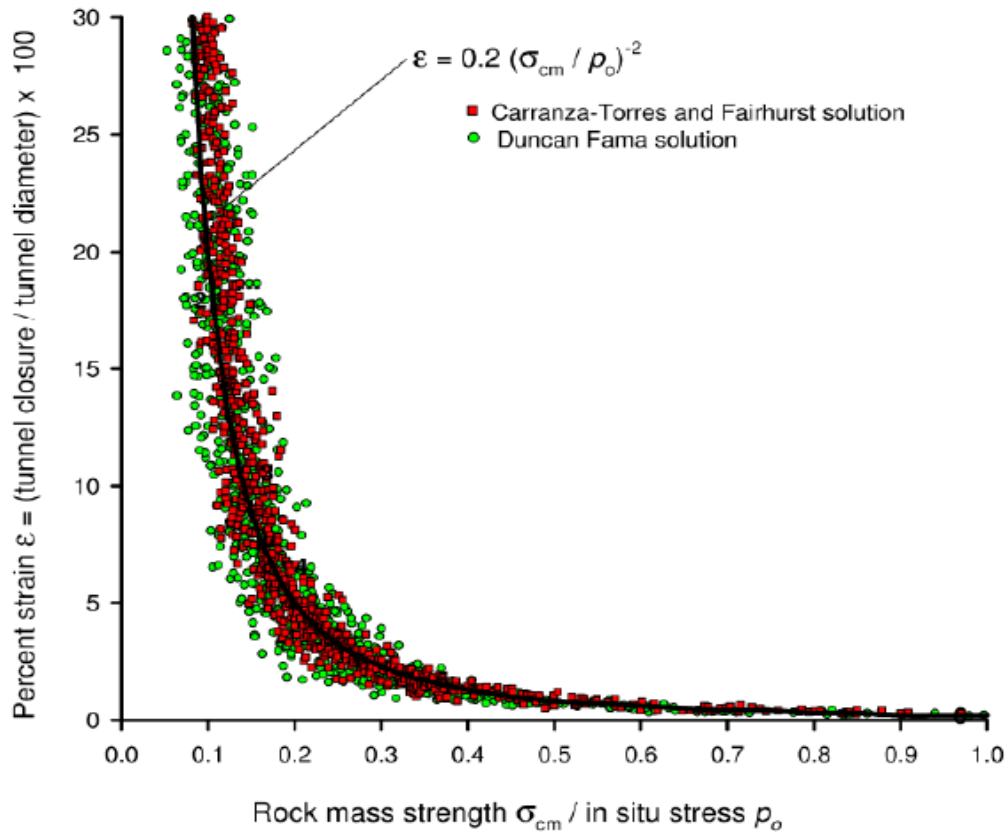
Figure 6-7: Tunnel convergence against the ratio of rock mass strength to in-situ stress (Hoek and Marinos, 2000)

Furthermore, (Hoek and Marinos, 2000) extended the analysis by including an internal pressure in tunnel to stimulate the effects of support and found a very similar trend for the size of the plastic zone surrounding the tunnel as shown in Figure 6-7. Using the fitting curve, they developed the following equations which determines the size of plastic zone and deformation of a tunnel in squeezing ground which is shown below:

$$\frac{d_p}{d_o} = \left(1.25 - 0.625\frac{p_i}{p_o}\right)\frac{\sigma_{cm}}{p_o}^{\left(\frac{p_i}{p_o} - 0.57\right)} \tag{6-6}$$

$$\varepsilon = \frac{\delta_i}{d_o} = \left(0.002 - 0.0025\frac{p_i}{p_0}\right)\frac{\sigma_{cm}}{p_o}^{\left(2.4\frac{p_i}{p_o} - 2\right)} \tag{6-7}$$

Where,

d_p = diameter of the plastic zone [m]

d_o = original tunnel diameter [m]

p_i = internal support pressure [MPa]

δi = tunnel sidewall deformation [m]

p_o = in-situ stress [MPa]

σ_{cm} = the rock mass strength [MPa]

Hoek and Marinos (2000) also proposed a classification system for squeezing severity based on strain percentage, as shown in Figure 6-8. Ranging from "extreme squeezing problems" to "few support system" there are five classes of severity of squeezing problems which are described further in Table 6-2. However, this analysis is based upon circular tunnel with isostatic stress field. Such conditions are rarely met in field in reference to the excavation method, tunnel shape and in-situ stress condition. Therefore Hoek and Marinos (2000) recommended to use numerical analysis in case of significant squeezing problem.
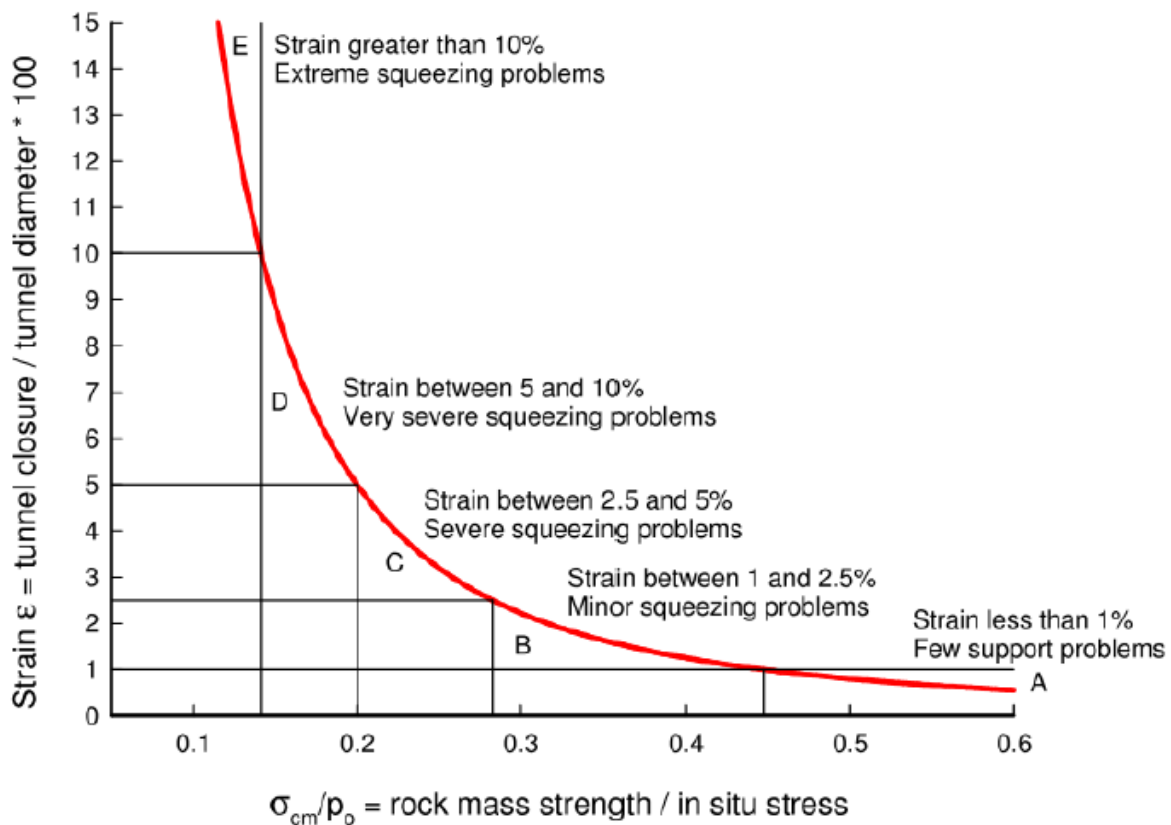

Figure 6-8: Relationship between tunnel strain and degree of severity of squeezing problems in case of unsupported tunnel, proposed by Hoek and Marinos (2000)

Table 6-2: Geotechnical issues and suggested support types for the 5 classes of squeezing severity (Hoek and Marinos, 2000)

	Strain ε %	Geotechnical issues	Support types
A	Less than 1	Few stability problems and very simple tunnel support design methods can be used. Tunnel support recommendations based upon rock mass classification provide an adequate basis for design.	Very simple tunneling conditions, with rock bolts and shotcrete typically used for support.
B	1 to 2.5	Convergence confinement methods are used to predict the formation of a 'plastic' zone in the rock mass surrounding a tunnel and of the interaction between the progressive development of this zone and different types of support.	Minor squeezing problems which are generally dealt with by rock bolts and shotcrete. sometimes with light steel sets or lattice girders are added for additional security.
C	2.5 to 5	Two-dimensional finite element analysis, incorporating support elements and excavation sequence, are normally used for this type of problem. Face stability is generally, not a major problem.	Severe squeezing problems requiring rapid installation of support and careful control of construction quality. Heavy steel sets embedded in shotcrete are generally required.
D	5 to 10	The design of the tunnel is dominated by face stability issues and, while two dimensional finite analyses are generally carried out, some estimates of the effects of fore poling and face reinforcement are required.	Very severe squeezing and face stability problems. Fore poling and face reinforcement with steel sets embedded in shotcrete are usually necessary.
E	More than 10	Severe face instability as well as squeezing of the tunnel make this an extremely difficult three-dimensional problem for which no effective design methods are	Extreme squeezing problems. Fore poling and face reinforcement are usually applied and yielding support

		currently available. Most solutions are based on experience.	may be required in extreme cases.

6.3.3 Analytical Method

Carranza-Torres and Fairhurst (2000) describes that the estimation of the support required to stabilize a tunnel excavation is four-dimensional problem. The three-dimensional redistribution of forces around the excavation which depends upon time and the nature of rock that is uncertain until it is exposed in the face. Labase (1949) describes the situation in two ways. First, the type of support to be used must be limited to one or two so that it would not disrupt the material supply in underground construction. Second, the need to install the precise support immediately after the excavation does not allow time to make calculations and fabricate the support. For the precise solution in each face, there is necessity to study each cross-section separately which requires several experiments and mathematical analysis. This may take a lot of time during which the excavation would certainly have collapsed.

Considering these constraints, analytical methods like Convergent-Confinement method proposed by (Carranza-Torres and Fairhurst, 2000) have been proposed. It addresses the nature of interplay between the rock mass that may vary and the installed support, and the effect of variation in assumed rock properties on the support loads. As there is no special analytical method for squeezing condition only, the general tunnel stability analysis like CCM can be used (Shrestha, 2006)

6.3.3.1 Convergent-Confinement Method

To understand the issues involved in the process of designing support in case of tunnel in weak rock mass, it is necessary to examine some very basic concepts of how a rock mass surrounding a tunnel deforms and how the support systems acts to control this deformation. The Convergent-Confinement method is a procedure that allows the estimation of load imposed on the support installed on the face of a tunnel. This method provides an interaction between the installed support and ground based on stresses and strains around a circular tunnel. This approach is mainly based on three different curves; Longitudinal Displacement Profile (LDP), the Ground Reaction Curve (GRC) and the Support Confining Curve (SCC) which are combined in order to calculate the equilibrium state between the support and the ground. The schematic representation of GRC, SCC and LDP is shown in Figure 6-9.
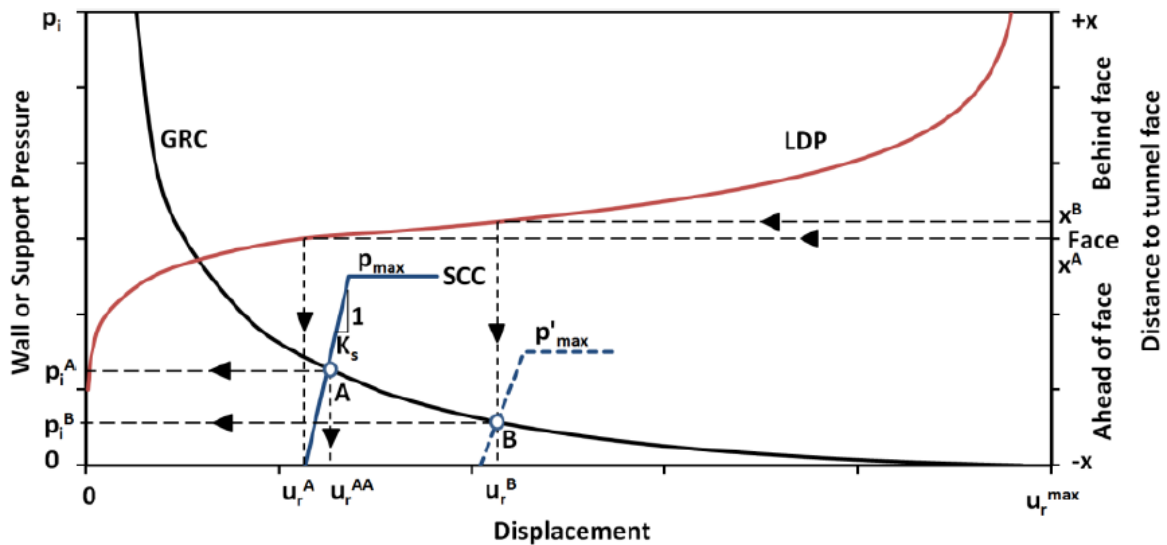
Figure 6-9: Schematic Representation of GRC, SCC and LDP of a circular tunnel (Shrestha, 2014)

CCM allows for estimation of the load imposed on the support installed immediately behind the face. Support installed immediately behind the face of a tunnel will not carry the full load for which it is designed; a part of the load will be carried by the face itself. As the tunnel advances, this 'face-effect' will decrease, and the support progressively carries more load. When the face has moved sufficiently far from the installed support, the full design load of the support is reached.

The Ground Reaction Curve (GRC)

GRC describes the relationship between the decreasing internal pressure (pi) and the increasing radial displacement of the wall. The internal pressure is not a true representation of reality, but rather a surrogate for the effect of the gradual reduction of the radial resistance provided by the initially present tunnel core (Vlachopoulos and Diederichs, 2009).

The Longitudinal Deformation Profile (LDP)

It is a graphical representation of radial displacement occurring along the axis of an unsupported cylindrical excavation, for sections behind and ahead of the face (Carranza-Torres and Fairhurst, 2000).

Support Characteristic Curve (SCC)

SCC is the relationship between the increasing internal pressure on the support, and the increasing radial displacement of the support. As shown in schematic representation as per

Figure 6-9 ,K corresponds to a support pressure at time of installation. Point R corresponds to the maximum pressure the support can accept before collapsing, p^{max} .

6.3.4   Numerical Analysis

6.3.4.1   General

The term "numerical modeling" means "discretization" of the rock mass into a large number of individual elements and the numerical models are made mostly to analyze the rock stress and deformation (Nilsen and Palmström, 2000). There is not any specialized software program particularly made for analyzing squeezing phenomena. However, there are various software tools like RS2 and RS3 which can be used for assessing the deformations around an underground opening. The deformation data from the numerical models can be compared with the results from empirical semi-analytical and analytical approaches of plastic deformation. All the empirical and analytical methods use the basic assumptions of homogeneous material and simple geometry (circular) which does not simulate the reality in most of the cases. Comparatively, the numerical models have the evident advantage in allowing complex geometry with complex interplay of geology and specified layouts. The advantages of numerical analysis over the other methods of plastic deformation analysis includes:

- complex geometry can be analyzed (i.e. anisotropy, in-homogeneity, groundwater, topography effect etc.)
- better understanding of mechanism since it provides visual effects and makes easier for interpretation
- extension of measurement results and laboratory data from field.
- it is quantitative analysis and can be used to verify the results obtained from other methods.

In this study, the main objective for the numerical analysis has been to verify, assess and analyze the rock mass parameters, induced stresses and the resulting deformations around the tailrace tunnel and the powerhouse cavern of AKHP. The verification of the results of numerical analysis has been done by comparing it with the existing measured deformation in the tailrace tunnel and the cavern. Also, it has been used to verify the validity of the empirical and analytical methods. For the analysis of the tailrace tunnel, the 2D finite element program RS2 by Rocscience has been used. Similarly, for the numerical analysis of powerhouse cavern, both RS2 and RS3 software have been used. The basic input parameters for deformation analysis in

RS2 include :loading conditions, material properties and support properties which are explained in Chapter 8 under numerical modeling.

6.4 Concluding remarks on the plastic deformation analysis

The empirical and semi-analytical methods of plastic deformation analysis can primarily be applied to predict the extent of squeezing. Both these methods does not include geometrical features of discontinuities and other parameter of rock mass.

Singh et al. (1992) approach only predicts the condition of squeezing but does not gives the amount of deformation of tunnel opening and support pressure. In this method, estimation of Q-value is most difficult since it depends on SRF value which is very sensitive for correct estimation of Q-value in most of the cases.

The method by Hoek and Marinos (2000) gives the amount of tunnel wall deformation along with the consideration of support pressure and the grade of squeezing. However, this method does not consider the deformation of tunnel at the time of support application and has no consideration of yielding of support. Another major lacking is that, it considers only the vertical stress due to gravity and do not include the effect of tectonic and topography stress in its analysis. Still, this method can be used to get information regarding deformation during the initial phase of analysis when the detailed rock mass parameters are not known.

Numerical modeling cannot be used directly to analyze the squeezing phenomenon in the tunnels. However, it can be used find the deformation of the excavation in squeezing condition and the major advantage over other methods is that it can represent the complex nature of the rock mass and geometry of excavation in its analysis.

7 Plastic deformation Analysis

7.1 General

As presented in the above chapters, plastic deformation (squeezing) in several stretches of tailrace tunnel had been the main challenge during the upgrading of AKHP. Along with that, during the longitudinal extension of the existing powerhouse cavern, minor squeezing was also noticed on the side walls of cavern. The plastic deformation analysis methods reviewed in Chapter 6 has been applied for the selected sections of tailrace tunnel and powerhouse cavern and compared with the measured deformations. Most of the rock mass parameters have been estimated corresponding to the theory presented in Chapter 2 and from the project report of AKHP. The overview of the performed analysis in the form of flowchart is shown Figure 7-1.

The empirical methods: (Singh et al., 1992) and Q-system and semi analytical method : (Hoek and Marinos, 2000) and analytical method: CCM has been applied using the estimated rock mass parameters, and the results has been compared to the measured deformations. Further numerical analysis of the same stretches of tailrace tunnel and powerhouse has also been carried out. Based on the comparison, the applicability and sensitivity of the methods regarding plastic deformations analysis in tunnel and cavern has been assessed.
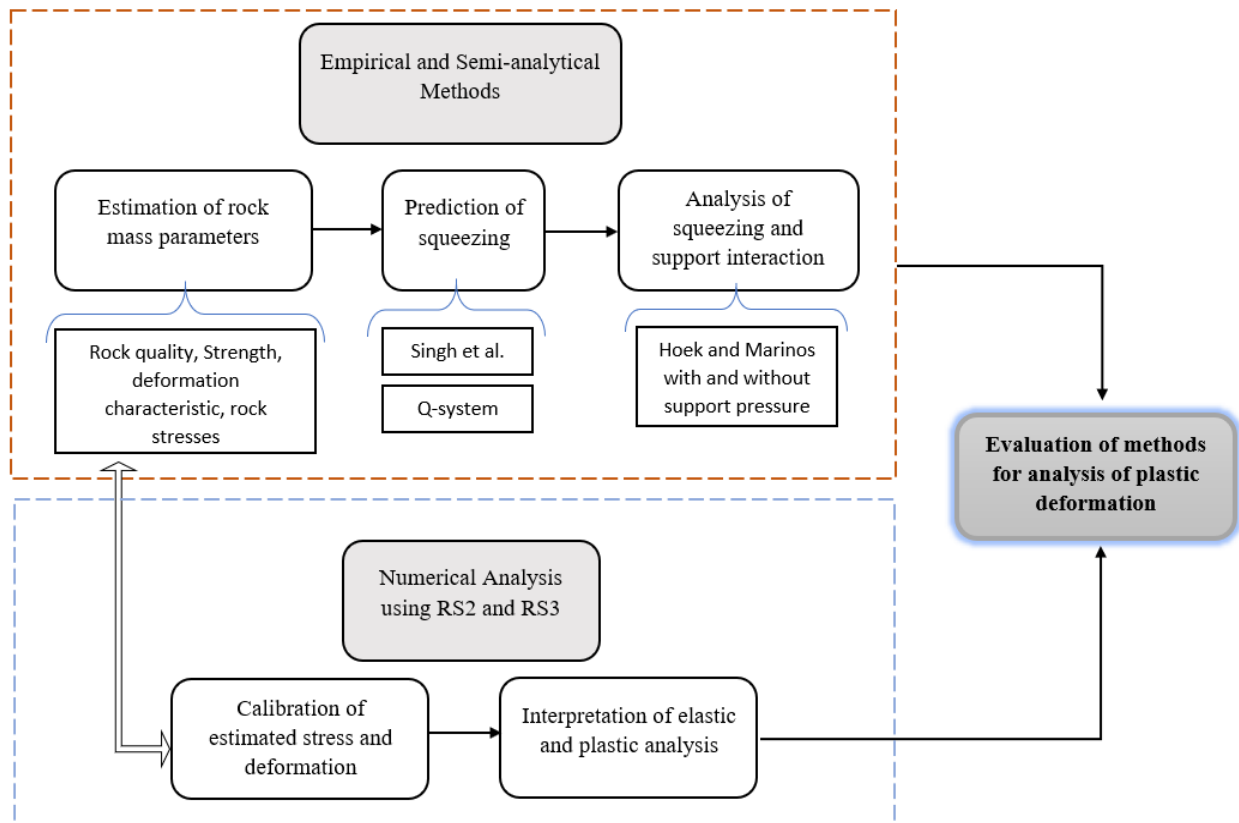
Figure 7-1: Overview of the performed analysis on plastic deformation

7.2 Input Data

The source of input data used in each methods and approaches are the AKHP Project Completion Report 2015, literature related to similar rock mass condition, hydropower projects in the nearby area of AKHP and discussion with supervisor. The details of geological setup, rock mass condition and convergence measurement of the components of AKHP i.e. powerhouse cavern and tailrace tunnel has already been presented in Chapter 4: Inspection and Data .

7.2.1 Rock mass parameters estimation

To estimate the initial values of rock mass parameters, various literatures such as scientific papers and journals, books, project report of AKHP, etc have been used. Also, the few input parameters from project located in same geological area of AKHP has been taken during the analysis.

Density and Poisson's ratio

The rock types along the tunnel sections considered for the analysis are phyllite and slate. The density of both the rocks are taken to be 2.72 t/m^3. The Poisson's ratio of the rocks are taken as 0.15 for slate and 0.1 for phyllite (Panthi, 2006)

Uniaxial compressive strength of intact rocks, σ$_{ci}$

The preliminary uniaxial compressive strength of intact, σci, has been estimated from data of nearby project Kaligandaki HP(Panthi, 2006) since no test were performed on the field. Later through back calculation from numerical modeling, σ$_{ci}$ of slate and phyllite are taken as 30 and 10 Mpa respectively.

Young's modulus of elasticity of intact rocks, Ei

There was not any measurement of Ei of intact rock thus, the value of similar rock type from project of same geological area has been taken as basis. The Young's modulus of elasticity of intact rock of the Slate is taken as 14Gpa and for phyllite the Ei value is considered to be 10Gpa. (Panthi, 2006)

Hoek and Brown constant, mi

According to Appendix A, the values of mi are taken as 10 and 7 for slate and phyllite respectively.

Tectonic stress

The tailrace tunnel and powerhouse cavern of AKHP are located near Kaligandaki Hydropower Project and the rock stress measurements carried out at Kaligandaki (Nepal 1999) showed that the tectonic stress component to be approximately 3 MPa (Nepal, 1999). Following (Panthi, 2012), in Central Himalaya, the general orientation of the direction of tectonic movement is close to north-south.

7.2.2   Rock mass strength calculation

Rock mass strength has been calculated using the different empirical relationships proposed by different authors. The equations of these approaches that are used for the calculation has been presented in Table 2-2 (Chapter 2)
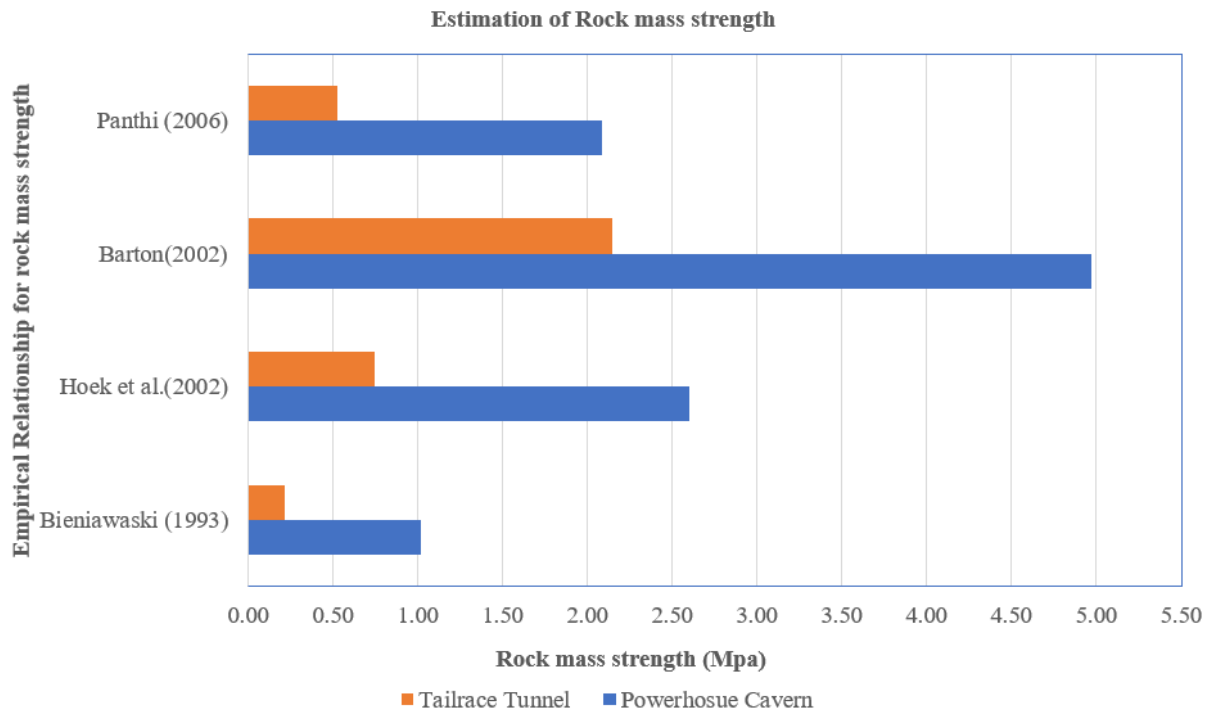
Figure 7-2: Rock mass strength estimation using different empirical methods

Figure 7-2 shows that Barton (2002) gives the highest values of rock mass strength for both the components i.e. powerhouse cavern and tailrace. Bieniawaski (1993) gives the lowest values for all the sections. Panthi (2006) and Hoek et al. (2002) gives the values almost average of all approaches. Panthi (2006) has been used to estimate the rock mass strength in Q-system (as discussed in section 2.3.3) to overcome the problem of loop of dependency in squeezing predicting criteria proposed by (Grimstad and Barton, 1993). Furthermore, in case of estimation of rock mass strength in Hoek and Marinos (2000) approach, the equations suggested by Hoek et al (2002) has been used.

7.2.3 Rock mass deformation modulus calculation

The rock mass deformation modulus has been calculated using different empirical relationship proposed by various authors. The equations used for estimation of the rock mass modulus are presented in Table 2-2. The comparison of the rock mass modulus values using various empirical methods are shown in Figure 7-3. It can be seen in Figure 7-3 that the Barton(2002) method have highest values of Erm whereas Hoek and Diederichs (2006) shows lowest values Panthi (2006) and Hoek et al. (2002) gives almost similar value. For further squeezing analysis, E_{rm} value from Hoek et al. (2002) has been used.
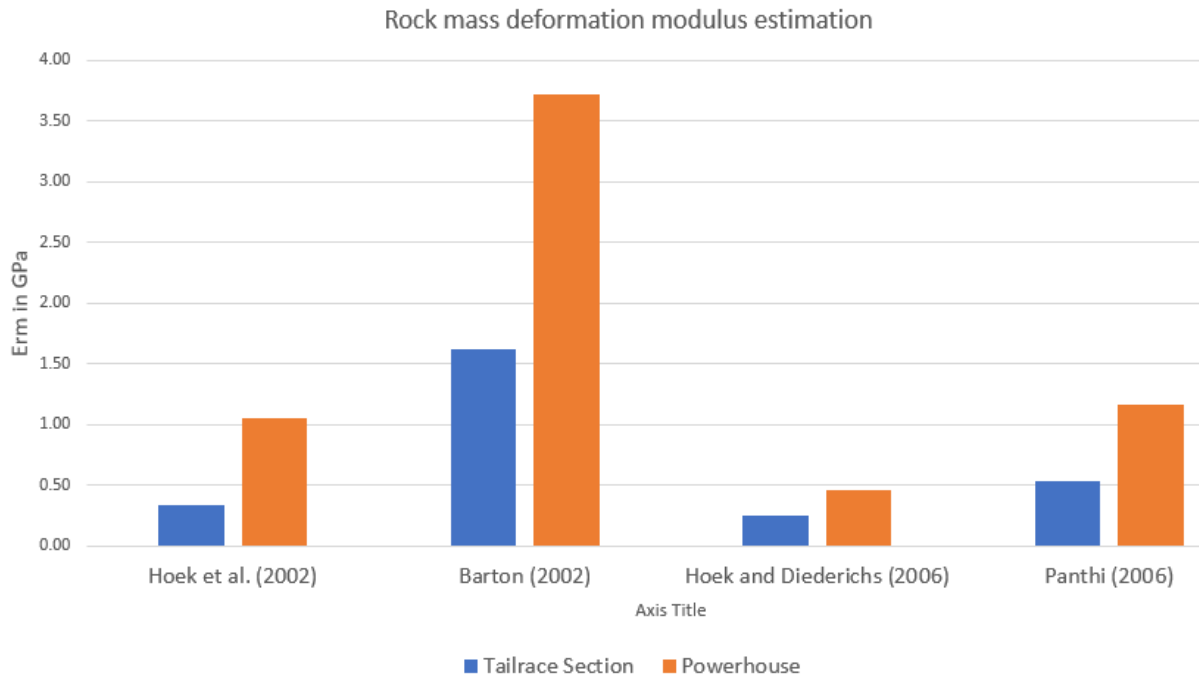
Figure 7-3: Rock mass Modulus estimation using different methods for selected tunnel section and powerhouse cavern

7.2.4 Squeezing prediction criteria

There methods such as Singh et al. (1992), Q-system (Grimstad and Barton, 1993) and Hoek and Marinos (2000) have been used to predict the squeezing phenomenon in tailrace tunnel of AKHP. The result of the analysis is shown in Table 7-1.

Table 7-1: Squeezing prediction according to Singh et al (1992), Q-system (Grimstad and Barton, 1993) and Hoek and Marinos (2000)

Component with Chainage	Rock type	Overburden Depth (m)	$\sigma 1$ (Mpa)	$\sigma 3$ (Mpa)	Singh et al. (1992)		Q-System (Barton and Grimstad, 1993)				Hoek and Marinos (2000)	
					Limiting value of H(m)	Squeezing condition	$\sigma\theta_{max}$	σ_{cm}	$\sigma\theta_{max}/\sigma_{cm}$	Squeezing condition	Strain % without support	Squeezing condition
Tailrace Tunnel 0+390	Phyllite	125	3.38	0.90	119.69	YES	9.23	0.74	12.43	Heavy Squeezing	4.13	Severe squeezing problem
Tailrace Tunnel 0+395	Phyllite	130	3.51	0.91	119.69	YES	9.62	0.74	12.96	Heavy Squeezing	4.47	Severe squeezing problem
Tailrace Tunnel 0+400	Phyllite	134	3.62	0.92	119.69	YES	9.93	0.74	13.38	Heavy Squeezing	4.75	Severe squeezing problem
Tailrace Tunnel 0+405	Phyllite	138	3.73	0.93	119.69	YES	10.24	0.74	13.80	Heavy Squeezing	5.04	Severe squeezing problem
Tailrace Tunnel 0+408	Phyllite	140	3.78	0.94	119.69	YES	10.4	0.74	14.01	Heavy Squeezing	5.18	Severe squeezing problem
Powerhouse	Slate	250	6.75	3.32	204.68	YES	6.21	2.50	6.21	Heavy Squeezing	1.25	Minor squeezing problem

Each analysis shows the mixed results for the squeezing prediction. Singh et al (1992) shows that there will be squeezing in all the selected components. According to Q-system, there will be heavy squeezing in powerhouse cavern and in the selected sections of tailrace tunnel. Similarly, according to Hoek and Marinos (2000) approach, there will be minor squeezing problems in powerhouse cavern and severe squeezing in all the tailrace tunnel sections. However, as per the field measurement of the squeezed tailrace tunnel, the maximum strain observed was 5-12 %.

Table 7-2: Strain % estimation with and without support using Hoek and Marinos (2000)

Sections	Overburden depth	Strain % = tunnel closure / tunnel diameter x100 Hoek and Marinos (2000)			Measured Strain
		Strain % Without support	Assumed support pressure, pi, Mpa	Strain % With support	
Tailrace Tunnel 0+390	125	4.13	0.15	2.23	5 %
Tailrace Tunnel 0+395	130	4.47	0.18	2.26	10 %
Tailrace Tunnel 0+400	134	4.75	0.20	2.54	12 %
Tailrace Tunnel 0+405	138	5.04	0.16	2.83	10 %
Tailrace Tunnel 0+408	140	5.18	0.18	2.97	8 %
Powerhouse	250	1.25	0.33	0.67	1.5 %

All the strain percentages in case of tailrace tunnel are above 2% even after the support application assumed using support pressure given by Barton. However there has been discrepancy in both the strain values when comparing the Hoek and Marinos and the measured deformation as shown in Figure 7-4.
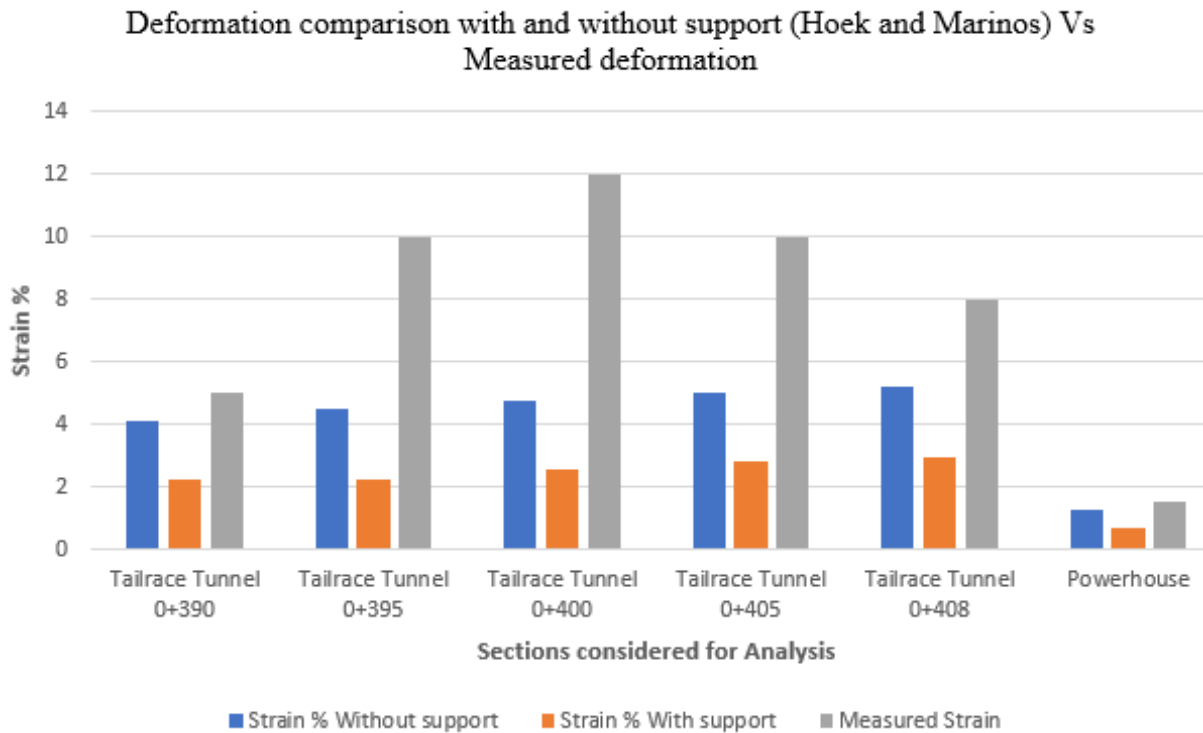
Figure 7-4: Comparison of measured deformation with the Hoek and Marinos approach

Also the instantaneous and final deformation of the selected section without support has been calculated using the equation 6-1 and 6-2 as per Panthi and Shrestha (2018). Comparing the value with other methods of plastic deformation, the value comes in accordance.

Table 7-3: Instantaneous and Final Strain estimation using Panthi and Shrestha (2018)

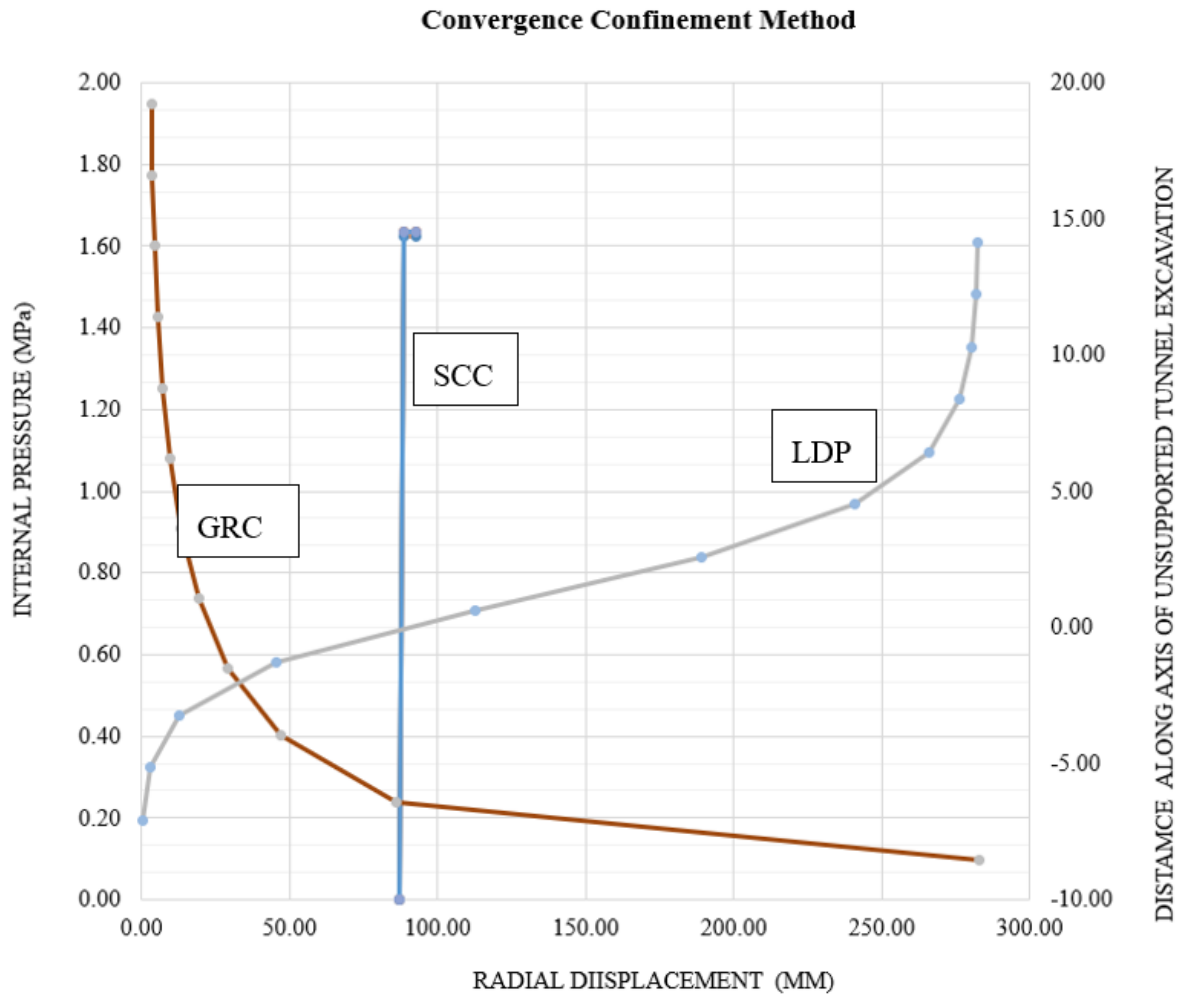| Sections considered for the analysis	Panthi and Shrestha (2018)		
	Rock type	Instantaneous strain	Final strain
Tailrace Tunnel 0+390	Phyllite	1.52 %	2.82 %
Tailrace Tunnel 0+395	Phyllite	1.64 %	3.03 %
Tailrace Tunnel 0+400	Phyllite	1.73 %	3.20 %
Tailrace Tunnel 0+405	Phyllite	1.83 %	3.38 %
Tailrace Tunnel 0+408	Phyllite	1.88 %	3.47 %
Powerhouse	Slate	0.76 %	1.42 %

Convergence Confinement Method

Figure 7-5: Results from Convergence Confinement Method for Tailrace Tunnel for chainage 0+400

7.2.5   Numerical Analysis

RS2 and RS3 program can used to determine the deformation of tunnel wall closure and the powerhouse cavern. The value of tunnel wall closure will determine the condition of ground whether it is squeezed or not.

At first, the back calculated intact rock strength along with other rock mass parameters has been taken as input to the program. The resulting deformation has been compared with measured deformation. The intact rock strength has been changed until the resulting deformation becomes equal to measured value. At that point, the intact rock strength value has been considered as more accurate value. The more detail procedure of using RS2 and RS3 program in this thesis is explained in Chapter 8: Numerical Modeling.

8 Numerical Modeling

8.1 Model setup

RS2 package from Rocscience has been used for numerical modeling of tailrace tunnel of AKHP whereas, for powerhouse cavern, both RS2 and RS3 software have been used. Analysis of the model with both elastic and plastic material type has been carried out. The redistribution of stress and strength factor of material has been analyzed using elastic material whereas the displacement and rock mass failure has been investigated using plastic material properties since the plastic property allows the material to yield. The model setup used in RS2 and RS3 are presented in Table 8-1.

Table 8-1: Model Setup in RS2 and RS3 modeling

Model Setup	RS2	RS3
Analysis Type	Plain Strain	Uncoupled
Solver Type	Gaussian Elimination	Automatic
Convergence Type	Absolute Force and Energy	Absolute Force and Energy
Field Stress Type	Constant	Constant
Failure Criterion	Generalized Hoek and Brown	Generalized Hoek and Brown
Mesh Type	3 Noded Graded	4 Noded Tetrahedron

Excavation boundary for each model has been made from project drawings of AKHP. The geological conditions (input parameters) have been finalized by calibrating the model using project report of AKHP, project drawings, geological information of the area, data from nearby projects and discussion with the supervisor. Input parameters, model analysis and interpretation of both structures i.e. the tailrace tunnel and the powerhouse cavern are presented separately in the following sections.

8.1.1 Numerical Modeling of Powerhouse

Initially, the RS2 model of powerhouse cavern has been created and calibrated using the basis of reference of the existing powerhouse cavern which was completely in stable condition before extension. Once the RS2 model demonstrated similar stability state as that of existing cavern, the same input parameters have been used to create the RS3 model to simulate the deformation occurred in the powerhouse cavern of AKHP after the extension work. The basic steps used in numerical modeling setup, analysis and interpretation is presented in Figure 8-1
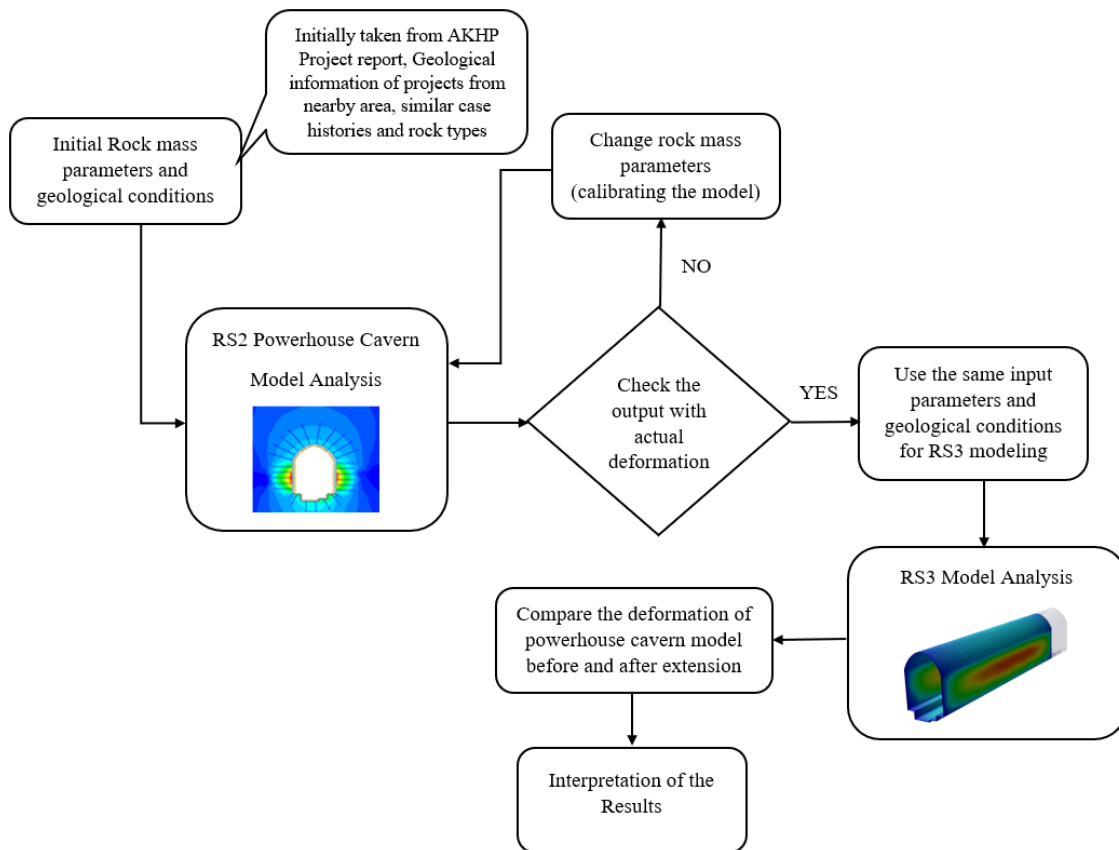
Figure 8-1: Flow chart of numerical modeling, analysis and interpretation of the powerhouse cavern of AKHP

8.1.1.1   Calibrating the model

The major intention for the calibration of the model has been to simulate the stability state of existing powerhouse cavern and to find the rock mass parameters which replicates the actual deformation condition of the existing powerhouse cavern before extension.

There was not any measurement of intact rock strength at the powerhouse cavern. So initially, the intact rock strength has been taken as per project report of AKHP, later it was calibrated and calculated using back analysis from the RS2 model. The basis of final deformation as reference has been found out considering the state of stability of existing powerhouse. As discussed in Chapter 4 Inspection and Data , the existing powerhouse cavern before extension had no deformation except for minor cracks on shotcrete which were negligible as per report of AKHP. Following that, the RS2 model has been created and assuming some relaxation of the cavern opening in long run of 30 years, the model was calibrated using final deformation value to be less than 1%.

To estimate the magnitude and orientation of major and minor principal stress acting around the opening of powerhouse cavern, a model in RS2 has been generated using actual ground surface as an external boundary. This model also accounts the effect of topography in stress

development around the excavation. However, the powerhouse cavern is deeply located around 240 meters below the surface, thus the topography effect is almost negligible which has been verified interpreting the model as shown in Figure 8-2. The major principal stress σ1 is almost vertical to the opening of cavern and minor principal stress σ3 is acting perpendicular to σ1.
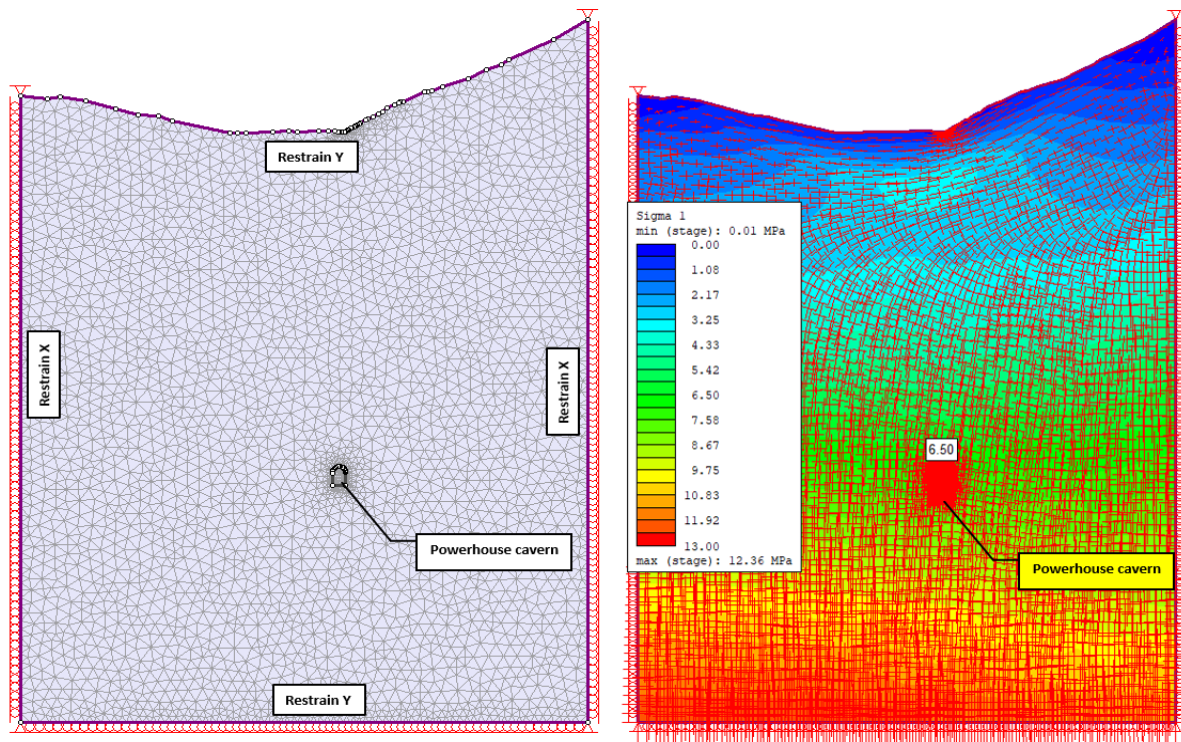

Figure 8-2: Model of powerhouse cavern in RS2 to verify the major principal stress orientation and magnitude around the cavern

Once the major and minor principal stresses were known, a box model in RS2 has been created with actual excavation contour as per project drawing of the powerhouse cavern of AKHP. The external boundary around the excavation has been set as a box with expansion factor of 5 which is assumed to be sufficient for rock mass to normalize towards the boundary as shown in Figure 8-4.
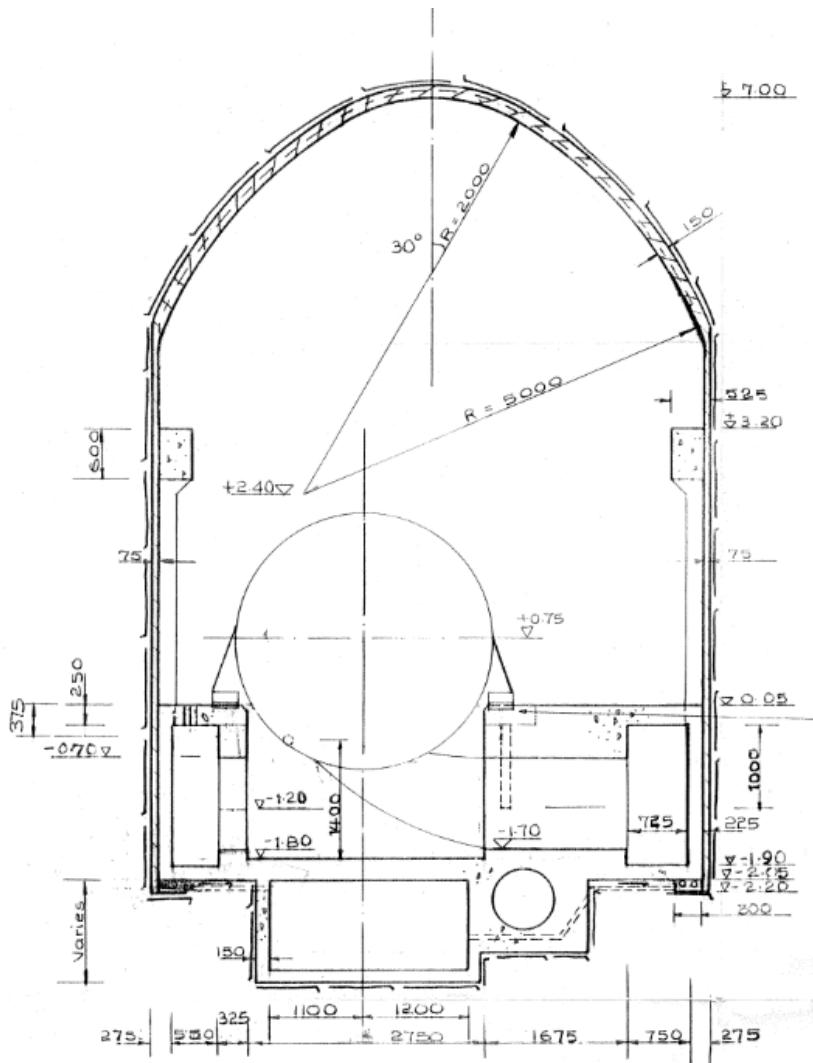
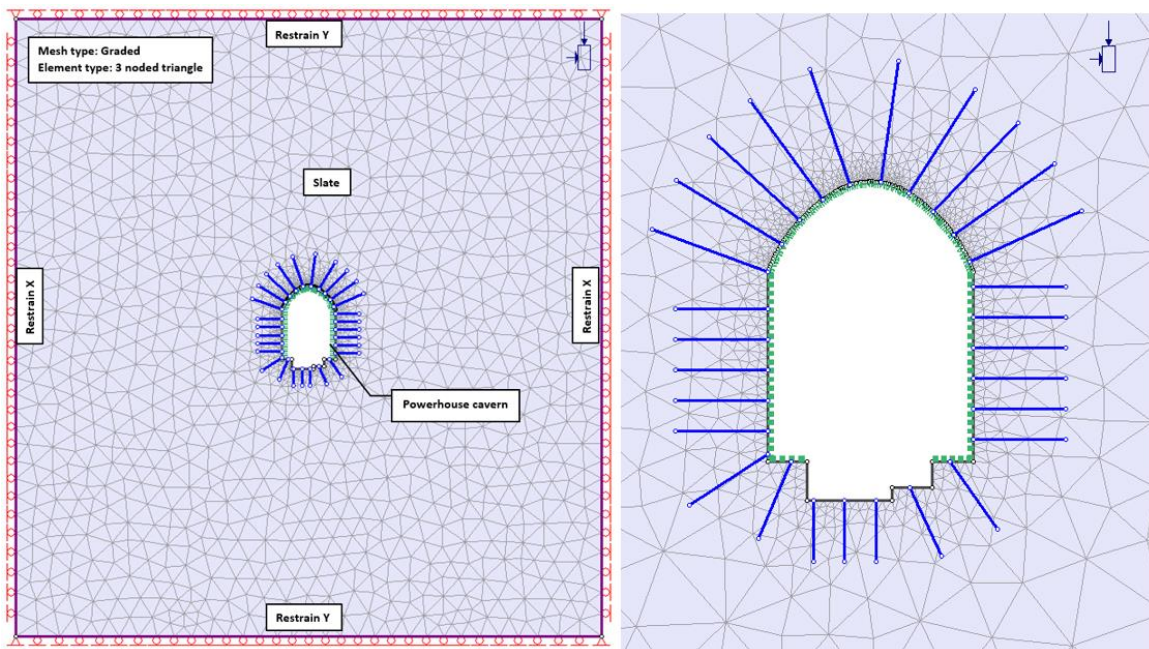Figure 8-3: Powerhouse cavern as built drawing issued in 1989,AKHP

Figure 8-4: RS2 model of powerhouse cavern of AKHP

8.1.1.2 Model Input of Powerhouse cavern:

Generalized Hoek and Brown criterion has been used to define the material properties of the model. Initially, the intact rock strength has been taken as per project report of AKHP, later it was calibrated and calculated using back analysis from the RS2 model. The Poisson's ratio of 0.1 and Modulus of Elasticity of 14Gpa has been used in the analysis according to (Panthi, 2006). AKHP is located near Kaligandaki Hydropower Project and the rock stress measurements carried out at Kaligandaki (Nepal 1999) showed that the tectonic stress component to be approximately 3 MPa (Nepal, 1999). Following (Panthi, 2012), in Central Himalaya, the general orientation of the direction of tectonic movement is close to north-south. AKHP is in central Himalaya and the powerhouse cavern is aligned almost $60°$ with the tectonic stress.

Table 8-2: Input parameters used in both elastic and plastic analysis of the model after calibration

Rock Type	Cavern depth	Density (MN/m^3)	Poisson's ratio	Ei (Mpa)	σci (Mpa)	GSI	mi	σ1 (Mpa)	σ3 (Mpa)	σz (Mpa)
Slate	240	0.027	0.1	14000	30	35	10	6.5	3.32	2.23
Tectonic stress value					3 Mpa					
Direction of tectonic stress movement					Approximately 0-degree NE					
Angle between powerhouse cavern and tectonic stress					60 degree					

In plane tectonic stress + horizontal stress due to vertical stress ($\sigma h = \frac{v}{1-v} x\ \sigma v + \sigma\text{tec\_in}$)	3.32 Mpa
Out plane tectonic stress + horizontal stress due to vertical stress ($\sigma h = \frac{v}{1-v} x\ \sigma v + \sigma\text{tec\_out}$)	2.23 Mpa

The support system used in the model is same as mentioned in the as built drawing of the existing powerhouse cavern. The details of the rock support are shown in Table 8-3.

Table 8-3: Existing rock support in powerhouse cavern (as per test holes, AKHP report)

Area	Rock Bolts (20 mm dia.)	Shotcrete
Crown	4 m long at 1 m c/c spacing alternately	Inner Layer: 7-10 cm thick plain shotcrete with combination of wire mesh Outer Layer: 2-5 cm thick steel fiber shotcrete
Wall	3 m long at 1 m c/c spacing alternately	Inner Layer: 7-10 cm thick plain shotcrete with combination of wire mesh Outer Layer: 2-5 cm thick steel fiber shotcrete
Floor	2 m long at 1 m c/c spacing alternately	
End Face	3 m long at 1 m c/c spacing alternately	1 layer of 75mm steel fiber shotcrete

8.1.1.3 RS2 Modeling of Powerhouse Cavern

Elastic Analysis

The main intention of the elastic analysis of the model is to evaluate the strength factor and stress distribution around the powerhouse cavern opening. As shown in Figure 8-5, the strength factor of the elastic model is less than one. This means that the material in the elastic model will fail (yield), and plastic analysis of the model is necessary for deformation analysis. Also, in elastic model, the deformation value is very less than the actual measured deformation which further reinforces the necessity of the plastic analysis.
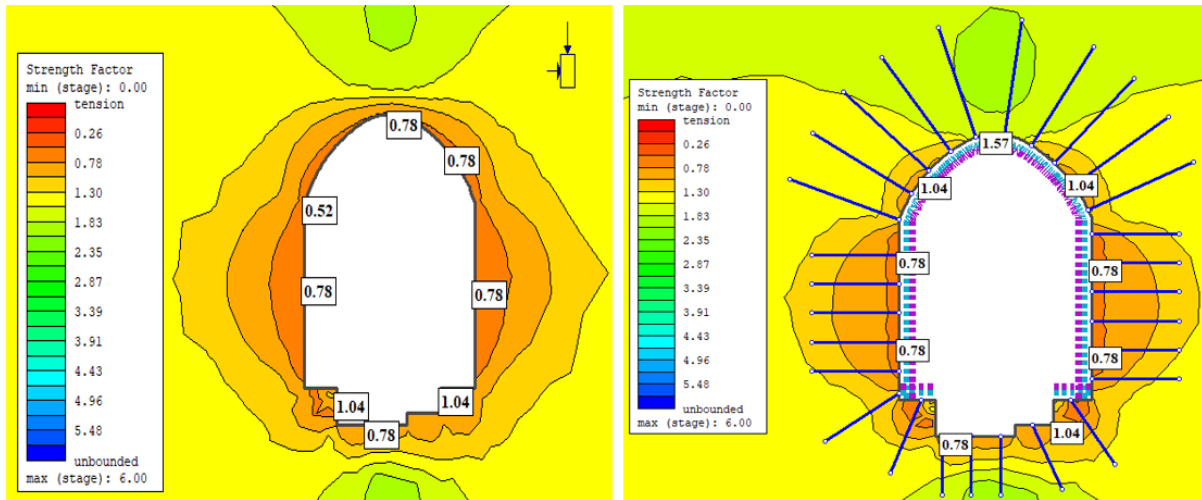
Figure 8-5: Strength factor for Elastic model of powerhouse cavern in RS2 without support (left) and with support (right)

For the RS2 elastic model without support, the strength factor around the whole contour except few areas in the invert has been found to be less than one. Whereas, in same elastic model after application of rock support, the strength factor around the crown has been found to be greater than one and rest all the contour has strength factor less than one. This signifies that the rock mass of crown portion of the powerhouse cavern will have less yielding than rest of the portion of the cavern. This is found to be true as per the results obtained from plastic analysis of the cavern as presented in Figure 8-8 which shows almost no yielding of crown portion with very less deformation.
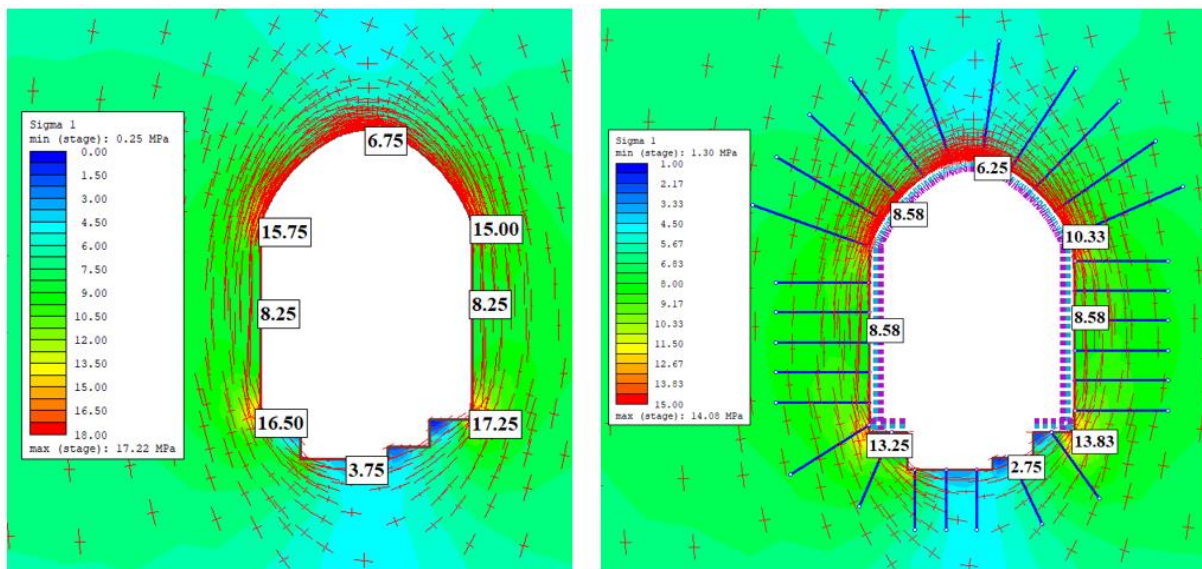

Figure 8-6: Major principal stress with trajectories in elastic model of powerhouse cavern without support(left) and with support(right)

It can be noticed that the stress concentration is mainly over the junction of crown and wall (spring line) portion and over the corners of invert portion. However, after the application of rock support, the stress concentration has comparatively reduced.

Plastic Analysis

Since the rock mass around the powerhouse cavern in elastic model yielded, plastic analysis of the same model has been carried out to find the deformation pattern around the contour of opening. The RS2 model has been created to simulate the existing condition of powerhouse cavern before the extension. Major intension creating this model was to find out the calibrated input parameters which can be used in the RS3 model. Two different models with and without rock support have been made The input rock mass parameters and rock supports that has been used for the analysis are discussed in Table 8-2 and Table 8-3 respectively.
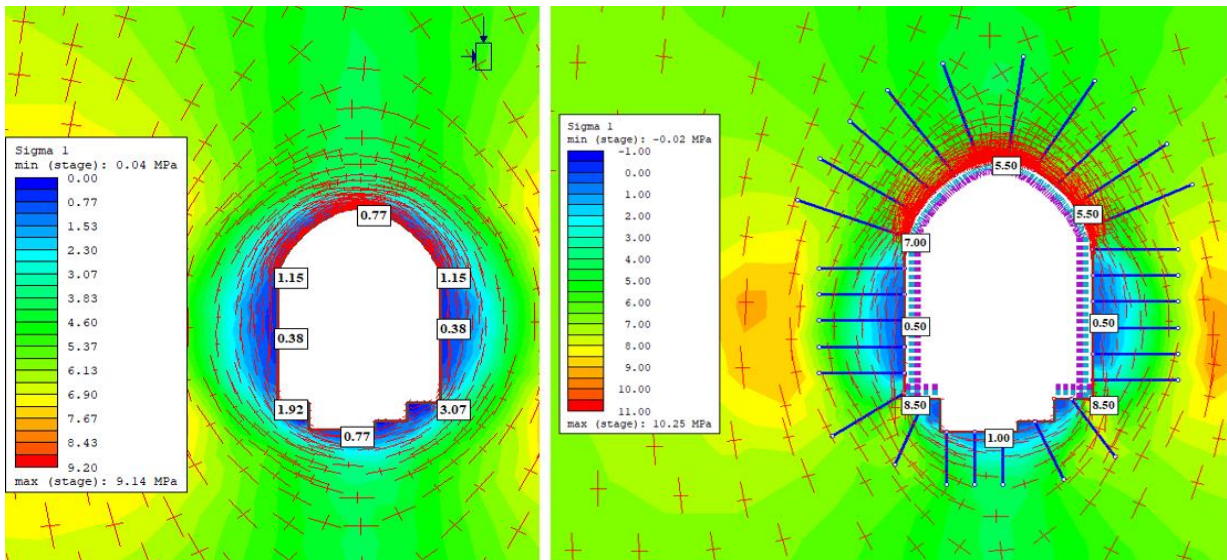

Figure 8-7: Major principal stress distribution with trajectories in Plastic model of powerhouse cavern without support (left) and with support (right)
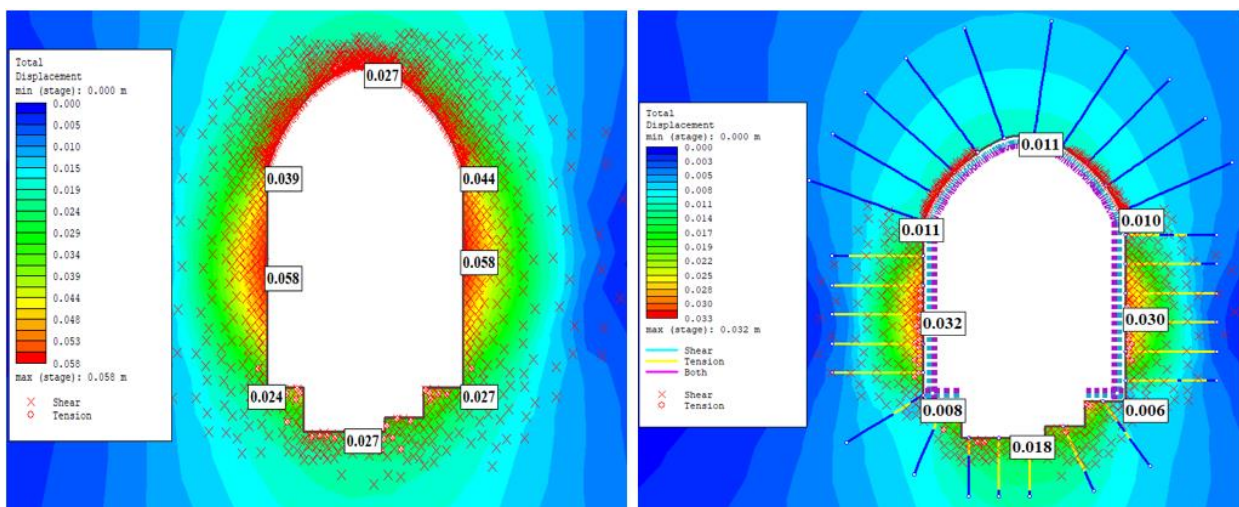

Figure 8-8: Total deformation for plastic analysis without support (left) and with support (right)

The above figure displays the total deformation and yielded elements in plastic model with and without support conditions. Failure of rock mass in shear and tension can be seen in model even after the rock support. It is observed that even after the rock support application, the displacement is almost 0.5% of the total width of powerhouse which is acceptable. Furthermore, the crown portion of the cavern does not display any failure of rock mass in tension but have yielded in shear up to few meters above spring line. The results obtained from the model seems reasonable since similar stability condition can be found in the existing powerhouse before the extension.

8.1.1.4 RS3 Modeling of Powerhouse Cavern

The main intension of creating the RS3 model of the powerhouse cavern has been to simulate the effect of longitudinal extension on the existing 37m long cavern which was in stable condition before the extension. The extension works later resulted in deformation of the side walls. Although, there has not been any exact measurement of convergence, the outward shifting of rail-track of EOT crane by 50-100mm has been taken as final deformation value. Thus, the deformation analysis was the major concern from this model. No other results except the deformation pattern and magnitude are presented in this section since other results are already presented and discussed in the RS2 modeling. Same rock mass properties and geological conditions as used in RS2 modeling has been used in creating this RS3 model of the powerhouse cavern. The analysis involves two stages which are presented below:

Stage 1: The stability condition of powerhouse cavern before the extension has been simulated in this stage. The excavation of 37m long powerhouse cavern with provided support system has been created. The support system and geological conditions in this RS3 model has been kept same as used in RS2 plastic analysis.

Stage 2: The longitudinal excavation of further 8m of powerhouse cavern along the existing cavern.
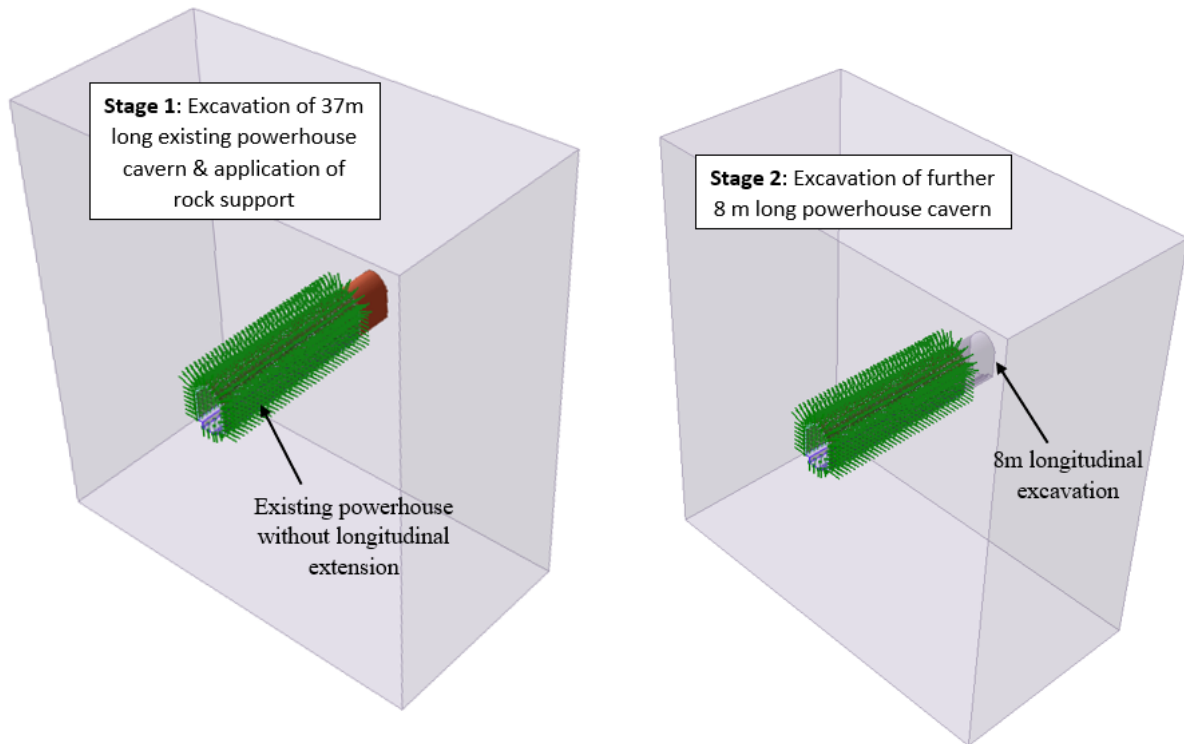
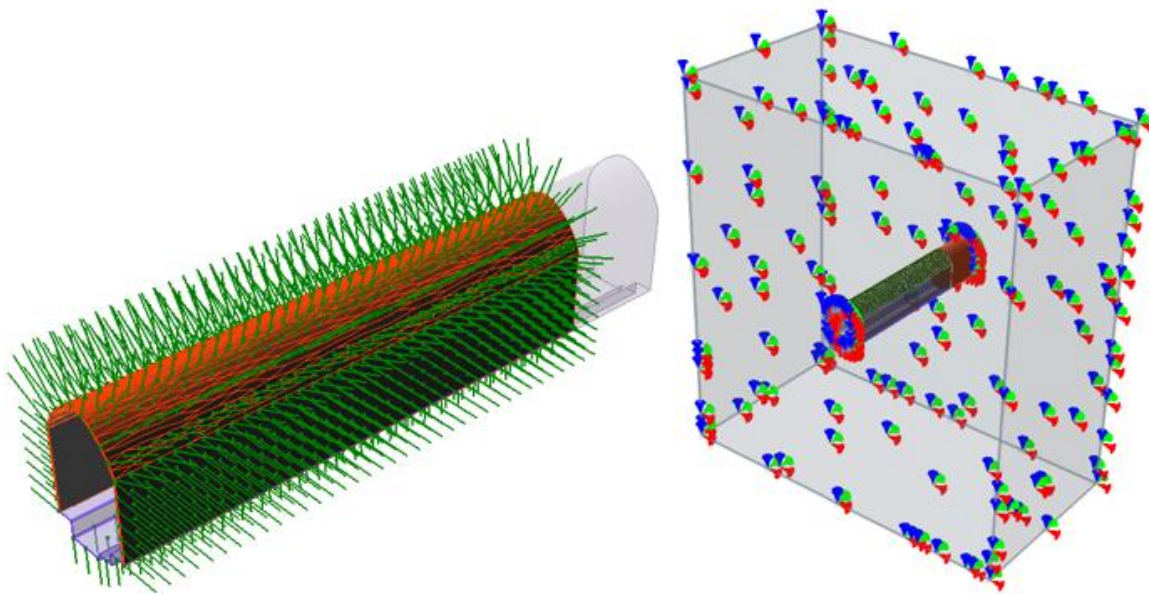Figure 8-9: Stages used in RS3 model of powerhouse cavern

Figure 8-10: Applied support to the existing powerhouse model (bolts and shotcrete) and restraints for the external boundary of RS3 model of cavern
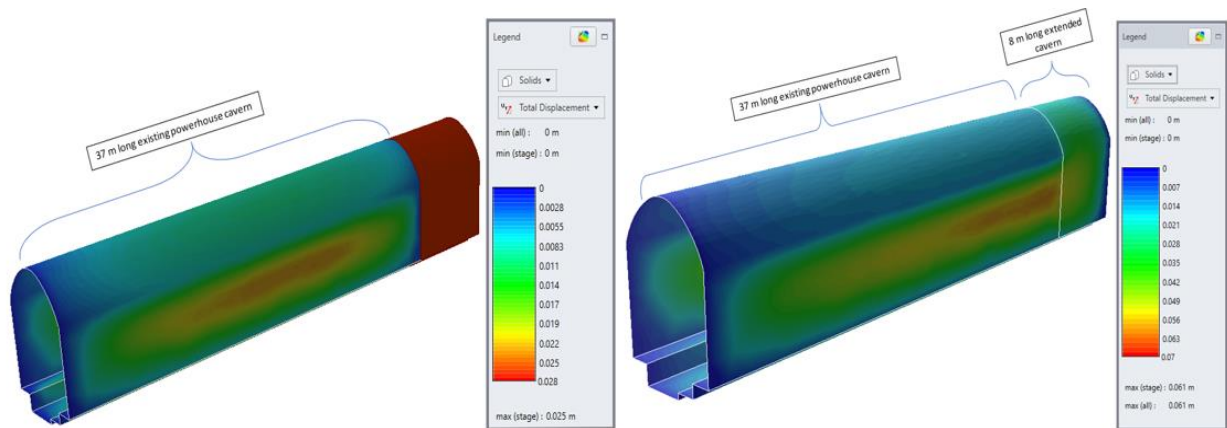
Figure 8-11: Total deformation in the RS3 powerhouse cavern model before(left) and after extension(right)

In both stages, the maximum deformation has been noticed on the walls of cavern. Before the extension of the powerhouse cavern, the deformation on the wall is found to be 2.5cm which is almost 0.4 % of total width of powerhouse. Whereas, the longitudinal extension has resulted in around 4cm increase in deformation on the side wall of the existing model of powerhouse cavern making the total deformation around 6cm. Thus, this RS3 model simulates the actual deformation of the powerhouse cavern of AKHP after the extension. The measured deformation of 5-10 cm was on the crane rail fitted on the wall and this model also shows the same pattern of deformation.

Figure 8-12: Total deformation in RS3 model of existing powerhouse cavern after extension of 8 m.

8.1.2 Numerical Modeling of Tailrace Tunnel

The main purpose of the numerical modeling of the tailrace tunnel of AKHP was to simulate the deformation behavior which was noticed on the walls of the tunnel after the base was excavate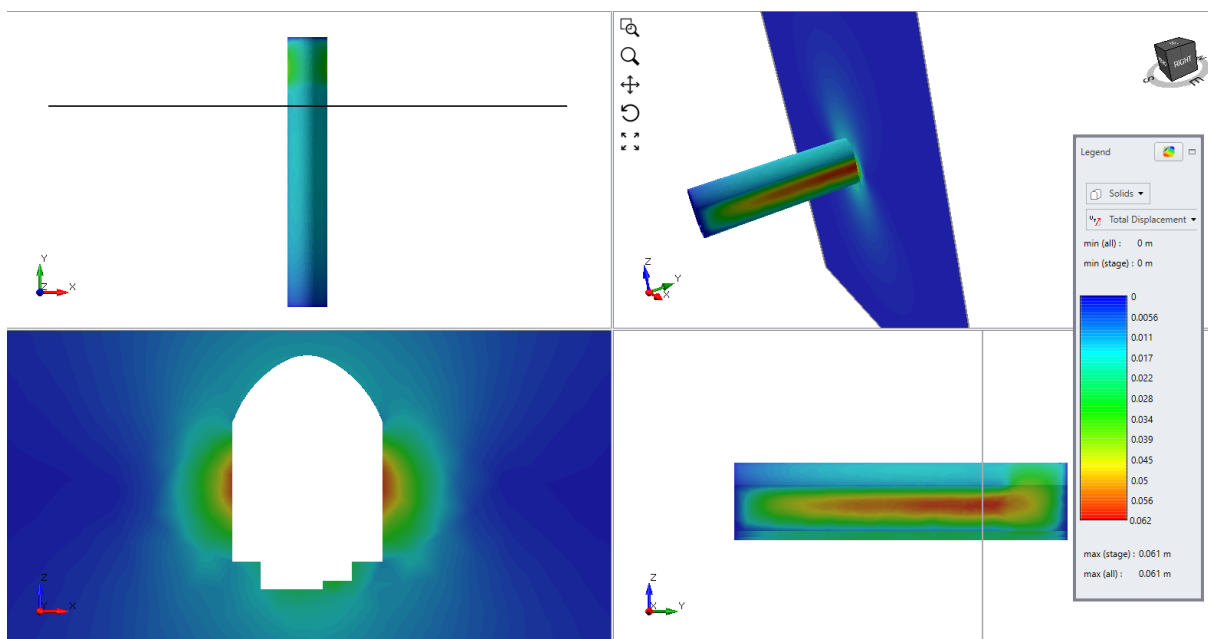d during upgrading work. Once the deformation result from the RS2 model is same as that measured in the site, the input parameters and assumed geological conditions can be considered as calibrated and thus can be used in theoretical methods of calculating deformation.

8.1.2.1 Background

The existing tailrace tunnel was in stable state before enlargement except for few sections which experienced bulging of invert. As presented in Chapter 4: Inspection and Data , the upgrading of AKHP needed the enlargement of cross section of existing tailrace tunnel by further lowering of the invert. The rock support applied to the enlarged section of the tunnel was inadequate and squeezing of the rock mass occurred along the tunnel from chainage 0+390 to 0+410. The convergence monitoring was carried out in July,2013 for 5 sections (chainage 0+390, 0+395, 0+400, 0+405 and 0+408). In this report only the RS2 model of chainage **0+400** has been presented and investigated in detail since this section experienced the maximum deformation due to squeezing.

Regarding the shape of the tailrace tunnel:
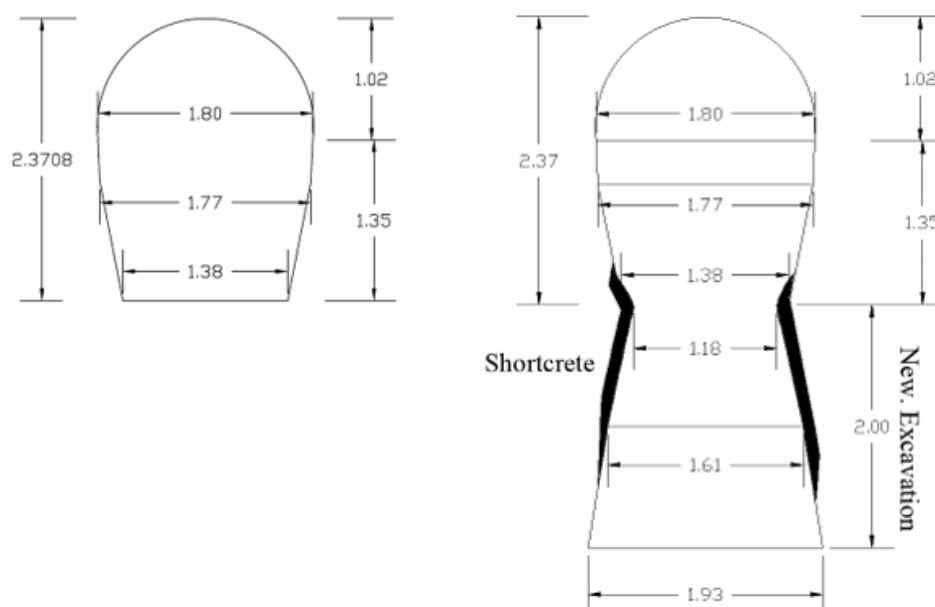

Figure 8-13: Existing tailrace tunnel cross section before enlargement (left) and after enlargement (right)

The tailrace tunnel shape before the enlargement was a modified horseshoe but after the excavation of invert further 2 m below, the new tunnel shape resulted in belly bottomed with height to width ratio being around 2.4. This unusual shape of tailrace tunnel was due to the

minimum clearance of required for the passage of wheel loader and mocking tractor during the construction. The same geometry has been used in the RS2 modeling of tailrace tunnel.

8.1.2.2 Model Generation

To estimate the magnitude and orientation of major principal stress acting around the opening of tailrace tunnel, a model in RS2 has been generated using actual ground surface as an external boundary. This model also accounts the effect of topography in stress development around the excavation.
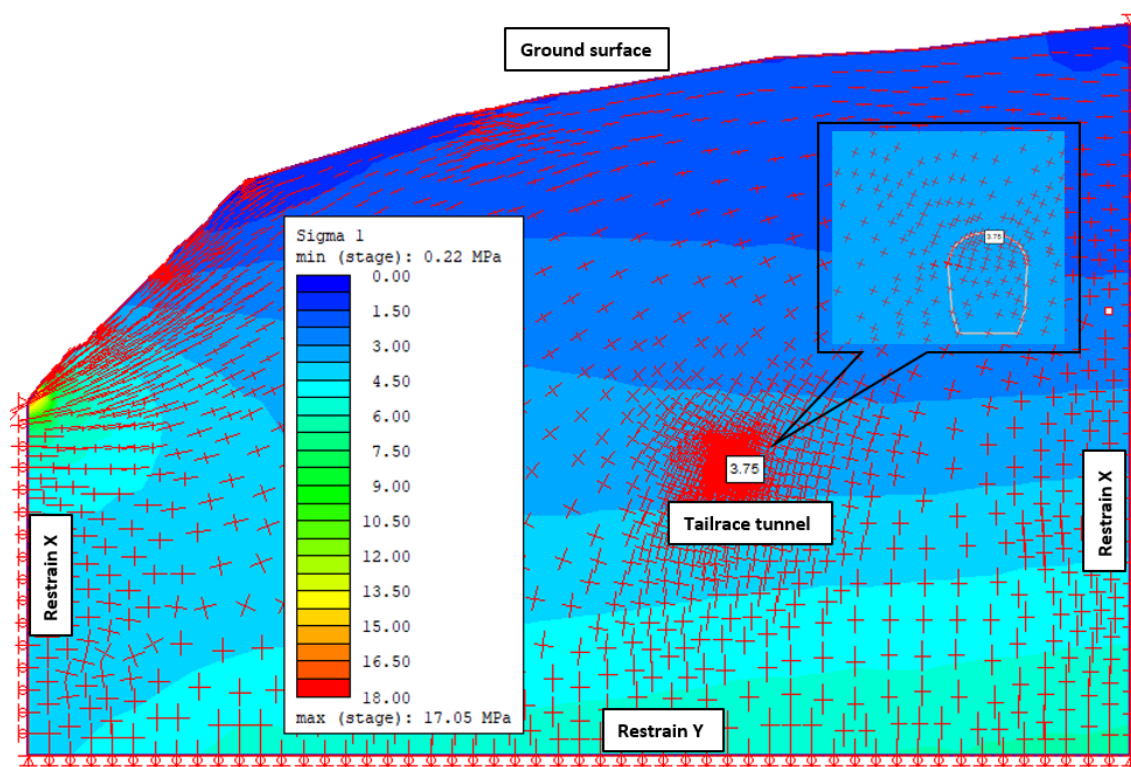
Figure 8-14: Major principal stress orientation and magnitude around the tailrace tunnel section at chainage 0+400 m

It can be noticed that there is the effect of topography acting on the stress development near the area of tailrace tunnel. The major stress is approximately oriented 70% with the horizontal and the magnitude of 3.75Mpa around the opening of tunnel as shown in Figure 8-14. Once the major stress was finalized, a box model with expansion factor of 5 having actual excavation contour of tailrace tunnel has been created as shown in Figure 8-15.
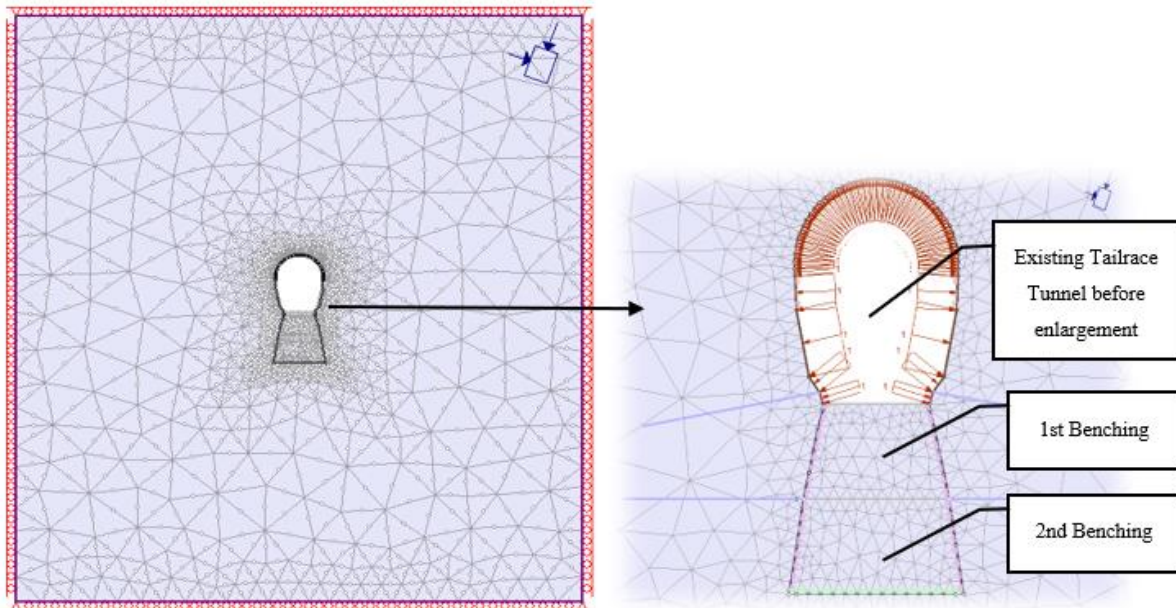
Figure 8-15: RS2 model of tailrace tunnel for chainage 0+400

8.1.2.3   Stages used in RS2 modeling of tailrace tunnel

Three stages have been created in RS2 model as per the excavation and support installation followed during the enlargement of tailrace tunnel of AKHP. The stages are explained in detail as follows:

Stage 1: Excavation of existing tunnel and applying field stress vectors

In this stage the existing tunnel has been excavated as shown in Figure 8-16. As per the AKHP project report, the existing tailrace tunnel was excavated 30 years ago and was in stable condition before the excavation of invert. However, even after the excavation of the bottom part, not the whole section of the opening was squeezed but only the side walls and invert were deformed. The crown and the springing parts were still stable and intact.

To simulate the existing condition in the numerical model of RS2, it is very important to assign the constraint at the nodes of finite elements especially in the part where there was zero deformation due to existing support condition. Thus, field stress vectors have been assigned to control deformation at such location and to simulate the real behavior of the opening as shown in Figure 8-16.
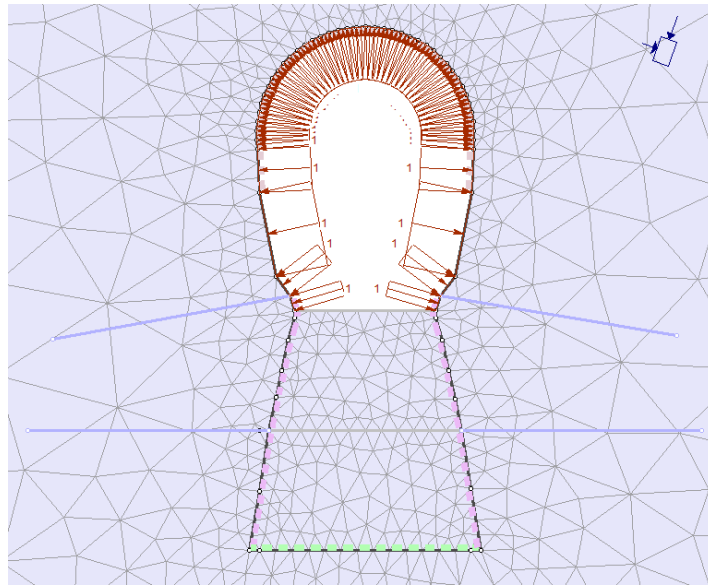
Figure 8-16: 1st Stage of RS2 model with excavation of existing tailrace tunnel and application of field stress vector

Stage 2: First benching (excavation) from the base of existing tailrace tunnel

This stage represents 1st stage of excavation of 1m from the base of existing tailrace tunnel. It was followed by application of 2m long rock bolts just above the invert level on both sides of wall and then 150 mm fiber reinforced shotcrete as shown in Figure. Furthermore, it has been assumed that certain relaxation of the tunnel opening in the long run of around 30 year would have happened. Thus 10% of the total field stress has been be released before the new excavation.
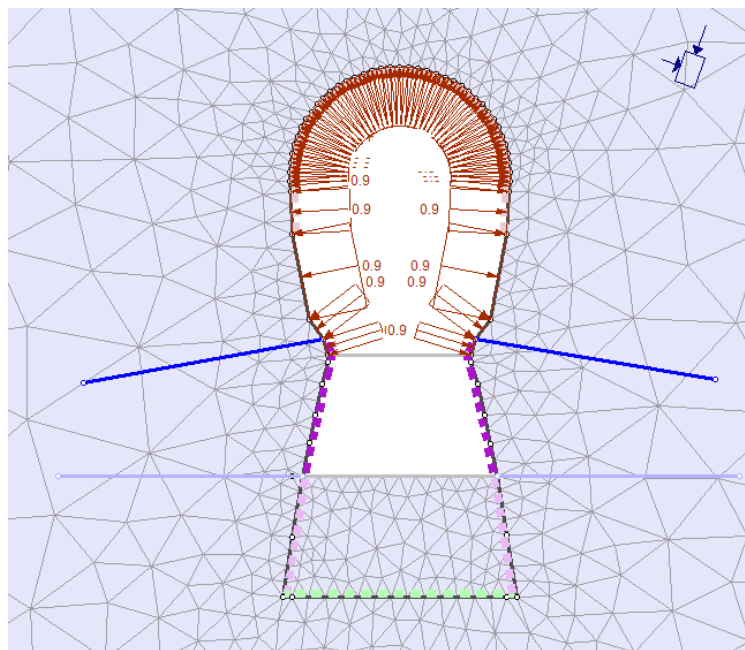
Figure 8-17: 2nd Stage of excavation in RS2 model of tailrace tunnel

Stage 3: 2nd Benching (excavation) of the base of existing tailrace tunnel

In this stage, following the 1st benching, further excavation of 1m has been made below the base. The newly excavated height of the invert excavation is about 2m from the existing level. It is followed by 150mm thick fiber reinforced shotcrete applied to the side walls and 200 mm thick reinforced concrete lining on the invert of the tailrace tunnel.
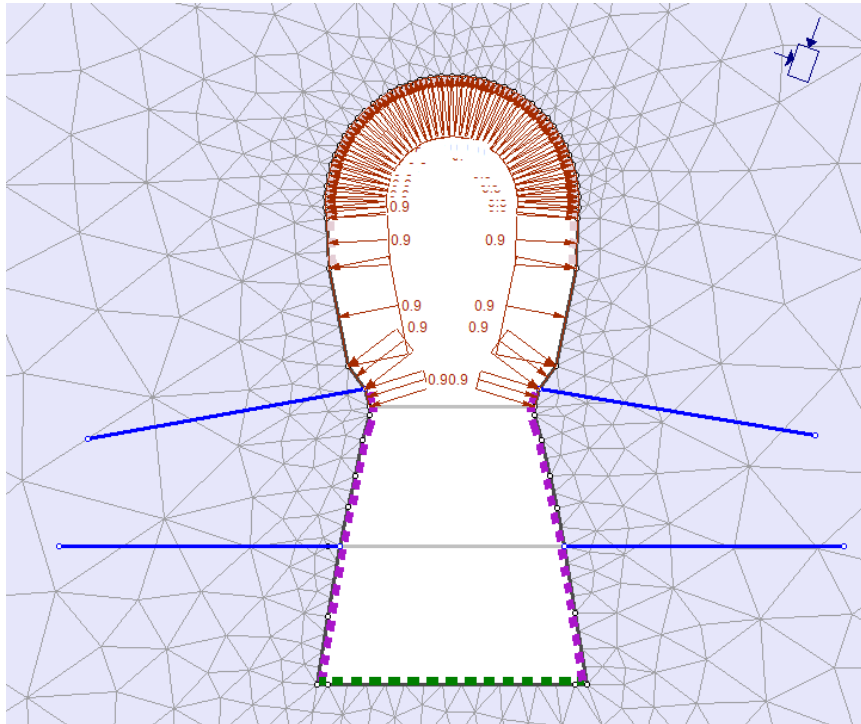
Figure 8-18: 3rd Stage of excavation of the base of existing tailrace tunnel

8.1.2.4 Model Input Parameters

Generalized Hoek and Brown criterion has been used to define the material properties of the model. The intact rock strength has been taken as per project report of AKHP. The Poisson's ratio of 0.1 and Modulus of Elasticity of 14Gpa has been used in the analysis according to (Panthi, 2006). The tectonic stress development around AKHP has already been discussed in numerical modeling of powerhouse, thus similar tectonic stress value has been taken for RS2 modeling of tailrace tunnel.

Table 8-4: Input parameters used in both elastic and plastic analysis of the model

Rock Type	Density (MN/m^3)	Poisson's ratio	Ei (Mpa)	σci (Mpa)	GSI	mi	σ1 (Mpa)	σ3 (Mpa)	σz (Mpa)
Phyllite	0.027	0.1	10000	10	23	7	3.62	0.92	3.47
Tectonic stress value				3 Mpa					

Direction of tectonic stress movement	Approximately 0-degree NE
Angle between tailrace tunnel alignment and tectonic stress	10 degree
In-plane tectonic stress + gravity led horizontal stress ($\sigma h = \frac{v}{1-v} x \ \sigma v + \sigma\text{tec\_in}$)	0.92 Mpa
Out-plane tectonic stress + gravity led horizontal stress ($\sigma h = \frac{v}{1-v} x \ \sigma v + \sigma\text{tec\_out}$)	3.47 Mpa

Table 8-5: Rock Support applied at various stages of excavation in RS2 Model of tailrace tunnel

Stages of Excavation	Rock support Type	
Stage 1	Opposing stress field vector applied along the contour of existing tailrace tunnel	
	Rock Bolts	Lining
Stage 2	2 m long at 0.5 m c/c spacing	150 mm thick fiber reinforced shotcrete on the walls of the newly excavated portion
Stage 3	2 m long at 1 m c/c spacing	150 mm thick fiber reinforced shotcrete on the walls of the newly excavated portion - On the new invert, 200mm thick C25 reinforced concrete lining, 12mm rebar with 150mm c/c spacing

8.1.2.5 Elastic Analysis

The main intention of the elastic analysis of the model is to evaluate the strength factor. As shown in Figure 8-19, after the excavation of base of tailrace tunnel, the strength factor of the elastic model is less than one. This means that the material in the elastic model will fail (yield), thus plastic analysis of the model is necessary for deformation analysis.
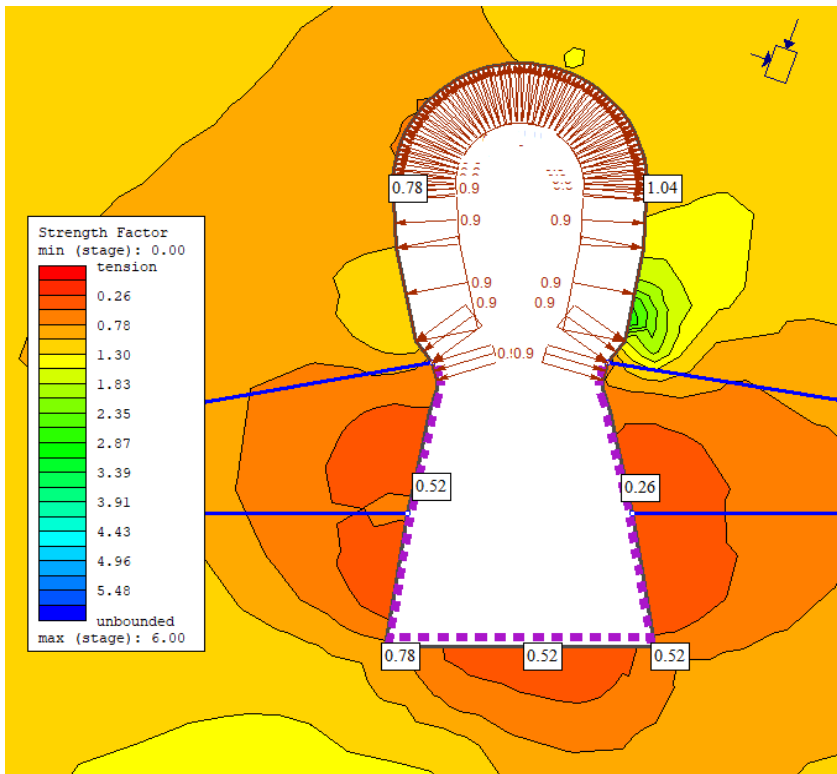
Figure 8-19: Strength factor around the newly excavated tailrace portion for Elastic Analysis of RS2 model
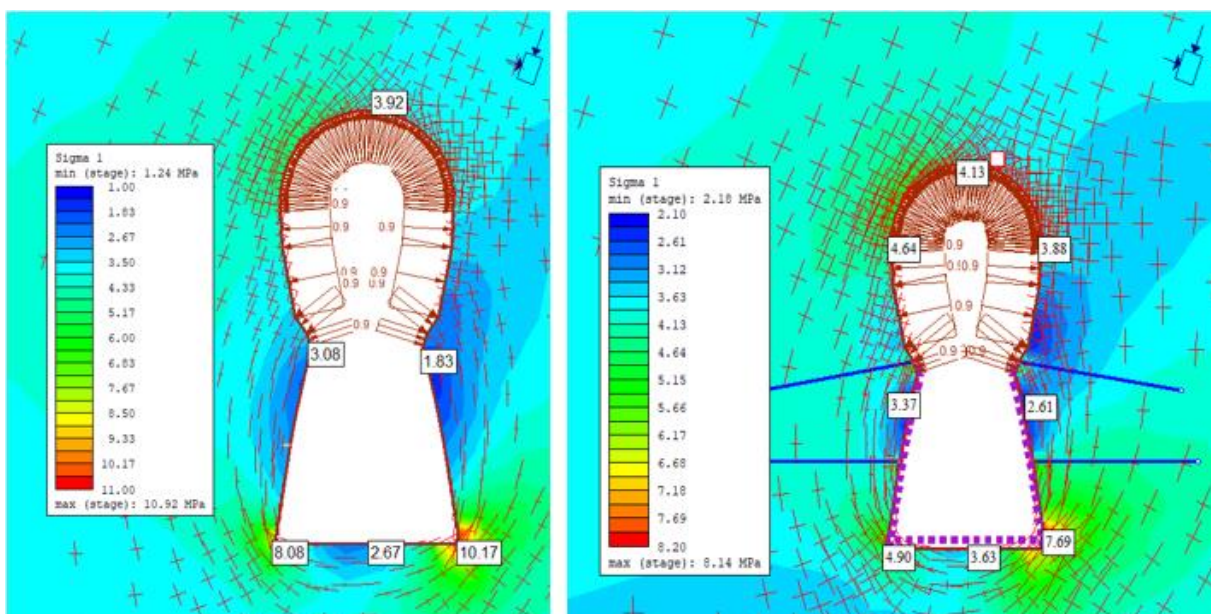
Figure 8-20: Major stress distribution around the tailrace tunnel after the enlargement with and without support

8.1.2.6 Plastic Analysis

The plastic analysis has been done to find the deformation around the tailrace tunnel with and without support. The deformation obtained from the RS2 model has been compared with the

measured convergence by calibrating the rock mass parameters and geological conditions. The deformation has been presented as per the stages of excavation followed during the enlargement of tailrace tunnel.

Stage 1 Deformation Result:
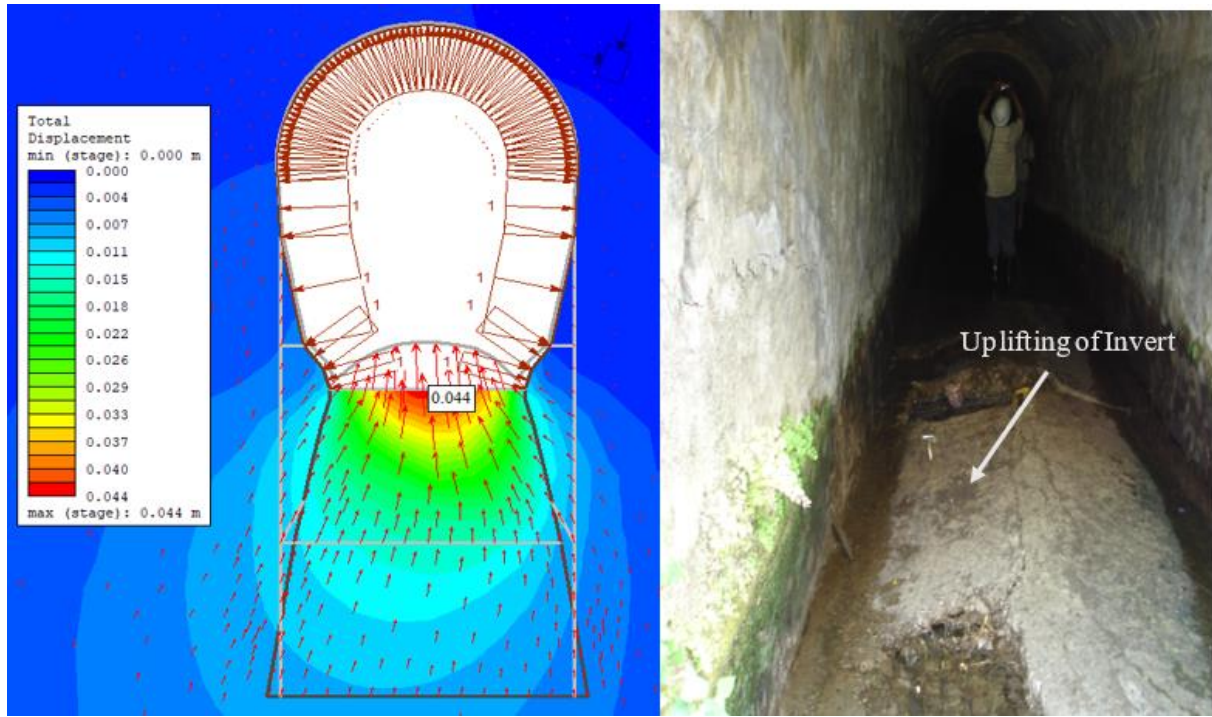
Figure 8-21: Total deformation at invert of the existing tailrace tunnel before enlargement (left) and uplifting of invert noticed during inspection before enlargement of tunnel

As per the above deformation result, it can be noticed that, the RS2 model has simulated the actual deformation pattern which was investigated during the inspection of tailrace tunnel before the enlargement. There was uplift of approximately 5-15 cm in the invert in the existing tailrace tunnel. The uplift (deformation) of 4cm has been found in the RS2 model which is nearly the same as site condition. The deformation value in the RS2 model is not very high since the opposing field stress has been applied throughout the contour of existing tunnel.
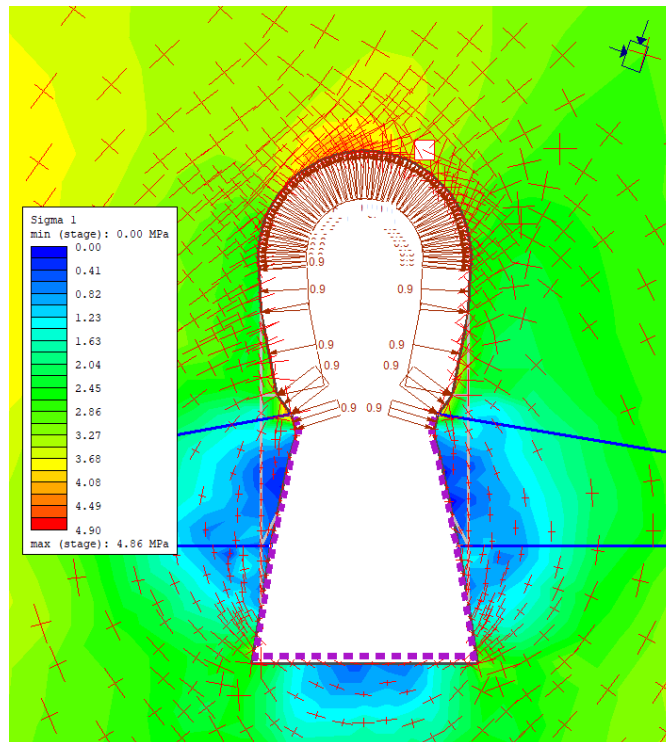
Figure 8-22: Major stress distribution around the tailrace tunnel after enlargement
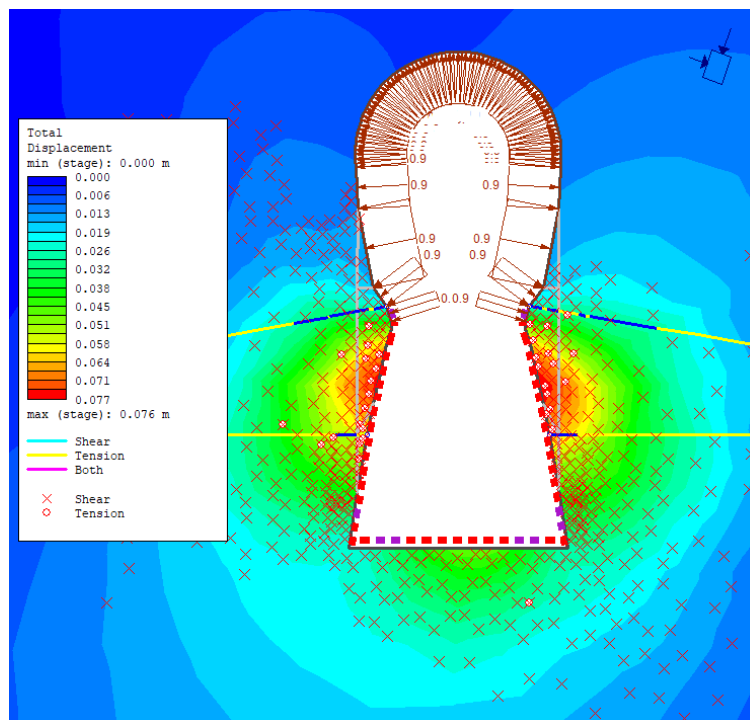
Figure 8-23:Total yielded elements around the enlarged tailrace tunnel

It can be noticed that the almost all the rock support have yielded and most of the area near the wall and invert have failed in shear.
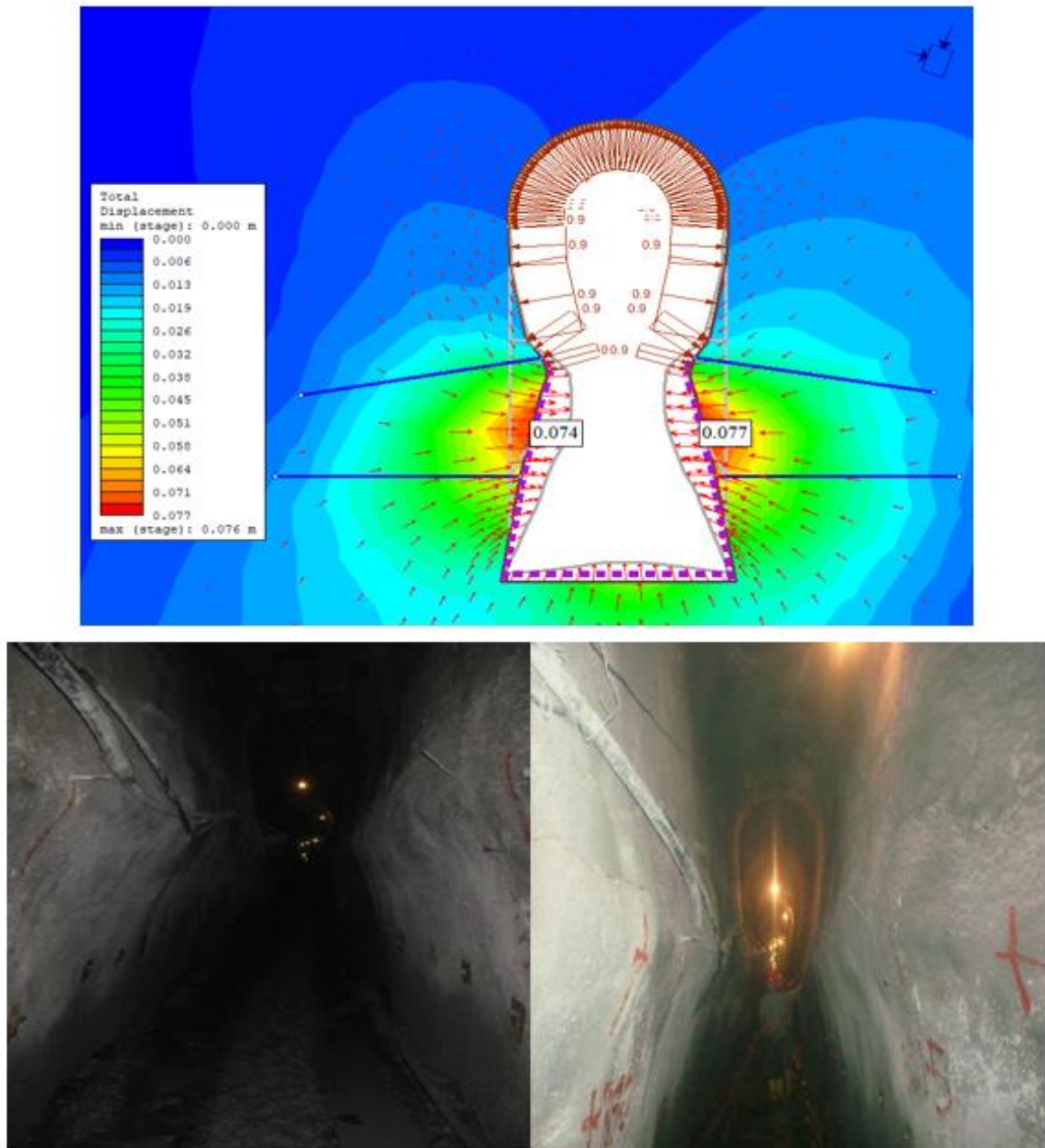
Figure 8-24: Total deformation (squeezing) after the tunnel enlargement in RS2 model (top) and squeezed section along chainage 0+390m to 0+410m (bottom left and right)

The above figure represents that the RS2 model has simulated the actual tunnel squeezing phenomena occurred during the enlargement of tailrace tunnel. As per the convergence monitoring, the maximum deformation measured at chainage 0+400 is 145mm and the RS2 model has resulted in total deformation of 151mm (deformation of both walls, as per Figure 8-24) which is approximately similar to the measured value. Thus, it can be assumed that the input parameters used are calibrated and accurate to be used in other analysis methods.

9 Conclusion and Recommendation

9.1 Conclusion

Plastic deformation or squeezing (in case of weak rock mass) in underground excavation is very common phenomena in the Himalayan region. Since the Himalayan region rock mass is mainly composed of very weak, highly schistose and fractured rock types and subjected to high tectonic stress, the plastic deformation (squeezing) has been experienced even in the lower overburden. Hence, analysis of plastic deformation phenomenon to find the accurate deformation values before excavation has been a challenge to tunnel engineers, especially in Himalayan region. There have been numerous cases of hydropower tunnels in Nepal which experienced such problem. In this thesis, the AKHP is one among them which has been chosen for the analysis of plastic deformation.

The upgrading of AKHP needed the enlargement of cross section of existing tailrace and longitudinal extension of powerhouse cavern. Both the structures were completely in stable condition before the enlargement during upgrading. The existing tailrace tunnel invert excavated further 2 m deep. The rock support applied to the enlarged section was inadequate and squeezing of the rock mass occurred along the tunnel from chainage 0+390 to 0+410. The maximum convergence measured in the tailrace tunnel was 145mm however, in case of powerhouse cavern, minor squeezing was noticed with maximum deformation was 50-100mm on the wall.

For this study, three main methods have been used to analyze the squeezing phenomenon viz. empirical methods such as Singh et al. (1992) and Q-system (Grimstad and Barton, 1993), semi-analytical method such as (Hoek and Marinos, 2000), and numerical modeling in RS2 and RS3. The inputs to squeezing analysis in each method are rock mass parameters and rock stresses. Therefore, quality of analysis largely depends upon the correct estimation of these input parameters. Form the analysis, the tectonic stress value has been found to be equal to 3.0 MPa in this area, but stress measurement will be necessary to verify this value. Following conclusions has been made from the squeezing analysis using different approaches.

- The main challenge that has been faced in squeezing analysis is the correct estimation of rock mass parameters. All methods depend on rock mass strength or quality, and their results are only as good as the quality of the estimated input. Due to lack of field measured data, the input parameters have been estimated with the help of different reports, literatures, and discussion with Supervisors, geological information from project in regional area. Thus, there has been discrepancy in the measured data and the

deformation data obtained from the various analytical and empirical methods. Thus, field measurement is the must for accurate analysis of plastic deformation.

- Singh et al (1992) method is empirical method which predicts the condition of ground whether there will be squeezing or not, but it does not give the amount of tunnel wall deformation and support pressure. The difficulty in this method is the estimation of correct value of SRF (one of the terms in Q) in some cases. The selection of SRF value is very sensitive for the correct estimation of Q-value. Also, this approach does not consider the rock mass strength.

- Hoek and Merinos (2000) method gives the amount of tunnel wall deformation and also considers the support pressure. But it does not consider the tunnel wall deformation at the time of support application and also does not specify the yielding of support. It considers only the isostatic stress condition but in reality, there will be considerable difference in stresses in different directions. However, it can be used to get the useful information at the beginning of analysis. It also gives the grade of squeezing phenomenon in terms of tunnel wall closure percentage. The method by Hoek and Marinos (2000) has proven the least applicable to analysis of squeezing in the powerhouse cavern. The classification and suggested support measures are evaluated about percentage strain. The conversion from strain to deformation would require use of an equivalent tunnel diameter. For a cavern with height to width ratio around 2, the equivalent diameter becomes twice the width of the cavern. Even then the deformations estimated by Hoek and Marinos were grossly underestimated for the assumed rock conditions.

- RS2 and RS3 of Rocscience software is considered a useful tool for the analysis of the deformation for any shape of underground excavation. It gives much better results than the empirical and analytical approach if the proper input parameters are used. The effect of high straight walls and corners in case of non-circular excavation is seen in the model. The input parameters can also be calibrated if the deformation data of the excavation is available. The program can also be used for analysis of the effect of enlargement on the existing underground opening.

- Thus, a dependable prediction of the extent of tunnel squeezing is very essential to propose stabilizing measures to reduce stability problems during underground excavation and optimizing the support condition in advance.

Stability of tunnels passing through weak and schistose rock mass is influenced by two important considerations, which are assessment of extent of tunnel deformation and requirement of support pressure (stiffness) to contain the deformation. Since the rock mass strength and in-situ stress, which are major parameters for calculation of tunnel deformation, are highly variable and use of a deterministic approach as mentioned above may not represent whole rock mass. Above all, numerical modeling gives more realistic and reliable information about deformation. As complex rock mass situation and the actual tunnel profile can be well defined in this model, more realistic result is obtained, and this could be compared with the results from other approaches along with actual measured deformation.

Most of these approaches that are available for assessing deformation result in total deformation. However, none of these discuss on the instantaneous and time dependent deformation which are important for rock support optimization in weak rock mass. (Panthi & Shrestha, 2018) have established that the time-dependent plastic deformation contributions are considerable in the recorded total deformations and it varies according to the engineering geological conditions along the tunnel alignment.

During tunneling in weak rock mass, if tunnel deformations are constrained at very early stage, squeezing will lead to long-term load build-up of rock support, causing bucking or even failure of rock support. For example, in case of large deformation, installation of stiff and heavy supports, immediately after excavation may not be able to sustain imposed stress and may be destroyed. Conversely, if the support installation is delayed, the rock mass moves into the tunnel creating risk to workers at the face of unsupported tunnel. Thus, the decision of installation of optimum support at right time is the major concern tunneling inside weak rock. The use of support systems that can provide high support resistance to limit the rock deformation and can accommodate large displacement should be prioritized for highly squeezed ground. To adjust excavation and support requirements under poor rock condition, careful monitoring of system behavior, up to date evaluation of monitoring data, detailed and continuous engineering geological mapping are very much essential.

9.2   Recommendations

Following recommendations can be applied for analysis of plastic deformation:

- Stress measurement at the site is essential for verification of the estimated value from various analysis methods.

- Field observations and laboratory test are very important for accurate estimation of rock mass properties since these input parameters are the most important factors for analysis.

- The analytical methods used during the plastic deformation analysis in severe squeezing rock mass condition should be verified using actual monitored deformation data, mapped geological conditions, and lab-tested rock mechanical properties. An erroneous understanding of the suggested methods may lead to inaccurate interpretation of the deformation magnitude and the effective tunnel support pressure required.

- If severe squeezing is anticipated, deformation measurements must be carried out in the tunnels and using the RS2 program one can correlate the deformations to rock mass parameters and stress conditions. Moreover, the input parameters can be calibrated, and thus more optimum design of rock support design and necessary precautions can be adopted.

- 3-dimentional numerical modeling will be necessary in case of large cavern for adequate estimation of plastic deformation. Mainly in cases where the modification in geometry is made in the existing cavern, the nature of stress orientation is drastically changed which cannot be replicated in 2D numerical modeling.

- Taking the basis of reference of rectangular tailrace tunnel of AKHP, the excavation geometry should be adopted as circular as possible in case of weak rock mass. The rectangular geometry should be avoided as far as possible since the stress concentration increases in the corners leading to other instability and stress anisotropy.

- In general, for weak and heterogeneous rock masses, it is extremely challenging to have undisturbed samples of intact core for laboratory testing. Even if such samples are obtained, they will not always be representative samples. Thus, Primary observation and Instrumented observation data can be used in various ways like interactive back analysis with numerical modeling to find out refined and representative input parameters.

References

Aydan, Ö., Akagi, T. & Kawamoto, T. 1993. The squeezing potential of rocks around tunnels; theory and prediction. *Rock mechanics and rock engineering,* 26**,** 137-163.

Aydan, Ö., Akagi, T. & Kawamoto, T. 1996. The squeezing potential of rock around tunnels: theory and prediction with examples taken from Japan. *Rock mechanics and rock engineering,* 29**,** 125-143.

Barla, G., Bonini, M. & Debernardi, D. 2010. Time dependent deformations in squeezing tunnels. *ISSMGE International Journal of Geoengineering Case Histories,* 2**,** 40-65.

Barton, N. 2002. Some new Q-value correlations to assist in site characterisation and tunnel design. *International journal of rock mechanics and mining sciences,* 39**,** 185-216.

Barton, N., Lien, R. & Lunde, J. 1974. Engineering classification of rock masses for the design of tunnel support. *Rock mechanics,* 6**,** 189-236.

Basnet, C. B., Shrestha, P. K. & Panthi, K. K. 2013. Analysis of Squeezing Phenomenon in the Headrace Tunnel of Chameliya Project, nepal.

Bieniawski, Z. T. 1989. *Engineering rock mass classifications: a complete manual for engineers and geologists in mining, civil, and petroleum engineering*, John Wiley & Sons.

Brady, B. & Brown, E. 2007. Rock strength and deformability. *Rock Mechanics for underground mining.* Springer.

Carranza-Torres, C. & Fairhurst, C. 1999. The elasto-plastic response of underground excavations in rock masses that satisfy the Hoek–Brown failure criterion. *International Journal of Rock Mechanics and Mining Sciences,* 36**,** 777-809.

Carranza-Torres, C. & Fairhurst, C. 2000. Application of The Convergence-Confinement Method of Tunnel Design to Rock Masses that Satisfy The Hoek-Brown Failure Criterion.". *Tunnelling and Underground Space Technology*.

Chapman, D., Metje, N. & Stärk, A. 2010. *Introduction to tunnel construction,* London, Spon Press.

Chern, J., Shiao, F. & Yu, C. 1998. *An empirical safety criterion for tunnel construction.*

Fama, M. E. D. 1993. Numerical modeling of yield zones in weak rock. *Analysis and design methods,* Journal of Comprehensive rock engineering**,** 49-75.

Goel, R. K., Jethwa, J. L. & Paithankar, A. G. 1995. Indian experiences with Q and RMR systems. *Tunnelling and Underground Space Technology,* 10**,** 97-109.

Goodman, R. E. 1989. *Introduction to rock mechanics*, Wiley New York.

Grimstad, E. & Barton, N. Updating the Q-system for NMT. Proceedings of the International Symposium on Sprayed Concrete-Modern use of wet mix sprayed concrete for underground support, Fagemes, Oslo, Norwegian Concrete Association, 1993, 1993.

Hoek, E. Estimating Mohr-Coulomb friction and cohesion values from the Hoek-Brown failure criterion. Intnl. J. Rock Mech. & Mining Sci. & Geomechanics Abstracts, 1990. 227-229.

Hoek, E. 2007c. Rock mass properties. *Practical rock engineering,* Ch.11**,** 190-236.

Hoek, E. & Brown, E. T. 1980. *Underground excavations in rock.*

Hoek, E., Carranza-Torres, C. & Corkum, B. 2002. Hoek-Brown failure criterion-2002 edition. *Proceedings of NARMS-Tac,* 1**,** 267-273.

Hoek, E. & Diederichs, M. S. 2006. Empirical estimation of rock mass modulus. *International journal of rock mechanics and mining sciences,* 43**,** 203-215.

Hoek, E. & Marinos, P. 2000. Predicting tunnel squeezing problems in weak heterogeneous rock masses. *Tunnels and tunnelling international,* 32**,** 45-51.

Hudson, J. A. & Harrison, J. P. 2000. *Engineering rock mechanics: an introduction to the principles*, Elsevier.

Kovári, K. 1998. Tunneling in squeezing rock. *Tunnel 5/98*.

Myrvang, A. 2001. Rock Mechanics. *Norway University of Technology (NTNU), Trondheim*.

Nepal, K. M. 1999. A review of in-situ testing of rock mechanical parameters in hydropower projects of Nepal. *J Nepal Geol Soc,* 19**,** 1-8.

Nilsen, B. & Palmström, A. 2000. Engineering geology and rock engineering. *Norwegian Soil and Rock Engineering Association (NJFF), Oslo*.

Nilsen, B. & Thidemann, A. 1993. Rock Engineering, Hydropower Development Vol. 9. *Norwegian Institute of Technology (NTH), 156p*.

Panthi, K. & Nilsen, B. 2007. Uncertainty analysis of tunnel squeezing for two tunnel cases from Nepal Himalaya. *Int. J. Rock Mech. Min. Sci.,* 44**,** 67-76.

Panthi, K. K. 2006. *Analysis of engineering geological uncertainties related to tunnelling in Himalayan rock mass conditions.* (Doctoral Thesis at NTNU 2006:41), Norwegian University of Science and Technology, Department of Geology and Mineral Resources Engineering.

Panthi, K. K. 2012. Evaluation of rock bursting phenomena in a tunnel in the Himalayas. *Bulletin of Engineering Geology and the Environment,* 71**,** 761-769.

Panthi, K. K. 2013. Predicting Tunnel Squeezing: A Discussion based on Two Tunnel Projects.

Panthi, K. K. & Shrestha, P. K. 2018. Estimating Tunnel Strain in the Weak and Schistose Rock Mass Influenced by Stress Anisotropy: An Evaluation Based on Three Tunnel Cases from Nepal. *Rock mechanics and rock engineering,* 51**,** 1823-1838.

Saari, K. H. 1982. *Analysis of Platic Deformations (squeezing) of Seams Intersecting Tunnels and Shafts in Rock*, University of California, Berkeley.

Sakurai, S. Displacement measurements associated with the design of underground openings. Field measurements in geomechanics. International symposium, 1984. 1163-1178.

Shrestha, G. L. 2006. *Stress induced problems in Himalayan tunnels with special reference to squeezing.* (Doctoral Thesis 2006:20), Norwegian University of Science and Technology, Faculty of Engineering Science and Technology, Department of Geology and Mineral Resources Engineering.

Shrestha, P. & Panthi, K. 2014a. Analysis of the plastic deformation behavior of schist and schistose mica gneiss at Khimti headrace tunnel, Nepal. *The official journal of the IAEG,* 73**,** 759-773.

Shrestha, P. K. 2014. *Stability of tunnels subject to plastic deformation : a contribution based on the cases from the Nepal Himalaya.* 2014:305, Norwegian University of Science and Technology, Faculty of Engineering Science and Technology, Department of Geology and Mineral Resources Engineering.

Shrestha, P. K. & Panthi, K. K. 2014b. Groundwater effect on faulted rock mass: an evaluation of Modi Khola pressure tunnel in the Nepal Himalaya. *Rock mechanics and rock engineering,* 47**,** 1021-1035.

Singh, B., Jethwa, J., Dube, A. & Singh, B. 1992. Correlation between observed support pressure and rock mass quality. *Tunnelling and Underground Space Technology,* 7**,** 59-74.

Steiner, W. 2000. Squeezing rock in tunnelling: identification and important factors. *Rivitsta Italiana di Geotecnica (1)*.

Sulem, J., Panet, M. & Guenot, A. An analytical solution for time-dependent displacements in a circular tunnel. International journal of rock mechanics and mining sciences & geomechanics abstracts, 1987. Elsevier, 155-164.

Vlachopoulos, N. & Diederichs, M. 2009. Improved longitudinal displacement profiles for convergence confinement analysis of deep tunnels. *Rock mechanics and rock engineering,* 42**,** 131-146.

Wood, A. M. M. 1972. Tunnels for roads and motorways. *Quarterly Journal of Engineering Geology and Hydrogeology,* 5**,** 111-126.

APPENDICES

Appendix A: Standard Chart and Figures

Determination of GSI (Hoek and Marinos, 2000)

GEOLOGICAL STRENGTH INDEX

From the description of structure and surface conditions of the rock mass, pick an appropriate box in this chart. Estimate the average value of the Geological Strength Index (GSI) from the contours. Do not attempt to be too precise. Quoting a range of GSI from 36 to 42 is more realistic than stating that GSI = 38. It is also important to recognize that the Hoek-Brown criterion should only be applied to rock masses where the size of the individual blocks or pieces is small compared with the size of the excavation under consideration. When individual block sizes are more than approximately one quarter of the excavation dimension, failure will generally be structurally controlled and the Hoek-Brown criterion should not be used.

STRUCTURE	SURFACE CONDITIONS	VERY GOOD Very rough, fresh unweathered surfaces	GOOD Rough, slightly weathered, iron stained surfaces	FAIR Smooth, moderately weathered and altered surfaces	POOR Slickensided, highly weathered surfaces with coatings or fillings of angular fragments	VERY POOR Slickensided, highly weathered surfaces with soft clay coatings or fillings
		DECREASING SURFACE QUALITY →				
INTACT OR MASSIVE – intact rock specimens or massive in situ rock with very few widely spaced discontinuities		90 / 80		N/A	N/A	N/A
BLOCKY - very well interlocked undisturbed rock mass consisting of cubical blocks formed by three orthogonal discontinuity sets			70 / 60			
VERY BLOCKY - interlocked, partially disturbed rock mass with multifaceted angular blocks formed by four or more discontinuity sets				50		
BLOCKY/DISTURBED - folded and/or faulted with angular blocks formed by many intersecting discontinuity sets				40	30	
DISINTEGRATED - poorly interlocked, heavily broken rock mass with a mixture of angular and rounded rock pieces						20
FOLIATED/LAMINATED – Folded and tectonically sheared foliated rocks. Schistosity prevails over any other discontinuity set, resulting in complete lack of blockiness		N/A	N/A			10 / 5

(Left margin: DECREASING INTERLOCKING OF ROCK PIECES ↓)

Disturbance factor D (Hoek et al., 2002)

Appearance of rock mass	Description of rock mass	Suggested value of D
	Excellent quality controlled blasting or excavation by Tunnel Boring Machine results in minimal disturbance to the confined rock mass surrounding a tunnel.	$D = 0$
	Mechanical or hand excavation in poor quality rock masses (no blasting) results in minimal disturbance to the surrounding rock mass. Where squeezing problems result in significant floor heave, disturbance can be severe unless a temporary invert, as shown in the photograph, is placed.	$D = 0$ $D = 0.5$ No invert
	Very poor quality blasting in a hard rock tunnel results in severe local damage, extending 2 or 3 m, in the surrounding rock mass.	$D = 0.8$
	Small scale blasting in civil engineering slopes results in modest rock mass damage, particularly if controlled blasting is used as shown on the left hand side of the photograph. However, stress relief results in some disturbance.	$D = 0.7$ Good blasting $D = 1.0$ Poor blasting
	Very large open pit mine slopes suffer significant disturbance due to heavy production blasting and also due to stress relief from overburden removal. In some softer rocks excavation can be carried out by ripping and dozing and the degree of damage to the slopes is less.	$D = 1.0$ Production blasting $D = 0.7$ Mechanical excavation

Description of ratings for input parameters for Q-system (Barton, 2002)

RQD (Rock quality designation, %)		J_n (Joint set number)	
Very poor	0 - 25	Massive, no or few joints	0.5 - 1
Poor	25 - 50	One joint set	2
Fair	50 – 75	One joint set + random joints	3
Good	75 – 90	Two joint sets	4
Excellent	90 - 100	Two joint sets + random	6
Notes:		Three joint sets	9
(i) where RQD is reported or measured as ≤ 10 (including 0), a nominal value of 10 is used to evaluate Q.		Three joint sets + random	12
		Four or more joint sets, heavily jointed, sugar cube etc	15
(ii) RQD intervals of 5 i.e. 100, 95, 90 etc., are successfully accurate.		Crushed rock, earthlike	20
		Note: For tunnel intersections, use (3 x J_n) and for portals use (2 x J_n)	

J_r (Joint roughness number)

(a) Rock wall contact		(b) Rock wall contact before 10 cm shear	
Discontinuous joints	4	Rough or irregular, undulating	1.5
Rough or irregular, undulating	3	Smooth, undulating	1
Smooth, undulating	2	Slickensided, undulating	0.5
Slickensided, undulating	1.5		

© *No rock wall contact when sheared*

Zone containing clay minerals thick enough to prevent rock wall contact	1
Sandy, gravely or crushed zone thick enough to prevent rock wall contact	1

Notes: (i) Description refers to small-scale features and intermediate scale features, in that order (ii) Add 1.0 if the mean spacing of the relevant joint set is greater than 3 m. (iii) Jr = 0.5 can be used for planner, slickenside joints having lineations, provided these are oriented for minimum strength. (iv) Jr and Ja classification is applied to the joint set that is least favorable for stability both from the point of view of orientation and shear resistance, $\tau \approx \sigma_n . \tan^{-1} (J_r/J_a)$

J_a (Joint alteration number)

(a) Rock wall contact (no mineral fillings, only coatings)	ϕ_r (appr.)	J_a
Tightly healed, hard, non-softening, impermeable filling i.e., quartz/epidote	-	0.75
Unaltered joint walls, surface staining only	25 - 35	1
Slightly altered joint walls, non-softening mineral coatings, sandy particles, clay free disintegrated rock ,etc.	25 - 30	2
Silty or sandy clay coatings, small clay fractions (non-softening)	20 - 25	3
Softening or low friction clay mineral coatings, i.e., kaolinite or mica. Also chlorite, talk, gypsum, graphite etc., and small quantities of swelling clay	8 - 16	4
(b) Rock wall contact before 10 cm shear (thin mineral fillings)		
Sandy particles, clay free disintegrated rock etc.	25 - 30	4
Strongly over-consolidated non-softening clay mineral fillings (continuous, but < 5mm thickness)	16 - 24	6

RMR classification of rock mass (Bieniawaski, 1989)

A. Classification parameters and their ratings

Parameters			Range of values or ratings						
1	Strength of Intact Rock	Point load strength index (MPa)	> 10	4 - 10	2 - 4	1 - 2	Low range uniaxial strength is preferred		
		Uniaxial compressive strength (MPa)	> 250	100-250	50-100	25-50	5- 25	1 - 5	< 1
		Rating	**15**	**12**	**7**	**4**	**2**	**1**	**0**
2	Drill core quality, RQD (%)		90-100	75-90	50-75	25-50	< 25		
	Rating		**20**	**17**	**13**	**8**	**5**		
3	Spacing of discontinuities (m)		> 2	0.6-2	0.2-0.6	0.06-0.2	< 0.06		
	Rating		**20**	**15**	**10**	**8**	**5**		
4	Condition of discontinuities	Length, persistence (m)	< 1	1-3	3-10	10-20	> 20		
		Rating	**6**	**4**	**2**	**1**	**0**		
		Separation (mm)	none	< 0.1	0.1-1	1-5	> 5		
		Rating	**6**	**5**	**4**	**1**	**0**		
		Roughness	very rough	rough	slightly rough	smooth	slickensided		
		Rating	**6**	**5**	**3**	**1**	**0**		
		Infilling (gouge) (mm)	none	hard filling < 5	hard filling > 5	soft filling < 5	soft filling > 5		
		Rating	**6**	**4**	**2**	**2**	**0**		
		Weathering	un-weathered	slightly weathered	moderately weathered	highly weathered	decomposed		
		Rating	**6**	**5**	**3**	**1**	**0**		
5	Ground water	Inflow per 10 meter tunnel length (l/min)	none	< 10	10-25	25-125	> 125		
		ρ_w / σ_1	0	0.0.1	0.1-0.2	0.2-0.5	> 0.5		
		General conditions	dry	damp	wet	dripping	flowing		
		Rating	**15**	**10**	**7**	**4**	**0**		

here, ρ_w is joint water pressure and σ_1 is major principle stress

B. Rating adjustment for discontinuity orientation

Tunnel alignment	very favorable	favorable	fair	unfavorable	very unfavorable
Rating adjustment	**0**	**-2**	**-5**	**-10**	**-12**

C. Rock mass classes determined from total ratings

Rating	100-80	80-61	60-41	40-21	< 20
Class No.	I	II	III	IV	V
Description	Very good	Good	Fair	Poor	Very poor

D. Meaning or rock mass classes

Class No.	I	II	III	IV	V
Average stand-up time	Can be estimated from Figure 4-4				
Cohesion of the rock mass (kPa)	> 400	3-400	2-300	1-200	< 00
Friction angle of the rock mass (degrees)	< 45	35-45	25-35	15-25	< 15

Support Pressure Estimation chart using Q-value
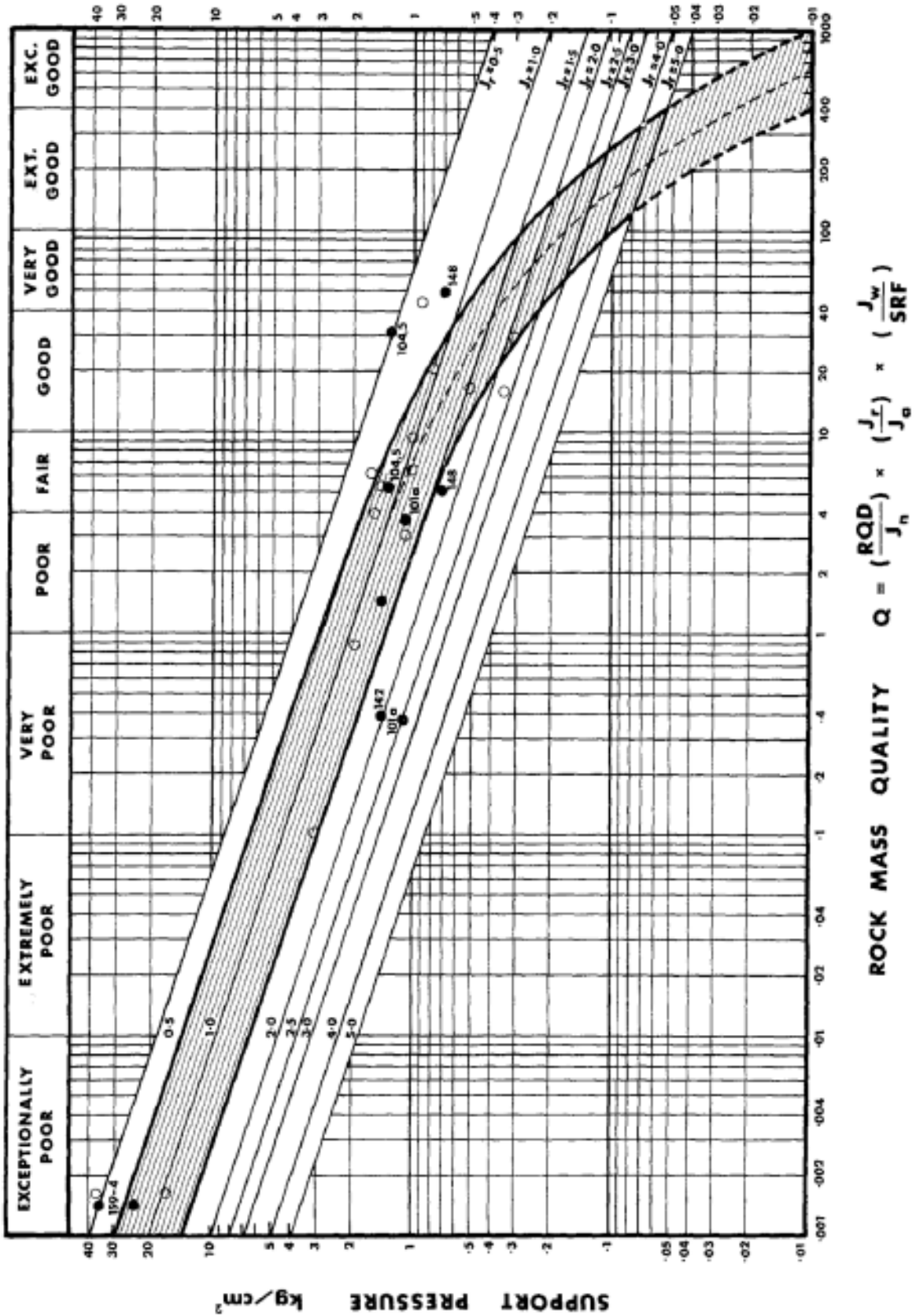
Q-system chart and various excavation support ratio categories

ROCK CLASSES

G	F	E	D	C	B	A
Exceptionally poor	Extremely poor	Very poor	Poor	Fair	Good	Very good / Extrem. good / Exce. good

Rock mass quality $Q = \dfrac{RQD}{Jn} \times \dfrac{Jr}{Ja} \times \dfrac{Jw}{SRF}$
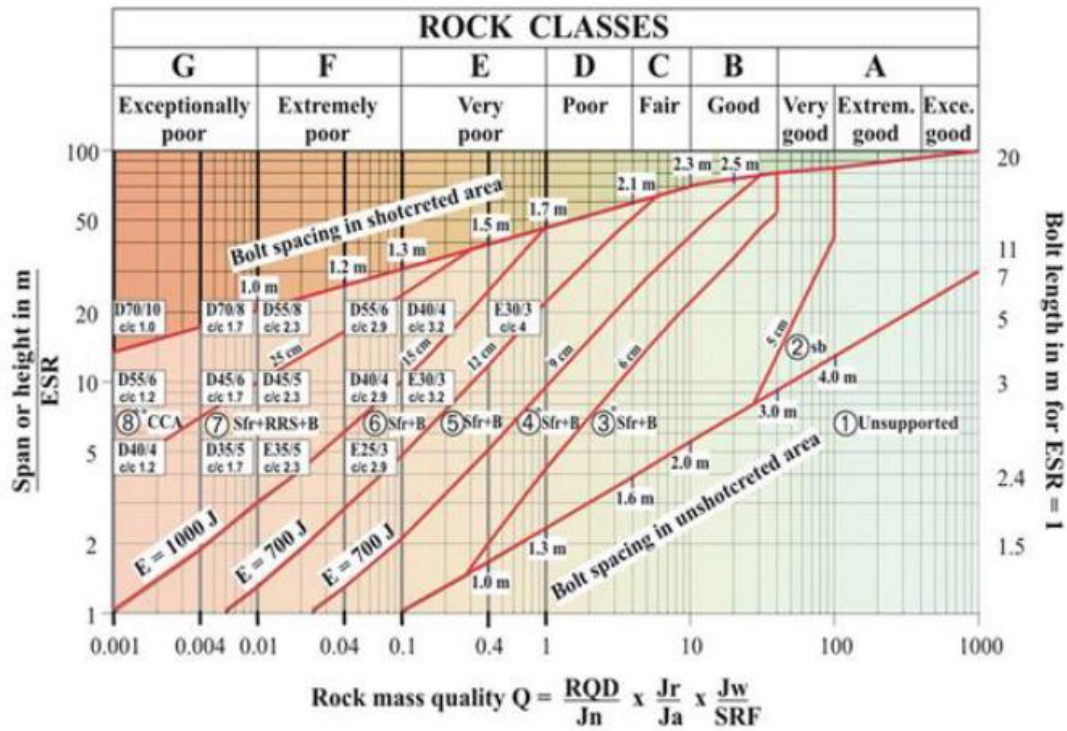
REINFORCEMENT CATEGORIES

1) Unsupported
2) Spot bolting, **sb**
3) Systematic bolting,
   (and unreinforced shotcrete, 5-6 cm), **B(+S)**
4) Fibre reinforced shotcrete and bolting, 6-9 cm, **Sfr+B**
5) Fibre reinforced shotcrete and bolting, 9-12 cm, **Sfr+B**
6) Fibre reinforced shotcrete and bolting, 12-15 cm, **Sfr+B**
7) Fibre reinforced shotcrete > 15 cm +
   reinforced ribs of shotcrete and bolting, **Sfr+RRS+B**
8) Cast concrete lining, **CCA** or **Sfr+RRS+B**

E) Energy absorbtion in fibre reinforced shotcrete at 25 mm bending during plate testing

$\begin{array}{|l} D45/6 \\ c/c\ 1.7 \end{array}$ = RRS with 6 reinforcement bars in double layer in 45 cm thick ribs with centre to centre (c/c) spacing 1.7 m. Each box corresponds to Q-values on the left hand side of the box. (See text for explanation)

*) Up to 10 cm in large spans
) Or **Sfr+RRS+B

	ESR = 3–5
Temporary mine openings	
Permanent mine openings, water tunnels for hydro power (excluding high pressure penstocks), pilot tunnels, drifts and headings for large excavations	1.6
Storage rooms, water treatment plants, minor road and railway tunnels, surge chambers, access tunnels	1.3
Power stations, major road and railway tunnels, civil defence chambers, portal intersections	1
Underground nuclear power stations, railway stations, sports and public facilities, factories	0.8

Appendix B: Project Information

Geological information of the squeezed tunnel section of AKHP

GEOLOGICAL LOG OF TUNNEL			
Location : Tailrace			→ N
Orientation			

LOG	LW		EXISTING STRUCTURE		
	RW				

	Chainage m			
Q System	RQD	10		
	JN	15		
	JR	1.5		
	JA	4		
	JW	1		
	SRF	10		
	Rock mass class	0.04		
RMR	RQD	3		
	UCS	4		
	J Spacing	8		
	J Condition	3		
	J-Orientation	-5		
	Ground Water	7		
	RMR	20		
GEOLOGY	DISCRIPTION	Moderately to highly weathered, closely foliated, fractured, dark grey, fine grain very weak phyllite with slate with 3 sets of joints clay filled multiple shear planes		

JOINT				
Attitude (dd/do)	F = 290/05	J1 = 120/65	J2 = 280/45
Persistence (m)	1-2m	<1m	0.5-1m
Spacing (cm)	3-15	20-40cm	2-5m
Aperature (cm)	>5mm	5-15mm	>5mm
Roughness	smooth	smooth	Rough
Filling	clay	clay	clay

Legends: Foliation Plane | Joint Plane | Shear Plane | XXXX Jointed Fractured

Convergence measurement at the tailrace tunnel wall

Chainage ➡	0+ 390	0+ 395	0+ 400	0+ 405	0+ 408
July 20, 2013	1.470	1.285	1.150	1.135	1.160
July 23, 2013	1.458	1.261	1.094	1.120	1.135
July 24, 2013	1.455	1.255	1.089	1.115	1.129
July 25, 2013	1.450	1.251	1.085	1.099	1.120
July 26, 2013	1.445	1.244	1.078	1.092	1.112
July 27, 2013	1.441	1.238	1.072	1.085	1.102
July 28, 2013	1.437	1.231	1.066	1.079	1.094
July 29, 2013	1.432	1.225	1.062	1.071	1.085
July 30, 2013	1.429	1.219	1.058	1.064	1.078
July 31, 2013	1.425	1.213	1.052	1.060	1.070
August 1, 2013	1.423	1.209	1.047	1.055	1.065
August 2, 2013	1.417	1.202	1.042	1.050	1.058
August 3, 2013	1.414	1.194	1.035	1.039	no bolt
August 4, 2013	1.413	1.191	1.031	1.034	
August 5, 2013	1.407	1.187	1.025	1.025	
August 6, 2013	1.399	1.183	1.021	1.018	
August 7, 2013	1.399	1.175	1.018	1.014	
August 8, 2013	1.395	1.170	1.013	1.010	
August 9, 2013	1.393	1.165	1.005		

The leftmost label spanning the date rows reads: "Reading of Tailrace Tunnel Monitoring bolts (meter)"

Rock support provided in newly extended powerhouse cavern (From as built drawing)

Rock Support	Location (chainage 0+000 start of newly extend cavern)	Rock Support	Quantity	
Spilling	Ch. 0+000	20 mm dia. 4 m long	39 nos.	
	Ch. 0+2.80		30 nos.	
	Ch. 0+5.10		33 nos.	
Rock Bolts	Ch. 0+0.05 m	20 mm dia. 3 m long	1 nos.	
	Ch. 0+0.06 m	20 mm dia. 4 m long 20 mm dia. 3 m long	3 nos. 2 nos.	
	Ch. 0+0.40 m	20 mm dia. 3 m long	1 nos. left side	
	Ch. 0+0.70 m	20 mm dia. 3 m long	1 nos. right side side	
	Ch. 0+0.90 m	20 mm dia. 3 m long	1 nos.+ 1 nos. left side	
	Ch. 0+1.80 m	20 mm dia. 4 m long 20 mm dia. 3 m long.	7 nos. @ 1.0 m spacing 2 nos.	

|				
	Ch. 0+2.0 m	20 mm dia. 3 m long	2 nos.	
	Ch. 0+2.20 m	20 mm dia. 3 m long	1 nos.	
	Ch. 0+2.30 m	20 mm dia. 3 m long	1 nos. right side	
	Ch. 0+2.45 m	20 mm dia. 4 m long	1 nos. extra @ crown face	
	Ch. 0+2.6 m	20 mm dia. 4 m long	1 nos.	
	Ch. 0+2.96 m	20 mm dia. 4 m long	6 nos. @ 1.0 m spacing	
	Ch. 0+3.40 m	20 mm dia. 4 m long	1 nos. right side	
	Ch. 0+3.6 m	20 mm dia. 3 m long	2 nos.	
	Ch. 0+3.7 m	20 mm dia. 3 m long	1 nos.	
	Ch. 0+4.0 m	20 mm dia. 3 m long	2 nos. right side	
	Ch. 0+4.5 m	20 mm dia. 4 m long	7 nos. @ 1.0 m spacing	
	Ch. 0+4.70 m	20 mm dia. 3 m long	2 nos. right side	
	Ch. 0+4.90 m	20 mm dia. 3 m long	2 nos. left side	
	Ch. 0+5.0 m	20 mm dia. 4 m long	1 nos. extra	
	Ch. 0+5.10 m	20 mm dia. 3 m long	1 nos.	
	Ch. 0+5.6 m	20 mm dia. 4 m long	1+1 nos. extra	
	Ch. 0+5.70 m	20 mm dia. 3 m long	1 nos. right side	
	Ch. 0+6.0 m	20 mm dia. 3 m long	1 nos.	
	Ch. 0+6.1 m	20 mm dia. 4 m long	6 nos. @ 1.0 m spacing	
	Ch. 0+6.20 m	20 mm dia. 3 m long	1 nos. left side	
	Ch. 0+6.60 m	20 mm dia. 3 m long	1 nos.	
	Ch. 0+6.70 m	20 mm dia. 3 m long	1-1 nos. right & left side	
	Ch. 0+6.75m	20 mm dia. 3 m long	3 nos.	
	Ch. 0+7.5 m	20 mm dia. 4 m long	5 nos. @ 1.0 m spacing	
	Ch. 0+7.60 m	20 mm dia. 3 m long	1 nos. left side	
	Ch. 0+7.9 m	20 mm dia. 3 m long	3 nos.	
	Ch. 0+8.0 m	20 mm dia. 3 m long	4+3+5+7 nos. @ face	
3	Shotcrete	steel fibre shotcrete	50 and 100 mm thick layer	

RS2 Powerhouse Cavern Model
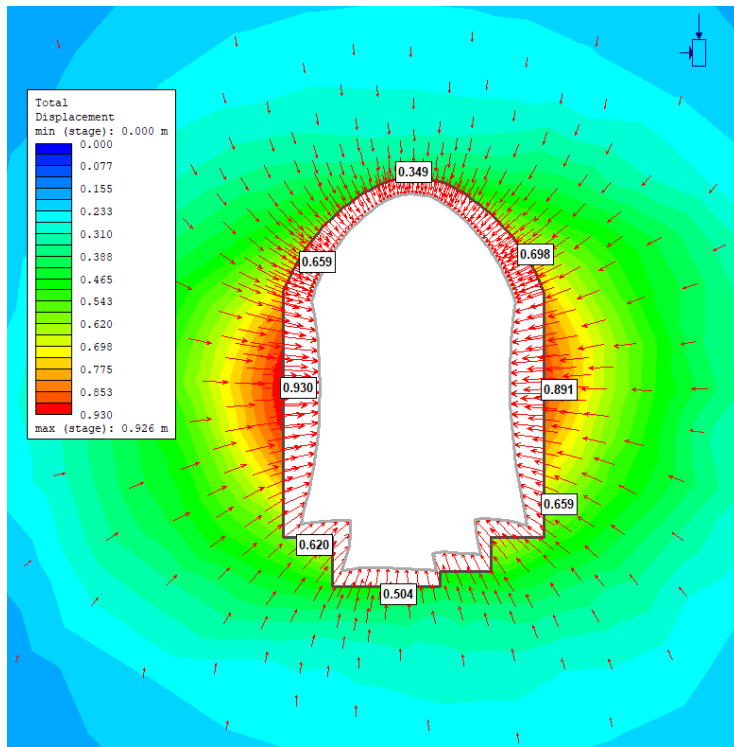
Figure: Total deformation for plastic analysis in the RS2 model of powerhouse cavern without support (As per the input parameters suggested in AKHP project completion report)

Table: Support system provided in RS2 Powerhouse cavern modeling as per AKHP project report

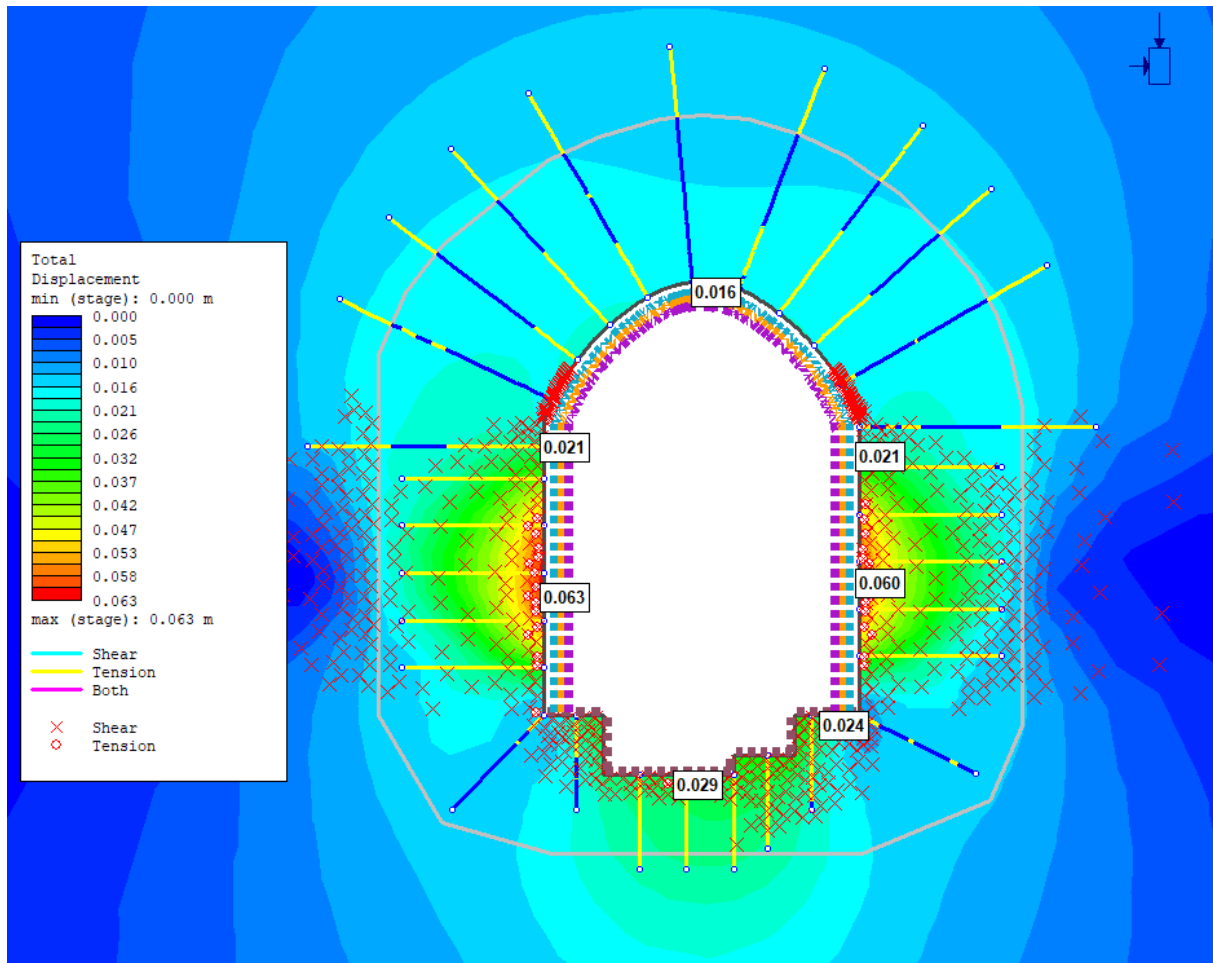| Rock Support			Crown	Wall	Invert
Perimeter grouting (Pre grouting)	Thickness (m)		3.5	3.5	-
Steel fiber reinforced shotcrete	Thickness (cm)	First layer	10	10	10
		Second layer	15	15	-
Fully bounded rock bolts	Length (m)		4	3	2
	Spacing (m) @ c/c		1	1	2
	Diameter (mm)		25	25	25
Steel ribs	I-Beam (area=0.00326 m²)		S150*25.7/reinforced ribs of shotcrete		-

Figure: Total deformation after applying the support system and input parameters as per AKHP project report.